Excited states from time-dependent density functional theory

Peter Elliott
Department of Physics and Astronomy, University of California, Irvine, CA 92697, USA

Kieron Burke
Department of Chemistry, University of California, Irvine, CA 92697, USA

Filipp Furche
Institut für Physikalische Chemie, Universität Karlsruhe, Kaiserstraße 12, 76128 Karlsruhe, Germany
(Dated: March 21, 2007)

Time-dependent density functional theory (TDDFT) is presently enjoying enormous popularity in quantum chemistry, as a useful tool for extracting electronic excited state energies. This article explains what TDDFT is, and how it differs from ground-state DFT. We show the basic formalism, and illustrate with simple examples. We discuss its implementation and possible sources of error. We discuss many of the major successes and challenges of the theory, including weak fields, strong fields, continuum states, double excitations, charge transfer, high harmonic generation, multiphoton ionization, electronic quantum control, van der Waals interactions, transport through single molecules, currents, quantum defects, and, elastic electron-atom scattering.

Contents

I. INTRODUCTION

Ground-state density functional theory [1–3] has become the method of choice for calculating ground-state properties of large molecules, because it replaces the interacting many-electron problem with an effective single-particle problem that can be solved much more quickly. It is based on rigorous theorems[1, 2, 4] and a hierarchy of increasingly accurate approximations, such as the local density approximation (LDA), generalized gradient approximations (GGA's)[5–7], and hybrids of exact exchange with GGA[8]. For example, a recent ground-state calculation[9] for crambin ($C_{203}H_{317}N_{55}O_{64}S_6$), a small protein, using TURBOMOLE[10] on a 1.5 GHZ HP itanium workstation took just 6h52m, extraordinarily fast for 2528 electrons. But, formally, ground-state density functional theory predicts only ground-state properties, not electronic excitations.

On the other hand, time-dependent density functional theory (TDDFT)[11–15] applies the same philosophy to time-dependent problems. We replace the complicated many-body time-dependent Schrödinger equation by a set of time-dependent single-particle equations whose orbitals yield the same time-dependent density. We can do this because the Runge-Gross theorem[16] proves that, for a given initial wavefunction, particle statistics and interaction, a given time-dependent density can arise from at most one time-dependent external potential. This means that the time-dependent potential (and all other properties) is a functional of the time-dependent density.

Armed with a formal theorem, we can then define time-dependent Kohn-Sham (TDKS) equations that describe non-interacting electrons that evolve in a time-dependent Kohn-Sham potential, but produce the same density as that of the interacting system of interest. Thus, just as in the ground-state case, the demanding interacting time-dependent Schrödinger equation is replaced by a much simpler set of equations to propagate.The price of this enormous simplification is that the exchange-correlation piece of the Kohn-Sham potential has to be approximated.

The most common time-dependent perturbation is a long-wavelength electric field, oscillating with frequency ω. In the usual situation, this field is a weak perturbation on the molecule, and one can perform a linear response analysis. From this, we can extract the optical absorption spectrum of the molecule due to electronic excitations. Thus linear response TDDFT predicts the transition frequencies to electronic excited states and many other properties. This has been the primary use of TDDFT so far, with lots of applications to large molecules.

Figure 1 compares TDDFT and experiment for the electronic CD spectrum of the chiral fullerene C_{76}. A total of 240 optically allowed transitions were required to simulate the spectrum. The accuracy is clearly good enough to assign the absolute configuration of C_{76}. TDDFT calculations of this size typically take less than a day on low-end personal computers.

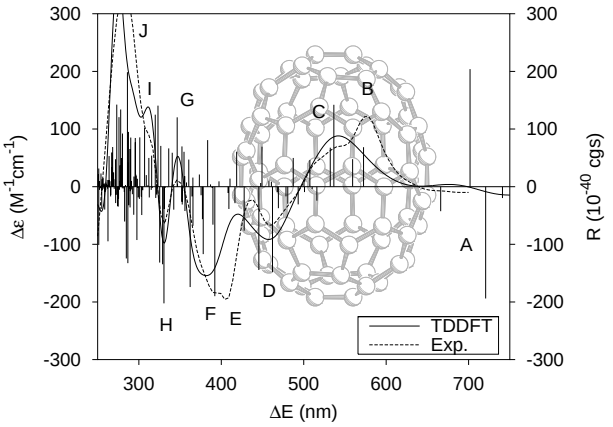

FIG. 1: TDDFT calculation and experiment for the electronic CD spectrum of fullerene (^fA)-C_{76}. TDDFT calculations were performed with the BP86 functional and an augmented SVP basis set [17]. The RI-J approximation together with TZVP auxiliary basis sets [18] was used. Experimental data (in CH_2Cl_2) are from [19].

A random walk through some recent papers using TDDFT gives some feeling for the breadth of applications. Most are in the linear response regime. In inorganic chemistry, the optical response of many transition metal complexes[20–35] has been calculated, and even some X-ray absorption[36, 37]. In organic chemistry, heterocycles[38–43] among others[44–46] have been examined. Other examples include the response of thiouracil[47], s-tetrazine[48], and annulated porphyrins[49]. We also see TDDFT's use in studying various fullerenes[50–55]. In biochemistry, TDDFT is finding many uses[56–66]. DNA bases are under examination, and an overview of their study may be found in Ref. [67]. In photobiology, potential energy curves for the trans-cis photo-isomerization of protonated Schiff base of retinal[68] have been calculated. Large calculations for green and blue fluorescent proteins have also been performed[69, 70]. Doing photochemistry with TDDFT[71], properties of chromophores[72–76] and dyes[77–83] have been computed. For these and other systems, there is great interest in charge-transfer excitations[84–92], but (as we later discuss) intermolecular charge transfer is a demanding problem for TDDFT.

Another major area of application is clusters, large and small, covalent and metallic, and everything inbetween[93–112], including Met-Cars[113]. Several studies include solvent effects[114–122], one example being the behavior of metal ions in explicit water[123]. TDDFT in linear response can also be used to examine chirality[124–127], including calculating both electric and magnetic circular dichroism[26, 128–132], and has been applied to both helical aromatics[133] and to artemisinin complexes in solution[134]. There have also been applications in materials[135, 136] and quantum dots[137] but, as discussed below, the optical response of bulk solids requires some non-local approximations[138].

Beyond the linear regime, there is also growing interest in second- and third-order response[139–142] in all these fields. In particular the field of non-linear optics has been heavily investigated[143–145], especially the phenomenon of two photon absorption[146, 146–153].

In fact, TDDFT yields predictions for a huge variety of phenomena, that can largely be classified into three groups: (i) the non-perturbative regime, with systems in laser fields so intense that perturbation theory fails, (ii) the linear (and higher-order) regime, which yields the usual optical response and electronic transitions, and (iii) back to the ground-state, where the fluctuation-dissipation theorem produces *ground-state* approximations from TDDFT treatments of excitations.

A. Overview

This work focuses primarily on the linear response regime. Throughout, we emphasize the difference between small molecules (atoms, diatomics, etc.) and the larger molecules that are of greater practical interest, where TDDFT is often the only practical first-principles method. We use napthalene ($C_{10}H_8$) as an example to show how the selection of the basis set and of the XC functional affects excitation energies and oscillator strengths computed using TDDFT. Small molecules are somewhat exceptional because they usually exhibit high symmetry which prevents strong mixing of the KS states due to configuration interaction; also, basis set requirements are often exacerbated for small systems. Naphthalene is large enough to avoid these effects, yet reasonably accurate gas phase experiments and correlated wavefunction calculations are still available.

We use atomic units throughout ($e^2 = \hbar = m_e = 1$), so that all energies are in Hartrees (1 H$\simeq$27.2 eV$\simeq$627.5 kcal/mol) and distances in Bohr ($\simeq$0.529 Å) unless otherwise noted. For brevity, we drop comma's between arguments wherever the meaning is clear. In DFT and TDDFT, there is a confusing wealth of acronyms and abbreviations. Table I is designed to aid the readers navigation through this maze.

The content of this review is organized as follows. Sections II and III cover the basic formalism of the theory, that is needed to understand where it comes from, why it works, and where it can be expected to fail. Section IV is all about details of implementation, especially basis-set selection. On the other hand, section V is devoted to performance, and analyzing the sources of error in the basis-set limit. In section VI, we then look at a few atoms in microscopic detail: this is because we know the *exact* ground-state Kohn-Sham potential in such cases, and so can analyze TDDFT performance in great depth. Section VII is devoted to the many attempts to go beyond standard functional approximations, and especially discusses where such attempts are needed. The last substantial section, section VIII, covers topics outside the usual linear response approach to excitations, including ground-state functionals derived from TDDFT, challenges for strong fields, and transport through single molecules. Section IX is a summary.

TABLE I: Table of acronyms and abbreviations.

AC	Asymptotically corrected
ALDA	Adiabatic LDA
A	Adiabatic
B88	Becke GGA
B3LYP	Hybrid functional using Becke exchange and LYP correlation
CASPT2	Complete active space 2^{nd} order perturbation theory
CC	Coupled cluster
CIS	Configuration-interaction singlets
ee	electron-electron
ext	external
EXX	Exact exchange
GGA	Generalized gradient approximation
HK	Hohenberg-Kohn
H	Hartree
HXC	Hartree plus exchange-correlation
KS	Kohn-Sham
LB94	van Leeuwen-Baerends asymptotically corrected functional
LDA	Local density approximation
LSDA	Local spin density approximation
LHF	Localized Hartree-Fock (accurate approximation to EXX)
LYP	Lee-Yang-Parr correlation
MAE	Mean absolute error
OEP	Optimised effective potential
PBE	Perdew-Burke-Ernzerhof GGA
PBE0	Hybrid based on PBE
RG	Runge-Gross
RPA	Random phase approximation
SPA	Single pole approximation
TDKS	Time-dependent Kohn-Sham
XC	Exchange-correlation

II. GROUND-STATE REVIEW

In this section, we review ground state DFT rather quickly. For a more comprehensive review, we recommend [154]. Many of the results discussed here are referred to in later sections.

A. Formalism

Ground-state DFT is a completely different approach to solving the many-electron problem than the traditional solution of the Schrödinger equation. The Hohenberg-Kohn (HK) theorem[1] of 1964 states that for a given non-degenerate ground-state density $n(\mathbf{r})$ of Fermions with a given interaction, the external potential $v_{\text{ext}}(\mathbf{r})$ that produced it is unique (up to an additive constant). Hence if the density is known, then $v_{\text{ext}}(\mathbf{r})$ is known and so $\hat{H}$, the Hamiltonian, is known. From this and the number of particles (determined by the integral of the density), all properties of the system may be determined. In particular, the ground-state energy of the system E would be known. This is what we mean when we say these properties are functionals of the density, e.g., $E[n]$. It was later shown that this holds even for degenerate ground-states[4], and modern DFT calculations use an analogous theorem applied to the spin densities, $n_\alpha(\mathbf{r}), n_\beta(\mathbf{r})$. Where $\alpha, \beta = \pm\frac{1}{2}$ respectfully.

The total energy for N electrons consists of three parts: the kinetic energy $T[\Psi]$, the electron-electron interaction $V_{\rm ee}[\Psi]$, and the external potential energy $V_{\rm ext}[\Psi]$, each of which is defined below:

$$T[\Psi] = \langle\Psi| - \frac{1}{2}\sum_{i=1}^{N}\nabla_i^2|\Psi\rangle \ , \tag{1}$$

$$V_{\rm ee}[\Psi] = \langle\Psi|\frac{1}{2}\sum_{i}^{N}\sum_{j\neq i}^{N}\frac{1}{|\mathbf{r}_i-\mathbf{r}_j|}|\Psi\rangle \ , \tag{2}$$

$$V_{\rm ext}[\Psi] = \langle\Psi|\sum_{i}^{N}v_{\rm ext}(\mathbf{r}_i)|\Psi\rangle \ . \tag{3}$$

By the Rayleigh-Ritz principle:

$$\begin{aligned} E &= \min_{\Psi}\langle\Psi|\hat{H}|\Psi\rangle \\ &= \min_{\Psi}\left(T[\Psi]+V_{\rm ee}[\Psi]+V_{\rm ext}[\Psi]\right) \ . \end{aligned} \tag{4}$$

If we simply rewrite the minimization as a two step process[155]:

$$E = \min_{n_\alpha,n\beta}\left\{\min_{\Psi\to(n_\alpha,n_\beta)}\left(T[\Psi]+V_{\rm ee}[\Psi]+V_{\rm ext}[\Psi]\right)\right\},$$

where the inner search is over all interacting wavefunctions yielding spin densities n_α, n_β. We may pull the last term out of the inner minimization:

$$\begin{aligned} E &= \min_{n_\alpha,n_\beta}\left(F[n_\alpha,n_\beta]+\sum_\sigma\int\ d^3r\ v_{{\rm ext}\sigma}(\mathbf{r})\ n_\sigma(\mathbf{r})\right) \\ &= \min_{n_\alpha,n_\beta}\left(E[n_\alpha,n_\beta]\right) \ , \end{aligned} \tag{5}$$

where

$$F[n_\alpha,n_\beta] = \min_{\Psi\to(n_\alpha,n_\beta)}\left(T[\Psi]+V_{\rm ee}[\Psi]\right) \tag{6}$$

$$= T[n_\alpha,n_\beta]+V_{\rm ee}[n_\alpha,n_\beta] \ , \tag{7}$$

is a universal functional independent of $v_{{\rm ext}\sigma}(\mathbf{r})$.

Minimizing the total energy density functional, Eq. (5), for both spin densities by taking the functional derivative $\delta/\delta n_\sigma$, and using the Euler-Lagrange multiplier technique leads to the equation:

$$\frac{\delta F[n_\alpha,n_\beta]}{\delta n_\sigma}+v_{{\rm ext}\sigma}(\mathbf{r}) = \mu \ , \tag{8}$$

where μ is the chemical potential of the system.

Next we imagine a system of non-interacting electrons with the same spin densities. Applying the HK theorem to this non-interacting system, the potentials, $v_{{\rm S}\sigma}(\mathbf{r})$, that give densities $n_\sigma(\mathbf{r})$ as the ground-state spin densities for this system are unique. This is the fictitious Kohn-Sham (KS) system[2], and the fully interacting problem is mapped to a non-interacting one which gives the exact same density. Solving the KS equations, which is computationally simple (at least compared to the fully interacting problem which becomes intractable for large particle numbers), then yields the ground-state density. The KS equations are

$$\left(-\frac{1}{2}\nabla^2+v_{{\rm S}\sigma}(\mathbf{r})\right)\phi_{j\sigma}(\mathbf{r}) = \epsilon_{j\sigma}\phi_{j\sigma}(\mathbf{r}) \ , \tag{9}$$

with spin densites

$$n_\sigma(\mathbf{r}) = \sum_{j=1}^{N_\sigma}|\phi_{j\sigma}(\mathbf{r})|^2 \ , \tag{10}$$

where $v_{{\rm S}\alpha}$,$v_{{\rm S}\beta}$ are the KS potentials and N_σ is the number of spin σ electrons , $(N_\alpha+N_\beta=N)$.

In Fig 2, we plot the exact density for the He atom from a highly accurate wavefunction calculation, and below we plot the *exact* KS potential for this system. One can see that the KS potential is very different from the external potential. This is due to the fact that the KS single effective potential for the non-interacting system must give the correct interacting electron density. Because the coulomb repulsion between the electrons shields the nucleus, and makes the charge density decay less rapidly than $e^{-4\mathbf{r}}$, the KS potential is shallower than $v_{\rm ext}(\mathbf{r})$.

To derive an expression for $v_{{\rm S}\sigma}(\mathbf{r})$ we note that the Euler equation that yields the KS equations is:

$$\frac{\delta T_{\rm S}[n_\alpha,n_\beta]}{\delta n_\sigma}+v_{{\rm S}\sigma}(\mathbf{r}) = \mu \ . \tag{11}$$

Here $T_{\rm S}$ is the kinetic energy of the KS electrons,

$$T_{\rm S} = \sum_\sigma\sum_{j=1}^{N_\sigma}\int\ d^3r\ \frac{1}{2}|\nabla\phi_{j\sigma}(\mathbf{r})|^2 \ .$$

If we rewrite $F[n_\alpha,n_\beta]$ in terms of the KS system:

$$F[n_\alpha,n_\beta] = T_{\rm S}[n_\alpha,n_\beta]+U[n]+E_{\rm XC}[n_\alpha,n_\beta] \ , \tag{12}$$

where $U[n]$ is the Hartree energy, given by

$$U[n] = \frac{1}{2}\sum_{\sigma\sigma'}\int\ d^3rd^3r'\ \frac{n_\sigma(\mathbf{r})n_{\sigma'}(\mathbf{r}')}{|\mathbf{r}-\mathbf{r}'|} \ , \tag{13}$$

and the exchange-correlation (XC) energy is defined by Eq. (7) and Eq. (12):

$$E_{\rm XC}[n_\alpha,n_\beta] = T[n_\alpha,n_\beta]-T_{\rm S}[n_\alpha,n_\beta]+V_{\rm ee}[n_\alpha,n_\beta]-U[n] \ . \tag{14}$$

Inserting this into Eq. (8) and comparing to Eq. (11) gives a definition of the KS potential:

$$v_{{\rm S}\sigma}(\mathbf{r}) = v_{\rm ext}(\mathbf{r})+v_{\rm H}(\mathbf{r})+v_{{\rm XC}\sigma}(\mathbf{r}) \ , \tag{15}$$

where the Hartree potential is the functional derivative of $U[n]$:

$$v_{\rm H}(\mathbf{r}) = \frac{\delta U[n]}{\delta n(\mathbf{r})} = \sum_{\sigma'} \int d^3r' \, \frac{n_{\sigma'}(\mathbf{r}')}{|\mathbf{r}-\mathbf{r}'|} \, , \qquad (16)$$

while the XC potential is given by the functional derivative of the XC energy:

$$v_{{\rm XC}\sigma}(\mathbf{r}) = \frac{\delta E[n_\alpha, n_\beta]}{\delta n_\sigma(\mathbf{r})} \, . \qquad (17)$$

This then closes the relationship between the KS system and the original physical problem. Once $E_{\rm XC}[n_\alpha, n_\beta]$ is known exactly or approximated, $v_{{\rm XC}\sigma}(\mathbf{r})$ is determined by differentiation. The KS equations can be solved self-consistently for the spin densities and orbitals, and the total energy found by inserting these into the total energy functional $E = T_{\rm S} + U + E_{\rm XC} + V_{\rm ext}$. Unfortunately $E_{\rm XC}[n_\alpha, n_\beta]$ is not known exactly and must be approximated. There exists a *functional soup* of many different approximations of varying accuracy and computational cost. Many of these are discussed in Section II B.

In Fig 2, when the KS equation is solved with this exact potential, the HOMO level is at -24.592 eV. This is minus the ionization energy for Helium. In exact DFT, Koopman's theorem, which states $I = -\epsilon_{HOMO}$, is exactly true[157]. In ground-state DFT, this is the only energy level of the fictitious KS system that has an immediate physical interpretation.

Before leaving the ground-state review, we mention the optimized effective potential (OEP) method[158, 159]. Here the XC functional is written as a functional of the KS orbitals (which in turn are functionals of the density). The exchange energy is then given by the familiar HF definition.

$$E_{\rm X} = -\frac{1}{2} \sum_{i,j=1}^{N} \sum_{\sigma} \int d\mathbf{r} d\mathbf{r}' \, \frac{\phi^*_{i\sigma}(\mathbf{r}) \phi^*_{j\sigma}(\mathbf{r}') \phi_{j\sigma}(\mathbf{r}) \phi_{i\sigma}(\mathbf{r}')}{|\mathbf{r}-\mathbf{r}'|} \qquad (18)$$

However in contrast to HF, a single effective potential $v_{\rm S}^{\rm XX}(\mathbf{r})$ is found via the chain rule. Accurate orbital dependent functionals for the correlation energy are extremely difficult to find, so often only exchange is used. In DFT, this is called exact exchange (EXX), since exchange is usually only treated approximately. EXX gives useful features such as derivative discontinuities and the correct asymptotic decay of the KS potential[160]. As we will see in Section V B, these are important for TDDFT linear response.

B. Approximate Functionals

In any ground-state DFT calculation, we must use approximations for the functional dependence of the XC energy on the spin densities. There now exists a hierarchy of such approximations. The simplest of these is the local density approximation (LDA), where the XC energy at a point $\mathbf{r}'$ is calculated as if it were a uniform electron gas with the spin densities $n_\sigma = n_\sigma(\mathbf{r}')$ in a constant positive background. The exchange energy for the uniform gas can be deduced analytically, but the correlation contribution is found using a combination of many-body theory and highly accurate Monte Carlo simulations for the electron gas of different densities[161–164].

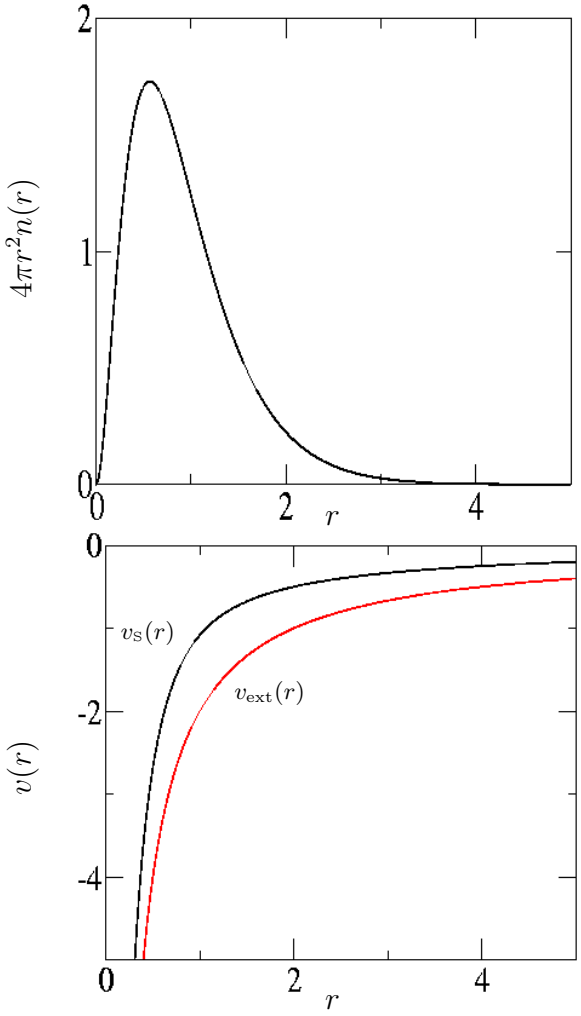

FIG. 2: Top panel – exact radial density for the He atom found via the QMC method[156]. Bottom panel – The external and KS potentials for the He atom. The KS potential is found by inverting the KS equations using the exact KS orbitals (easily found for He if exact density is known).

LDA works remarkably well, given the vast different between homogeneous electron gases and atoms or molecules. However total energies are generally underestimated. Typically the XC energy is underestimated by

about 7%. When the performance of LDA is examined carefully, this comes about via a nice (but not completely accidental) cancellation of errors between the exchange part (underestimated by about 10%) and correlation (overestimated by 200% − 300%), which is typically 4 times smaller than exchange.

An obvious improvement to LDA would be to include information about how rapidly the density is changing via its gradient. This leads to the generalized gradient approximation (GGA). In the original Kohn-Sham paper of 1965, the simplest of these was suggested. The gradient expansion approximation (GEA) is found by examining the slowly varying limit of the electron gas[2, 165]. However it was soon found that GEA failed to improve on the accuracy of LDA and sometimes made things worse. It was not until the late 80's that accurate GGA's were constructed. The most popular of these are BLYP (B88[5] for exchange and LYP[6] for correlation) and PBE[7]. These generally reduce atomization errors of LDA by a factor of $2-5$.

PBE is a functional designed to improve upon the performance of LDA without losing the features of LDA which are correct. As such it reduces to LDA for the uniform electron gas. A GGA should also satisfy as many exact conditions as possible, such as the Lieb-Oxford bound or the form of the exchange energy in the slowly varying limit of the electron gas. In this regard, PBE is a non-empirical functional where all parameters are determined by exact conditions. Because of its ability to treat bulk metals, it is the functional of choice in solid-state calculations and increasingly so in quantum chemistry. When choosing a GGA, using PBE or not PBE should no longer be a question. (Although the crambin calculation of the introduction used BP86, for reasons explained in [9].)

Finally, hybrid functionals mix in some fraction of exact exchange with a GGA. This is the Hartree-Fock exchange integral, Eq. (18), evaluated with the KS orbitals (which are functionals of the density). Only a small fraction of exact exchange ($20\% - 25\%$) is mixed in, in order to preserve the cancellation of errors which GGA's make use of[166]. The most widely used functional in chemistry is the hybrid function B3LYP, which contains 3 experimentally fitted parameters[6, 8, 167] (although the parameter in B88 has recently been derived [168]). Other hybrid functionals include PBE0, where 25% of exact exchange is mixed in with the PBE functional[169].

A less well-known feature to users of ground state DFT is that while their favourite approximations yield very good energies (and therefore structures, vibrations, thermochemistry, etc.) and rather good densities, they have poorly behaved potentials, at least far from nuclei. Figure 3 illustrates this for the He atom, showing the LDA potential compared to the exact KS potential. While the potential is generally good in the region $r < 2$, it decays much too fast far from the nucleus. The true KS potential falls off as $-1/r$ whereas LDA decays exponentially. Hence the KS eigenvalues and eigenvalues will be poor for the higher levels. To understand why poor potentials do not imply poor energies (and why these potentials are not as bad as they look), see Ref. [170]. But, as we shall see in section V, this has major consequences for TDDFT.

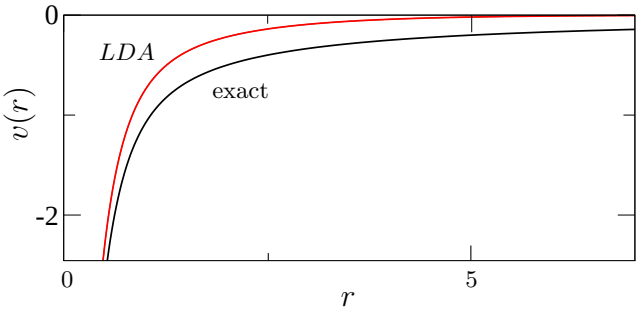

FIG. 3: Exact and LDA KS potentials for the He atom. While the exact potential falls off as $-1/r$, the LDA decays much too quickly. This is common for nearly all present functionals and has major consequences for TDDFT.

Over the past decade, the technology for treating orbital-dependent functionals has developed, and such functionals help cure this problem[158]. This is called the optimized effective potential (OEP)[171–173]. The first useful orbital functional was the self-interaction corrected LDA of Perdew and Zunger[162]. More generally, the OEP method can handle any orbital-dependent functional including treating exchange exactly. Orbital-dependent functionals naturally avoid the self-interaction error that is common in density functionals. An (almost) exact implementation of the OEP equations is localized Hartree-Fock (LHF)[174, 175], available in TURBOMOLE[10].

C. Basis Sets

To actually solve the KS equations, the KS orbitals $\phi_{p\sigma}(\mathbf{r})$ are expanded in a *finite* set of basis functions $\chi_\nu(\mathbf{r})$,

$$\phi_{p\sigma}(\mathbf{r}t) = \sum_\nu C_{p\nu\sigma}\ \chi_\nu(\mathbf{r}). \tag{19}$$

The most common choice by far for the basis functions in quantum chemistry are atom-centered contracted Cartesian Gaussians[176],

$$\chi_\nu(\mathbf{r}) = \sum_i c_{i\nu} x^{l_x(\nu)} y^{l_y(\nu)} z^{l_z(\nu)} e^{-\zeta_{i\nu}(\mathbf{r}-\mathbf{R}_\nu)^2}. \tag{20}$$

$l_x(\nu)$, $l_y(\nu)$, and $l_z(\nu)$ are positive integers or zero, and $l(\nu) = l_x(\nu) + l_y(\nu) + l_z(\nu)$ is somewhat loosely called l-quantum number of χ_ν. ($l = 0, 1, 2, 3, \ldots$ corresponds to

TABLE II: Single-point calculations using PBE functional for the reaction energy for naphthalene combustion using PBE/TZVP/RI geometries. Reference value computed using standard enthalpies of formation(from NIST[178]) using thermal and ZVPE corrections at the PBE/TZVP/RI level.

Basis set	Negative reaction energy (kcal/mol)
SV	916.8
SV(P)	1060.0
6-31G*	1047.1
SVP	1108.6
aug-SV(P)	1115.5
TZVP	1124.5
TZVPP	1131.2
cc-pVTZ	1129.0
aug-TZVP	1130.2
aug-TZVP/RI	1130.2
QZVP	1140.3
Reference Value	1216.3

$s, p, d, f, \ldots$ type Cartesian Gaussians.) The exponents $\zeta_{i\mu}$ and the contraction coefficients $c_{i\nu}$ are optimized in atomic calculations. Other common basis functions in use are Slater type orbitals, plane waves, or piecewise defined functions on a numerical grid.

The approximation of the orbitals $\phi_{p\sigma}(\mathbf{r})$ by a finite linear combination of basis functions (also called LCAO, linear combination of atomic orbitals), Eq. (19), leads to a finite number of MOs. Thus, the KS equations and all derived equations are approximated by *finite*-dimensional matrix equations. These equations can be treated by established numerical linear and non-linear algebra methods. When the basis set size is systematically increased, the computed properties converge to their basis set limit.

In a finite basis set, all operators become finite matrices; the matrix elements are integrals, e.g.,

$$H_{\mu\nu\sigma}[n] = \int d^3r\, \chi_\mu(\mathbf{r}) H_\sigma[n] \chi_\nu(\mathbf{r}). \tag{21}$$

The calculation and processing of such integrals is the main effort in virtually all DFT calculations. Gaussian basis functions have the distinct advantage that most integrals can be evaluated analytically, and that they are spatially local. The latter implies that many integrals vanish and need not be calculated. Whether a certain integral vanishes or not can be decided in advance by so-called pre-screening techniques[177].

To illustrate the effect of choosing various basis sets, we show in Fig. II, the reaction energy for naphthalene combustion in the gas phase:

$$C_{10}H_8 + 12O_2 \rightarrow 10CO_2 + 4H_2O \tag{22}$$

The basis sets are listed in order of increasing size, and are well-know in quantum chemistry (and are described in detail in section IV). We see that hydrogen polarization functions (basis sets ending in P) are important, because C-H bonds are broken and O-H bonds are formed. Augmentation (aug-) with diffuse functions somewhat improves the smaller basis-set results, but is not economical in this case. Using the resolution of the identity for the Coulomb operator (RI) saves computational time, with no loss of accuracy. Reasonable results are found with SVP, but convergence improves all the way to TZVP. We can see after the TZVPP result, the basis set error is below the functional error and the result is effectively converged. We have reached the stage where adding more orbitals, which increases the computational cost, is no longer going to drastically improve the result. (On the other hand, the crambin calculation mentioned in the introduction is very large and so only an SV(P) basis set could be used).

On first impression, comparison to the reference value indicates quite a large error, ΔE= 76 kcal/mol. However, given that 48 electron pair bonds are broken and formed, the error per carbon atom, 7.6 kcal/mol, is typical for this functional.

III. TIME-DEPENDENT THEORY

In this section, we introduce all the basis elements of TDDFT, and how it differs from the ground-state case.

A. Runge-Gross theorem

The analog of the Hohenberg-Kohn theorem for time-dependent problems is the Runge-Gross theorem[16], which we state here. Consider N non-relativistic electrons, mutually interacting via the Coulomb repulsion, in a time-dependent external potential. The Runge-Gross theorem states that the densities $n(\mathbf{r}t)$ and $n'(\mathbf{r}t)$ evolving from a common initial state $\Psi_0 = \Psi(t=0)$ under the influence of two external potentials $v_{\rm ext}(\mathbf{r}t)$ and $v'_{\rm ext}(\mathbf{r}t)$ (both Taylor expandable about the initial time 0) are always different provided that the potentials differ by more than a purely time-dependent ($\mathbf{r}$-independent) function:

$$\Delta v_{\rm ext}(\mathbf{r}t) \neq c(t)\ , \tag{23}$$

where

$$\Delta v_{\rm ext}(\mathbf{r}t) = v_{\rm ext}(\mathbf{r}t) - v'_{\rm ext}(\mathbf{r}t)\ . \tag{24}$$

Thus there is a one-to-one mapping between densities and potentials, and we say that the time-dependent potential is a functional of the time-dependent density (and the initial state).

The theorem was proven in two distinct parts. In the first (RGI), one shows that the corresponding current densities differ. The current density is given by

$$\mathbf{j}(\mathbf{r}t) = \langle\Psi(t)|\ \hat{\mathbf{j}}(\mathbf{r})\ |\Psi(t)\rangle \tag{25}$$

where

$$\hat{\mathbf{j}}(\mathbf{r}) = \frac{1}{2i}\sum_{j=1}^{N}(\nabla_j\delta(\mathbf{r}-\mathbf{r}_j)+\delta(\mathbf{r}-\mathbf{r}_j)\nabla_j) \tag{26}$$

is the current density operator. The equation of motion for the difference of the two current densities gives[16]:

$$\left.\frac{\partial\Delta j(\mathbf{r}t)}{\partial t}\right|_{t=0} = -n_0(\mathbf{r})\nabla\Delta v_{\rm ext}(\mathbf{r},0) \tag{27}$$

If the Taylor-expansion about $t=0$ of the difference of the two potentials is not spatially uniform for some order, then the Taylor-expansion of the current density difference will be non-zero at a finite order. This establishes that the external potential is a functional of the current density, $v_{\rm ext}[\,\mathbf{j},\Psi_0](\mathbf{r},t)$.

In the second part of the theorem (RGII), continuity is used:

$$\frac{\partial n(\mathbf{r}t)}{\partial t} = -\nabla\cdot\mathbf{j}(\mathbf{r}t) \tag{28}$$

which leads to:

$$\left.\frac{\partial^2\Delta n(\mathbf{r}t)}{\partial t^2}\right|_{t=0} = \nabla\cdot(n_0(\mathbf{r})\nabla\Delta v_{\rm ext}(\mathbf{r},0)) \tag{29}$$

Now, suppose $\Delta v_{\rm ext}(\mathbf{r},0)$ is not uniform everywhere. Might not the left-hand-side still vanish? Apparently not, for real systems, because it is easy to show[179]:

$$\begin{aligned}\int d^3r\ \ &\Delta v_{\rm ext}(\mathbf{r},0)\nabla\cdot(n_0(\mathbf{r})\nabla\Delta v_{\rm ext}(\mathbf{r},0)) \\ = &\int d^3r\ \ [\nabla\cdot(\Delta v_{\rm ext}(\mathbf{r},0)n_0(\mathbf{r})\nabla\Delta v_{\rm ext}(\mathbf{r},0)) \\ &-n_0|\nabla\Delta v_{\rm ext}(\mathbf{r},0)|^2\ ]\end{aligned} \tag{30}$$

Using Green's theorem, the first term on the right vanishes for physically realistic potentials (i. e., potentials arising from normalizable external charge densities), because for such potentials, $\Delta v_{\rm ext}(\mathbf{r})$ falls off at least as $1/r$. But the second term is definitely negative, so if $\Delta v_{\rm ext}(\mathbf{r},0)$ is non-uniform, the integral must be finite, causing the densities to differ in 2nd order in t. This argument applies to each order and the densities $n(\mathbf{r},t)$ and $n'(\mathbf{r},t)$ will become different infinitesimally later than t. Thus, by imposing this boundary conditions, we have shown that $v_{\rm ext}[n,\Psi_0](\mathbf{r}t)$.

Notes:

- The difference between $n(\mathbf{r}t)$ and $n'(\mathbf{r}t)$ is non-vanishing already in first order of $\Delta v_{\rm ext}(\mathbf{r}t)$, ensuring the invertibility of the linear response operators of section III C.
- Since the density determines the potential up to a time-dependent constant, the wavefunction is in turn determined up to a time-dependent phase, which cancels out of the expectation value of any operator.
- We write

  $$v_{\rm ext}[n;\Psi_0](\mathbf{r}t)$$

  because it depends on both the history of the density and the initial wavefunction. This functional is a very complex one, much more so than the ground-state case. Knowledge of it implies solution of all time-dependent Coulomb interacting problems.
- If we always begin in a non-degenerate ground-state[180, 181], the initial-state dependence can be subsumed by the Hohenberg-Kohn theorem[1], and then $v_{\rm ext}(\mathbf{r}t)$ is a functional of $n(\mathbf{r}t)$ alone:

  $$v_{\rm ext}[n](\mathbf{r}t)$$

- A spin-dependent generalization exists, so that $v_{\rm ext}(\mathbf{r}t)$ will be a functional of the spin densities n_α, n_β[182].

B. Kohn-Sham equations

Once we have a proof that the potential is a functional of the time-dependent density, it is simple to write the TD Kohn-Sham (TDKS) equations as

$$i\frac{\partial\phi_{j\sigma}(\mathbf{r}t)}{\partial t} = \left(-\frac{\nabla^2}{2}+v_{{\rm S}\sigma}[n](\mathbf{r}t)\right)\phi_{j\sigma}(\mathbf{r}t) \quad , \tag{31}$$

whose potential is uniquely chosen (via the RG theorem) to reproduce the exact spin densities:

$$n_\sigma(\mathbf{r}t) = \sum_{j=1}^{N_\sigma}|\phi_{j\sigma}(\mathbf{r}t)|^2\ , \tag{32}$$

of the interacting system. We *define* the exchange-correlation potential via

$$v_{{\rm S}\sigma}(\mathbf{r}t) = v_{{\rm ext}\sigma}(\mathbf{r}t)+\int d^3r'\ \frac{n(\mathbf{r}'t)}{|\mathbf{r}-\mathbf{r}'|}+v_{{\rm XC}\sigma}(\mathbf{r}t)\ , \tag{33}$$

where the second term is the familiar Hartree potential.

Notes:

- The exchange-correlation potential, $v_{{\rm XC}\sigma}(\mathbf{r}t)$, is in general a functional of the entire history of the densities, $n_\sigma(\mathbf{r}t)$, the initial interacting wavefunction $\Psi(0)$, and the initial Kohn-Sham wavefunction, $\Phi(0)$[181]. But if both the KS and interacting initial wavefunctions are non-degenerate ground-states, it becomes a simple functional of $n_\sigma(\mathbf{r}t)$ alone.
- By inverting the single doubly-occupied KS equation for a spin-unpolarized two-electron system, it is quite straightforward (but technically demanding) to find the TDKS potential from an exact time-dependent density, and has been done several times[183–185].

- In practical calculations, some approximation is used for $v_{\rm XC}(\mathbf{r}t)$ as a functional of the density, and so modifications of traditional TDSE schemes are needed for the propagation[186].

- Unlike the ground-state case, there is no self-consistency, merely forward propagation in time, of a density dependent Hamiltonian.

- Again, contrary to the ground-state, there is no central role played by a single-number functional, such as the ground-state energy. In fact, an action was written down in the RG paper, but extremizing it was later shown not to yield the TDKS equations[187].

C. Linear response

The most common application is the response to a weak long-wavevlength optical field,

$$\delta v_{\rm ext}(\mathbf{r}t) = -\xi \exp(i\omega t)\mathbf{z} \ . \tag{34}$$

In the general case of the response of the ground-state to an arbitrary weak external field, the system's first-order response is characterized by the non-local susceptibility

$$\delta n_\sigma(\mathbf{r}t) = \sum_{\sigma'} \int dt' \int d^3r' \chi_{\sigma\sigma'}[n_0](\mathbf{r},\mathbf{r}';t{-}t')\ \delta v_{{\rm ext}\sigma'}(\mathbf{r}'t'). \tag{35}$$

This susceptibility χ is a functional of the *ground-state* density, $n_0(\mathbf{r})$. A similar equation describes the density response in the KS system:

$$\delta n_\sigma(\mathbf{r}t) = \sum_{\sigma'} \int dt' \int d^3r' \chi_{{\rm S}\sigma\sigma'}[n_0](\mathbf{r},\mathbf{r}';t{-}t')\ \delta v_{{\rm S}\sigma'}(\mathbf{r}'t'). \tag{36}$$

Here $\chi_{\rm S}$ is the *Kohn-Sham* response function, constructed from KS energies and orbitals:

$$\chi_{{\rm S}\sigma\sigma'}(\mathbf{r}\mathbf{r}'\omega) = \delta_{\sigma\sigma'} \sum_q \left\{ \frac{\Phi_{q\sigma}(\mathbf{r})\ \Phi^*_{q\sigma'}(\mathbf{r}')}{\omega-\omega_q+i0_+} - \frac{\Phi^*_{q\sigma}(\mathbf{r})\ \Phi_{q\sigma'}(\mathbf{r}')}{\omega+\omega_q-i0_+} \right\} \tag{37}$$

where q is a double index, representing a transition from occupied KS orbital i to unoccupied KS orbital a, $\omega_{q\sigma} = \epsilon_{a\sigma} - \epsilon_{i\sigma}$, and $\Phi_{q\sigma}(\mathbf{r}) = \phi^*_{i\sigma}(\mathbf{r})\phi_{a\sigma}(\mathbf{r})$. 0_+ means the limit as 0_+ goes to zero from above (i.e., along the positive real axis). Thus $\chi_{\rm S}$ is completely determined by the ground-state KS potential. It is the susceptibility of the non-interacting electrons sitting in the KS ground-state potential.

To relate the KS response to the true response, we examine how the KS potential in Eq. (33) changes:

$$\delta v_{{\rm S}\sigma}(\mathbf{r},t) = \delta v_{{\rm ext}\sigma}(\mathbf{r},t) + \delta v_{{\rm HXC}\sigma}(\mathbf{r}t) \ . \tag{38}$$

Since $\delta v_{{\rm HXC}\sigma}(\mathbf{r}t)$ is due to an infinitesimal change in the density, it may be written in terms of its functional derivative, i.e.,

$$\delta v_{{\rm HXC}\sigma}(\mathbf{r}t) = \sum_{\sigma'} \int d^3r' \int dt'\ f_{{\rm HXC}\sigma\sigma'}(\mathbf{r}\mathbf{r}', t{-}t')\ \delta n_{\sigma'}(\mathbf{r}'t') \ , \tag{39}$$

where

$$f_{{\rm HXC}\sigma\sigma'}[n_0](\mathbf{r}\mathbf{r}', t-t') = \left.\frac{\delta v_{{\rm HXC}\sigma}(\mathbf{r}t)}{\delta n_{\sigma'}(\mathbf{r}'t')}\right|_{n_0} . \tag{40}$$

The Hartree contribution is found by differentiating Eq. (16):

$$\begin{aligned} f_{\rm H}[n_0](\mathbf{r}\mathbf{r}', t-t') &= \frac{\delta v_{\rm H}(\mathbf{r}t)}{\delta n_{\sigma'}(\mathbf{r}'t')} \\ &= \frac{\delta(t-t')}{|\mathbf{r}-\mathbf{r}'|} \end{aligned} \tag{41}$$

while the remainder $f_{{\rm XC}\sigma\sigma'}[n_0](\mathbf{r}\mathbf{r}', t-t')$ is known as the XC kernel.

By the definition of the KS potential, $\delta n_\sigma(\mathbf{r}t)$ is the same in both Eq. (35) and Eq. (36). We can then insert Eq. (39) into Eq. (36), equate with Eq. (35) and solve for a general relation for any $\delta n_\sigma(\mathbf{r}t)$. After Fourier transforming in time, the central equation of TDDFT linear response[188] is a Dyson-like equation for the true χ of the system:

$$\begin{aligned} \chi_{\sigma\sigma'}(\mathbf{r}\mathbf{r}'\omega) \ &= \ \chi_{{\rm S}\sigma\sigma'}(\mathbf{r}\mathbf{r}'\omega) + \sum_{\sigma_1\sigma_2} \int d^3r_1 \int d^3r_2\ \chi_{{\rm S}\sigma\sigma_1}(\mathbf{r}\mathbf{r}_1\omega) \\ &\times \ \left(\frac{1}{|\mathbf{r}_1-\mathbf{r}_2|} + f_{{\rm XC}\sigma_1\sigma_2}(\mathbf{r}_1\mathbf{r}_2\omega) \right) \chi_{\sigma_2\sigma'}(\mathbf{r}_2\mathbf{r}'\omega), \end{aligned} \tag{42}$$

Notes:

- The XC kernel is a much simpler quantity than $v_{{\rm XC}\sigma}[n](\mathbf{r}t)$, since the kernel is a functional of only the ground-state density.

- The kernel is non-local in both space and time. The non-locality in time manifests itself as a frequency dependence in the Fourier transform, $f_{{\rm XC}\sigma\sigma'}(\mathbf{r}\mathbf{r}'\omega)$.

- If $f_{\rm XC}$ is set to zero in Eq. (42), physicists call it the Random Phase Approximation (RPA). The inclusion of $f_{\rm XC}$ is an exactification of RPA, in the same way the inclusion of $v_{\rm XC}(\mathbf{r})$ in ground-state DFT was an exactification of Hartree theory.

- The Hartree kernel is instantaneous, i.e., local in time, i.e., has no memory, i.e., given exactly by an adiabatic approximation, i.e., is frequency independent.

- The frequency-dependent kernel is a very sophisticated object, since its frequency-dependence makes the solution of an RPA-type equation yield the exact χ (including all vertex corrections at every higher order term). It defies physical intuition and arguments based on the structure of the TDDFT equations are at best misleading. If any argument cannot be given in terms of many-body quantum mechanics, Eq. (42) cannot help.
- The kernel is, in general, complex, with real and imaginary parts related via Kramers-Kronig[189].

Next, Casida[190] used ancient RPA technology, to produce equations in which the poles of χ are found as the solution to an eigenvalue problem. The key is to expand in the basis of KS transitions. We write $\delta n_\sigma(\mathbf{r}t)$ as:

$$\delta n_\sigma(\mathbf{r}\omega) = \sum_q \left(P_{q\sigma}(\omega)\Phi^*_{q\sigma}(\mathbf{r}) + P_{\bar{q}\sigma}(\omega)\Phi_{q\sigma}(\mathbf{r}) \right) \quad (43)$$

where $\bar{q} = (a,i)$ if $q = (i,a)$. This representation is used to solve Eq. (36) self-consistently using Eq. (39), and yields two coupled matrix equations[191]:

$$\left[\begin{pmatrix} \mathbf{A} & \mathbf{B} \\ \mathbf{B}^* & \mathbf{A}^* \end{pmatrix} - \omega \begin{pmatrix} -\mathbb{1} & 0 \\ 0 & \mathbb{1} \end{pmatrix} \right] \begin{pmatrix} \mathbf{X} \\ \mathbf{Y} \end{pmatrix} = - \begin{pmatrix} \delta\mathbf{v} \\ \delta\mathbf{v}^* \end{pmatrix} \quad (44)$$

where $A_{q\sigma q'\sigma'} = \delta_{qq'}\delta_{\sigma\sigma'}\omega_{q\sigma} + K_{q\sigma q'\sigma'}$, $B_{q\sigma q'\sigma'} = K_{q\sigma q'\sigma'}$, $X_{q\sigma} = P_{q\sigma}$, $Y_{q\sigma} = P_{\bar{q}\sigma}$ and

$$K_{q\sigma q'\sigma'}(\omega) = \int d\mathbf{r} \int d\mathbf{r}' \; \Phi_{q\sigma}(\mathbf{r}) \; f_{\mathrm{HXC}\sigma\sigma'}(\mathbf{r}\mathbf{r}'\omega) \; \Phi^*_{q'\sigma'}(\mathbf{r}') \; , \quad (45)$$

with

$$\delta v_{q\sigma}(\omega) = \int d\mathbf{r} \; \Phi_{q\sigma}(\mathbf{r}) \; \delta v_{\mathrm{ext}}(\mathbf{r}\omega) \; . \quad (46)$$

At an excitation energy, $\delta v = 0$ and choosing real KS orbitals and since $(\mathbf{A} - \mathbf{B})$ is positive definite, we get:

$$\sum_{q'\sigma'} \tilde{\Omega}_{q\sigma q'\sigma'}(\omega) \; \vec{a}_{q'\sigma'} = \omega^2 \; \vec{a}_{q\sigma}, \quad (47)$$

where

$$\tilde{\Omega} = (\mathbf{A} - \mathbf{B})^{1/2}(\mathbf{A} + \mathbf{B})(\mathbf{A} - \mathbf{B})^{1/2} \; ,$$

or

$$\tilde{\Omega}_{q\sigma q'\sigma'}(\omega) = \omega^2_{q\sigma}\delta_{qq'}\delta_{\sigma\sigma'} + 2\sqrt{\omega_{q\sigma}\omega_{q'\sigma'}}K_{q\sigma q'\sigma'} \; . \quad (48)$$

Oscillator strengths f_q may be calculated[190] from the normalized eigenvectors using

$$f_{q\sigma} = \frac{2}{3}\left(|\vec{x}^T\mathbf{S}^{-1/2}\vec{a}_q|^2 + |\vec{y}^T\mathbf{S}^{-1/2}\vec{a}_q|^2 + |\vec{z}^T\mathbf{S}^{-1/2}\vec{a}_q|^2 \right) , \quad (49)$$

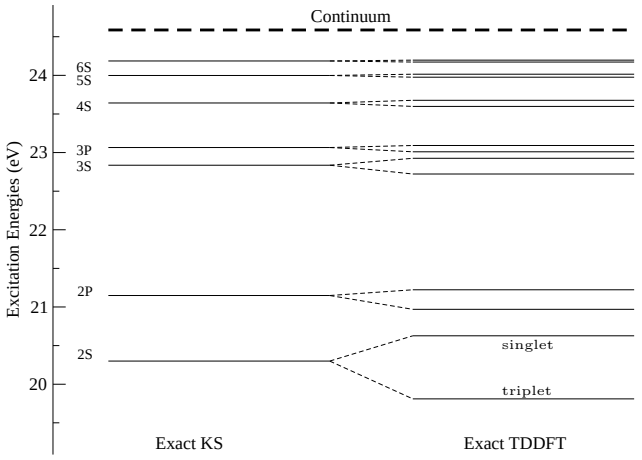

FIG. 4: Transitions for the Helium atom using in ground-state DFT on the left, and TDDFT on the right. In both cases, the exact functionals have been used. The results for employing the exact XC kernel in TDDFT linear response are known from calculations using Ref. [192]. In each pair of lines on the right, the triplet is the lower.

where

$$S_{qq'} = \delta_{qq'}\delta_{\sigma\sigma'}/w_{q'} \; .$$

Figure 4 shows the results of *exact* DFT calculations for the He atom. On the left, we consider just transitions between the exact ground-state KS occupied (1s) to unoccupied orbitals. These are *not* the true excitations of the system, nor are they supposed to be. However, applying TDDFT linear response theory, using the exact kernel on the exact orbitals, yields the exact excitations of the He atom. Spin-decomposing produces both singlet and triplet excitations.

D. Approximations

As in the ground-state case, while all the equations above are formally exact, a practical TDDFT calculation requires an approximation for the unknown XC potential. The most common approximation in TDDFT is the *adiabatic* approximation, in which

$$v^{\mathrm{adia}}_{\mathrm{XC}\sigma}[n](\mathbf{r}t) = v^{\mathrm{gs}}_{\mathrm{XC}\sigma}[n_0](\mathbf{r})|_{n_{0\sigma}(\mathbf{r})=n_\sigma(\mathbf{r}t)}, \quad (50)$$

i.e., the XC potential at any time is simply the ground-state XC potential at that instant. This obviously becomes exact for sufficiently slow perturbations in time, in which the system always stays in its instantaneous ground-state. Most applications, however, are not in this slowly varying regime. Nevertheless, results obtained within the adiabatic approximation are remarkably accurate in many cases.

Any ground-state approximation (LDA, GGA, hybrid) automatically provides an adiabatic approximation for use in TDDFT. The most famous is the adiabatic local density approximation (ALDA). It employs the functional form of the static LDA with a time-dependent density:

$$v_{\mathrm{XC}\sigma}^{\mathrm{ALDA}}[n](\mathbf{r}t) = v_{\mathrm{XC}}^{\mathrm{unif}}(n_\alpha(\mathbf{r}t), n_\beta(\mathbf{r}t)) = \left.\frac{de_{\mathrm{XC}}^{\mathrm{unif}}}{dn_\sigma}\right|_{n_\sigma = n_\sigma(\mathbf{r}t)}. \tag{51}$$

Here $e_{\mathrm{XC}}^{\mathrm{unif}}(n_\alpha, n_\beta)$ is the accurately known exchange-correlation energy density of the uniform electron gas of spin densities $n_\uparrow, n_\downarrow$. For the time-dependent exchange-correlation kernel of Eq. (40), Eq. (51) leads to

$$f_{\mathrm{XC}\sigma\sigma'}^{\mathrm{ALDA}}[n_0](\mathbf{r}t, \mathbf{r}t') = \delta^{(3)}(\mathbf{r}-\mathbf{r}')\,\delta(t-t')\left.\frac{d^2 e_{\mathrm{XC}}^{\mathrm{unif}}}{dn_\sigma dn_{\sigma'}}\right|_{n_\sigma = n_{0\sigma}(\mathbf{r})}. \tag{52}$$

The time Fourier-transform of the kernel has no frequency-dependence at all in any adiabatic approximation. Via a Kramers-Kronig relation, this implies that it is purely real[189].

Thus, any TDDFT linear response calculation can be considered as occuring in two steps:

1. An approximate ground-state DFT calculation is done, and a self-consistent KS potential found. Transitions from occupied to unoccupied KS orbitals provide zero-order approximations to the optical excitations.

2. An approximate TDDFT linear response calculation is done on the orbitals of the ground-state calculation. This corrects the KS transitions into the true optical transitions.

In practice both these steps have errors built into them.

IV. IMPLEMENTATION AND BASIS SETS

In this section we discuss how TDDFT is implemented numerically. TDDFT has the ability to calculate many different quantities and different techniques are sometimes favored for each type. For some purposes, e.g., if strong fields are present, it can be better to propagate forward in time the KS orbitals using a real space grid[193, 194] or with plane waves[195]. For finite-order response, Fourier transforming to frequency space with localized basis functions may be preferable[196]. Below, we discuss in detail how this approach works, emphasizing the importance of basis-set convergence.

A. Density matrix approach

Instead of using orbitals, we can write the dynamics of the TDKS systems in terms of the one-particle density matrix $\gamma_\sigma(\mathbf{r}\mathbf{r}'t)$ of the TDKS determinant. $\gamma_\sigma(\mathbf{r}\mathbf{r}'t)$ has the spectral representation

$$\gamma_\sigma(\mathbf{r}\mathbf{r}'t) = \sum_{j=1}^{N} \phi_{j\sigma}(\mathbf{r}t)\phi_{j\sigma}^*(\mathbf{r}'t), \tag{53}$$

i.e., the N_σ TDKS orbitals are the eigenfunctions of γ_σ. The eigenvalue of all TDKS orbitals, which is their *occupation number*, is always 1, which reflects the fact that the TDKS system is non-interacting. Equivalently, γ_σ satisfies the idempotency constraint

$$\gamma_\sigma(\mathbf{r}\mathbf{r}'t) = \int dx_1 \gamma_\sigma(\mathbf{r}\mathbf{r}_1 t)\gamma_\sigma(\mathbf{r}_1\mathbf{r}'t). \tag{54}$$

The normalization of the TDKS orbitals implies that the trace of γ_σ be N_σ.

Using the TDKS equations (31), one finds that the time-evolution of γ_σ is governed by the von-Neumann equation

$$i\frac{\partial}{\partial t}\gamma_\sigma(t) = \big[H_\sigma[n](t), \gamma_\sigma(t)\big], \tag{55}$$

where $H_\sigma[n](\mathbf{r}t) = -\nabla^2/2 + v_{s\sigma}[n](\mathbf{r}t)$ is the TDKS one-particle Hamiltonian. Although γ_σ has no direct physical meaning, it provides the interacting density and current density: The density is simply

$$n_\sigma(\mathbf{r}t) = \gamma_\sigma(\mathbf{r}\mathbf{r}t), \tag{56}$$

and the current density can be obtained from

$$\mathbf{j}_\sigma(\mathbf{r}t) = \left.\frac{1}{2i}\big(\nabla_{\mathbf{r}} - \nabla_{\mathbf{r}'}\big)\gamma_\sigma(\mathbf{r}\mathbf{r}'t)\right|_{\mathbf{r}'=\mathbf{r}}. \tag{57}$$

Thus, one can either propagate the TDKS orbitals using the TDKS equations (31), or equivalently one can propagate the TDKS one-particle density matrix γ_σ using the von-Neumann equation (55), subject to the idempotency contstraint (54) and normalized to N_σ.

In practice, it is often preferable to use γ_σ instead of the TDKS orbitals. γ_σ is unique (up to a gauge transformation), while the orbitals can be mixed arbitrarily by unitary transformations. Both n_σ and $\mathbf{j}_\sigma$ are linear in γ_σ, while they are quadratic in the orbitals; also, the TDKS equations are inhomogeneous in the orbitals due to the density dependence of H_σ, while they are homogeneous in γ_σ. A response theory based on the TDKS density matrix is therefore considerably simpler than one based on the orbitals. Finally, the use of γ_σ is computationally more efficient than using orbitals[196].

B. Basis Sets

In response theory, the basis functions $\chi_\nu(\mathbf{r})$ are usually chosen to be time-independent; for strong fields or coupled electron-nuclear dynamics, time-dependent basis functions can be more appropriate.

C. Naphthalene converged

Table III shows the basis set convergence of the first six singlet excitation energies of naphthalene computed using the PBE XC functional; the corresponding oscillator strengths for some of the transitions are also given. Similar basis-set convergence studies on small model systems should precede applications to large systems. In practice, the systems and states of interest, the target accuracy, the methods used, and the computational resources available will determine which basis set is appropriate.

With a model small molecule, we can find the basis-set convergence limit of a method. Both excitation energies and oscillator strengths are essentially converged within the aug-QZVP basis set. QZVP stands for a quadruple zeta valence basis set with polarization functions[199], and the prefix aug- denotes additional diffuse functions on non-hydrogen atoms, which were taken from Dunning's aug-cc-pVQZ basis set[200]. For C and H, this corresponds to $[8s5p4d3f2g]$ and $[4s3p2d1f]$, respectively, where the numbers in brackets denote shells of contracted Gaussian type orbitals (CGTOs), as usual. We will take the aug-QZVP results as a reference to assess the effect of smaller basis sets.

D. Double zeta basis sets

The smallest basis in Table III is of split valence (SV) or double zeta valence quality[201], without polarization functions. This basis set consists of two CGTOs per valence orbital and one per core orbital, i.e. $[3s2p]$ for C and $[2s]$ for H. Another popular double zeta valence basis set is 6-31G [202]. The SV basis set can be used to obtain a very rough qualitative description of the lowest valence excited states only, e.g. $1\ ^1B_{3u}$ and $1\ ^1B_{2u}$. Higher and diffuse excitations, such as $1\ ^1A_u$, are much too high in energy or can be missed completely in the spectrum. Since unpolarized basis sets also give poor results for other properties such as bond lengths and energies, their use is generally discuraged nowadays.

E. Polarization functions

By adding a single set of polarization functions to non-hydrogen atoms, the SV results for valence excitations can be considerably improved, at still moderate computational cost. The resulting basis set is termed SV(P) and consists of $[3s2p1d]$ for C and $[2s]$ for H[201]. The basis set errors in the first two valence excitation energies is reduced by about 50%. There is also a dramatic improvement in the oscillator strength of the dipole allowed transitions. This is expected from the limiting case of a single atom, where the first dipole allowed transition from a valence shell of l quantum number l_v generally involves orbitals with l-quantum number $l_v + 1$. Basis sets of SV(P) or similar quality are often the first choice for TDDFT applications to large systems, especially if only the lowest states are of interest and/or diffuse excitations are quenched, e.g. due to a polar environment. The popular 6-31G* basis set [202, 203] has essentially the same size as SV(P) but performs slightly poorer in our example.

Adding a single set of p type polarization functions to hydrogen atoms produces the SVP basis set[201]. These functions mainly describe C-H σ^* type excitation in molecules which usually occur in the far UV and are rarely studied in applications. In our example, going from SV(P) to SVP has no significant effect. This may be different for molecules containing strongly polarized hydrogen-element or hydrogen bridge bonds.

Next, aug-SV(P) is an SV(P) basis set augmented by a $[1s1p1d]$ set of primitive Gaussians with small exponents (from Dunning's aug-cc-pVDZ [200]), often called "diffuse functions". As shown in Table III, the effect of diffuse augmentation is a moderate downshift of less than 0.1 eV for the first two singlet excitation energies. This behavior is typical of lower valence excited states having a similar extent as the ground-state. Our example also shows that diffuse functions can have a significant effect on higher excitations. An extreme case is the $1\ ^1A_u$ state which is an excitation into the $10au$ orbital having the character of a $3s$ Rydberg state (of the entire molecule). The excitation energy of this state is lowered by more than 1 eV upon diffuse augmentation.

While polarization functions are necessary for a qualitatively correct description of transition dipole moments, additional diffuse polarization functions can account for radial nodes in the first-order KS orbitals, which further improves computed transition moments and oscillator strengths. These benefits have to be contrasted with a significant increase of the computational cost: In our example, using the aug-SV(P) basis increases the computation time by about a factor of 4. In molecules with more than 30-40 atoms, most excitations of interest are valence excitations, and the use of diffuse augmentation may become prohibitively expensive because the large extent of these functions confounds integral prescreening.

F. Triple zeta basis sets

In such cases, triple zeta valence (TZV) basis sets can be a better alternative. The TZVP (def-2-TZVP, Ref. [204]) basis set corresponds to $[5s3p2d1f]$ on C and $[3s1p]$ on H. It provides a description of the valence electrons that is quite accurate for many purposes when density functionals are used. At the same time, there is a second set of polarization functions on non-hydrogen atoms. The excitation energies of valence states are essentially converged in this basis set, see Table III. However, diffuse states are too high in energy. There is very little change going to the TZVPP basis, which differs from TZVP only by an additional set of polarization functions on H. Dunning's cc-pVTZ basis set [205] performs similar to TZVP

TABLE III: Basis set convergence of the first six singlet excitation energies (in eV) and oscillator strengths (length gauge) of naphthalene. The basis set acronyms are defined in the text. $N_{\rm bf}$ denotes the number of Cartesian basis functions, and CPU denotes the CPU time (seconds) on a single processor of a 2.4 GHz Opteron Linux workstation. The PBE functional was used for both the ground-state and TDDFT calculations. The ground-state structure was optimized at the PBE/TZVP/RI-level. Experimental results were taken from Ref. [197].

Basis set	$1\ ^1B_{3u}$	$1\ ^1B_{2u}$ (Osc. Str.)	$2\ ^1A_g$	$1\ ^1B_{1g}$	$2\ ^1B_{3u}$ (Osc. Str.)	$1\ ^1A_u$	$N_{\rm bf}$	CPU
SV	4.352	4.246 (0.0517)	6.084	5.254	5.985 (1.1933)	6.566	106	24
SV(P)	4.272	4.132 (0.0461)	5.974	5.149	5.869 (1.1415)	6.494	166	40
6-31G*	4.293	4.154	6.021	5.185	5.902	7.013	166	40
SVP	4.262	4.125 (0.0466)	5.960	5.136	5.852 (1.1402)	6.505	190	48
aug-SV(P)	4.213	4.056 (0.0417)	5.793	4.993	5.666 (1.1628)	5.338	266	168
TZVP	4.209	4.051 (0.0424)	5.834	5.030	5.715 (1.1455)	6.215	408	408
TZVPP	4.208	4.050 (0.0425)	5.830	5.027	5.711 (1.1464)	6.231	480	568
cc-pVTZ	4.222	4.064 (0.0427)	5.870	5.061	5.747 (1.1355)	6.062	470	528
aug-TZVP	4.193	4.031 (0.0407)	5.753	4.957	5.622 (1.1402)	5.141	608	2000
aug-TZVP/RI	4.193	4.031 (0.0407)	5.752	4.957	5.621 (1.1401)	5.142	608	400
QZVP	4.197	4.036 (0.0416)	5.788	4.989	5.667 (1.1569)	5.672	1000	6104
aug-QZVP	4.192	4.029 (0.0406)	5.748	4.954	5.616 (1.1330)	5.071	1350	28216
expt.	3.97, 4.0	4.45, 4.7 (0.102, 0.109)	5.50, 5.52	5.28, 5.22	5.63, 5.55, 5.89 (1.2, 1.3)	5.6		

and TZVPP. However, Dunning basis sets are based on a generalized contraction scheme for valence orbitals, as opposed to the segmented contracted SV, TZV and QZV basis sets. The latter are more efficient for larger systems, because more integrals vanish.

G. Diffuse functions

Adding a $[1s1p1d1f]$ set of diffuse functions to TZVP we obtain the aug-TZVP basis set. The aug-TZVP excitation energies of all states except the $1\ ^1A_u$ Rydberg state are within 0.01 eV of the reference aug-QZVP results and can be considered essentially converged for the purposes of present TDDFT. A similar observation can be made for the oscillator strengths in Table III.

Going to the even larger quadruple zeta valence (QZV) basis sets, the results change only marginally, but the computation times increase substantially. In density functional theory, these basis sets are mainly used for bechmarks and calibration.

H. Resolution of the identity

For comparison, we have included results that were obtained using the resolution of the identity approximation for the Coulomb energy (RI-J) [206, 207]. It is obvious that the error introduced by the RI-J approximation is much smaller than the basis set error, while the computation time is reduced by a factor of 5. The RI-J approximation is so effective because the computation of the Coulomb (Hartree) energy and its respose is the bottleneck in conventional (TD)DFT calculations. RI-J replaces the four-index Coulomb integrals by three-index and two-index integrals, which considerably lowers the algorithmic pre-factor[208]. It is generally safe to use with the appropriate auxiliary basis sets. As soon as hybrid functionals are used, however, the computation of the exact exchange becomes rate-determining.

I. Summary

To summarize, for larger molecules, SV(P) or similar basis sets are often appropriate due to their good cost-to-performance ratio. We recommend to check SV(P) results by a TZVP calculation whenever possible. Diffuse functions should be used sparingly for molecules with more than about 20 atoms.

V. PERFORMANCE

This chapter is devoted to studying and analyzing the performance of TDDFT, assuming basis-set convergence. We dissect many of the sources of error in typical TDDFT calculations.

To get an overall impression, a small survey is given by Furche and Ahlrichs[209]. Typical chemical calculations are done with the B3LYP[167] functional, and typical results are transition frequencies within 0.4 eV of experiment, and structural properties of excited states are almost as good as those of ground-state calculations (bond lengths to within 1%, dipole moments to within 5%, vibrational frequencies to within 5%). Most importantly, this level of accuracy appears sufficient in most cases to qualitatively identify the nature of the most intense transitions, often debunking cruder models that have been used for interpretation for decades. This is proving especially useful for the photochemistry of biologically relevant molecules[69]

TABLE IV: Performance of various density functionals for the first six singlet excitation energies (in eV) of naphthalene. An aug-TZVP basis set and the PBE/TZVP/RI ground-state structure was used. The "best" estimates of the true excitations were from experiment and calculations, as described in text.

Method	$1\ ^1B_{3u}$	$1\ ^1B_{2u}$	$2\ ^1A_g$	$1\ ^1B_{1g}$	$2\ ^1B_{3u}$	$1\ ^1A_u$
Pure density functionals						
LSDA	4.191	4.026	5.751	4.940	5.623	5.332
BP86	4.193	4.027	5.770	4.974	5.627	5.337
PBE	4.193	4.031	5.753	4.957	5.622	5.141
Hybrids						
B3LYP	4.393	4.282	6.062	5.422	5.794	5.311
PBE0	4.474	4.379	6.205	5.611	5.889	5.603
"best".	4.0	4.5	5.5	5.5	5.5	5.7

TABLE V: Performance of various wavefunction methods for the excitations of Table I. The aug-TZVP basis set and the PBE/TZVP/RI ground-state structure was used for all except the CASPT2 results, which were taken from Ref. [197]. Experimental results are also from Ref. [197].

Method	$1\ ^1B_{3u}$	$1\ ^1B_{2u}$	$2\ ^1A_g$	$1\ ^1B_{1g}$	$2\ ^1B_{3u}$	$1\ ^1A_u$
CIS	5.139	4.984	7.038	6.251	6.770	5.862
CC2	4.376	4.758	6.068	5.838	6.018	5.736
CASPT2	4.03	4.56	5.39	5.53	5.54	5.54
expt.	3.97, 4.0	4.45, 4.7	5.50, 5.52	5.28, 5.22	5.63,5.55 5.89	
"best".	4.0	4.5	5.5	5.5	5.5	5.7

TABLE VI: Performance of various density functionals and correlated wavefunction methods for the oscillator strengths of the first three dipole-allowed transitions of naphthalene. A aug-TZVP basis set and the PBE/TZVP/RI ground-state structure was used for all except the CASPT2 results, which were taken from Ref. [197].

Method	$1\ ^1B_{3u}$	$1\ ^1B_{2u}$	$2\ ^1B_{3u}$
LSDA	0.0000	0.0405	1.1517
BP86	0.0000	0.0411	1.1552
PBE	0.0000	0.0407	1.1402
B3LYP	0.0000	0.0539	1.2413
PBE0	0.0000	0.0574	1.2719
LHF/LSDA	0.0000	0.0406	1.2089
LHF/PBE	0.0000	0.0403	1.2008
CIS	0.0002	0.0743	1.8908
CC2	0.0000	0.0773	1.4262
CASPT2	0.0004	0.0496	1.3365
expt.	0.002	0.102, 0.109	1.2, 1.3

A. Example: Napthalene Results

As an illustration, compare the performance of various density functionals and wavefunction methods for the first singlet excited states of naphthalene in Tables IV, V and VI. All calculations were performed using the aug-TZVP basis set; the complete active space SCF with second-order perturbation theory (CASPT2) results from Ref. [197] were obtained in a smaller double zeta valence basis set with some diffuse augmentation. The experimental results correspond to band maxima from gas-phase experiments; however, the position of the band maximum does not necessarily coincide with the vertical excitation energy, especially if the excited state structure differs significantly from the ground-state structure. For the lower valence states, the CASPT2 results can therefore be expected to be at least as accurate as the experimental numbers. For higher excited states, the basis set used in the CASPT2 calculations appears rather small, and the approximate second-order coupled cluster values denoted RICC2 [210–212] might be a better reference. Thus our best guess (denoted "best" in the Tables) is from experiment for the first 4 transitions, CASPT2 for the 5th, and RICC2 for the 6th.

We begin with some general observations.

- The excitation energies predicted by the GGA functionals BP86 and PBE differ only marginally from the LSDA results (an exception being the $1\ ^1A_u$ Rydberg state, whose PBE excitation energy is substantially lower than those of all other methods). Note however that GGA functionals generally improve over LSDA results for other excited state properties such as structures or vibrational frequencies.

- Hybrid mixing leads to systematically higher excitation energies. On average, this is an improvement over the GGA results which are systematically too low. However, while diffuse excitations benefit from hybrid mixing due to a reduction of self-interaction error, valence excitation energies are not always improved, as is obvious for the $1\ ^1B_{3u}$ and $2\ ^1B_{3u}$ valence states.

- The $1\ ^1B_{2u}$ state is erroneously predicted below the $1\ ^1B_{3u}$ state by all density functionals, which is a potentially serious problem for applications in photochemistry; this is not corrected by hybrid mixing.

- The configuration-interaction singles (CIS) method which uses a Hartree-Fock reference that is computationally as expensive as hybrid TDDFT produces errors that are substantially larger, especially for valence states. The coupled cluster and CASPT2 methods are far more expensive, and scale prohibitively as the system size grows.

The $1\ ^1B_{2u}$ excitation is polarized along the short axis of the naphthalene molecule. In Platt's nomenclature of excited states of polycyclic aromatic hydrocarbons (PAHs), $1\ ^1B_{2u}$ corresponds to the ^1L_a state. This state is of more ionic character than the $1\ ^1B_{3u}$ or ^1L_b state. Parac and Grimme have pointed out [213] that GGA functionals considerably underestimate the excitation energy of the ^1L_a state in PAHs. This agrees with the observation that the $1\ ^1B_{2u}$ excitation of naphthalene is computed 0.4-0.5 eV too low in energy by LSDA

and GGA functionals, leading to an incorrect ordering of the first two singlet excited states.

B. Influence of the ground-state potential

From the very earliest calculations of transition frequencies[188, 190], it was recognized that the inaccuracy of standard density functional approximations (LDA, GGA, hybrids) for the ground-state XC potential leads to inaccurate KS eigenvalues. Because the approximate KS potentials have incorrect asymptotic behavior (they decay exponentially, instead of as $-1/r$, as seen in Fig. 3), the KS orbital eigenvalues are insufficiently negative, the ionization threshold is far too low, and Rydberg states are often unbound.

Given this disastrous behavior, many methods have been developed to asymptotically correct potentials[214, 215]. Any corrections to the ground-state potential are dissatisfying, however, as the resulting potential is *not* a functional derivative of an energy functional. Even mixing one approximation for $v_{\rm XC}(\mathbf{r})$ and another for $f_{\rm XC}$ has become popular. A more satisfying route is to use the optimized effective potential (OEP) method[159, 173] and include exact exchange or other self-interaction-free functionals[216]. This produces a far more accurate KS potential, with the correct asymptotic behavior. The chief remaining error is simply the correlation contribution to the position of the HOMO, i.e, a small shift. All the main features below and just above I are retained.

1. N_2, a very small molecule

A simple system to see the effect of the various ground-state potentials is the N_2 molecule. In all the cases discussed below, a SCF step was carried out using the ground-state potential to find the KS levels. These are then used as input to Eq. (47) with the ALDA XC kernel.

In Table VII, the KS energy levels for the LDA functional are shown. It is very clear to see that the eigenvalues for the higher unoccupied states are positive. As mentioned this is due to the LDA potential being too shallow and not having the correct asymptotic behavior. Comparing the basis-set calculation with the basis-set-free calculation, the occupied orbitals are in good agreement. However for the unoccupied states that are unbounded in LDA, basis sets cannot describe these correctly and give a positive energy value which can vary greatly from one basis set to another.

In Table VIII, the bare KS transition frequencies between these levels are shown. Note that they are in rough agreement with the experimental values and that they lie inbetween the singlet-singlet and singlet-triplet

TABLE VII: Orbital energies of the KS energy levels for N_2 at separation $R = 2.0744$a.u. Orbitals calculated using the LDA potential are shown for two different numerical methods. The first is fully numerical basis set free while the other uses the Sadlej (52 orbitals) basis set[217]. The OEP method uses the EXX (KLI) approximation and is also calculated basis set free.

	Energies in (eV)		
Orbital	LDA basis set free[a]	LDA Sadlej[b]	OEP[a]
Occupied orbitals			
$1\sigma_g$	-380.05	-380.82	-391.11
$1\sigma_u$	-380.02	-380.78	-391.07
$2\sigma_g$	-28.24	-28.52	-35.54
$2\sigma_u$	-13.44	-13.40	-20.29
$1\pi_u$	-11.89	-11.86	-18.53
$3\sigma_g$	-10.41	-10.38	-17.15
Unoccupied orbitals			
$1\pi_g$	-2.21	-2.23	-8.44
$4\sigma_g$	-0.04	0.66	-5.05
$2\pi_u$	> 0	1.93	-4.04
$3\sigma_u$	> 0	1.35	-3.54
$1\delta_g$	> 0	-	-2.76
$5\sigma_g$	> 0	3.20	-2.49
$6\sigma_g$	> 0	-	-2.33
$2\pi_g$	> 0	3.89	-2.17
$3\pi_u$	> 0	-	-2.04

[a]From Ref.[218]. [b]from Ref.[219].

TABLE VIII: Comparison of the vertical excitation energies for the first twelve excited states of N_2 calculated using different methods for the SCF step. In all cases the KS orbitals from the SCF step are inputed into Casida's equations with the ALDA XC kernel. For the LDA calculated with the Sadlej basis set, the bare KS transition frequencies are given to demonstrate how they are corrected towards their true values using Casida's equations. Also given are the mean absolute errors for each method, errors in backets are calculated for the lowest eight transitions only.

		Excitation energy (eV)					
State	Excitation	BARE KS[a]	ALDA[a]	ALDA[b]	LB94[c]	OEP[d]	Expt[e]
Singlet → singlet transitions							
$w^1\Delta_u$	$1\pi_u \to 1\pi_g$	9.63	10.20	10.27	9.82	10.66	10.27
$a'^1\Sigma_u^-$	$1\pi_u \to 1\pi_g$	9.63	9.63	9.68	9.18	10.09	9.92
$a^1\Pi_g$	$3\sigma_g \to 1\pi_g$	8.16	9.04	9.23	8.68	9.76	9.31
$a''^1\Sigma_g$	$3\sigma_g \to 4\sigma_g$	-	-	10.48	-	12.47	12.20
$o^1\Pi_u$	$2\sigma_u \to 1\pi_g$	-	-	13.87	-	14.32	13.63
$c^1\Pi_u$	$3\sigma_g \to 2\pi_u$	-	-	11.85	-	13.07	12.90
Singlet → triplet transitions							
$C^3\Pi_u$	$2\sigma_u \to 1\pi_g$	11.21	10.36	10.44	10.06	11.05	11.19
$B'^3\Sigma_u^-$	$1\pi_u \to 1\pi_g$	9.63	9.63	9.68	9.18	10.09	9.67
$W^3\Delta_u$	$1\pi_u \to 1\pi_g$	9.63	8.80	8.91	8.32	9.34	8.88
$B^3\Pi_g$	$3\sigma_g \to 1\pi_g$	8.16	7.50	7.62	7.14	8.12	8.04
$A^3\Sigma_u^+$	$1\pi_u \to 1\pi_g$	9.63	7.84	8.07	7.29	8.51	7.74
$E^3\Sigma_g^+$	$3\sigma_g \to 4\sigma_g$	-	-	10.33	12.32	11.96	12.00
Mean Absolute Error		(0.61)	(0.27)	0.54	(0.63)	0.34	

[a]Using Sadlej basis set. From Ref.[219].
[b]Basis set free. From Ref.[218].
[c]From Ref.[220].
[d]Using KLI approximation. From Ref.[218].
[e]Computed in [221] from the spectroscopic constants of Huber and Herzberg [222].

transitions[223]. The ALDA XC kernel $f_{\rm XC}^{\rm ALDA}$ then shifts the KS transitions towards their correct values. For the eight lowest transitions LDA does remarkably well, the mean absolute error (MAE) being 0.27eV for the Sadlej basis set. For higher transitions it fails drastically, the MAE increases to 0.54eV when the next four transitions are included. This increase in the MAE is attributed to a cancellation of errors that lead to good frequencies for the lower transitions[218]. Since LDA binds only two unoccupied orbitals, it cannot accurately describe transitions to higher orbitals. In basis set calculations, the energies of the unbound orbitals which have *converged* will vary wildly and cannot give trusted transition frequencies.

One class of XC functionals that would not have this problem are the asymptotically corrected (AC) functionals [214, 215, 224–226]. LB94[227] is one such of these and its performance is shown in Table VIII. AC XC potentials tend to be too shallow in the core region, so the KS energy levels will be too low while the AC piece will force the higher KS states to be bound and their energies will cluster below zero. Thus it is expected that using AC functionals will consistently underestimate the transitions frequencies.

A much better approach is using the OEP method. The KS orbitals found using this method are self-interaction free and are usually better approximations to the true KS orbitals. OEP will also have the correct asymptotic behavior and as we can see in Table VII, all orbital energies are negative. In Table VIII, the MAE for OEP is 0.34eV, much lower than LDA. Since OEP binds all orbitals, it allows many more transitions to be calculated. A common OEP functional is exact exchange (or the KLI approximation[228] to it) which neglects correlation effects, but these are generally small contributions to the KS orbitals. Using these with ALDA for $f_{\rm XC}$ (which does contain correlation) leads to good transition frequencies as shown in Table VIII. Although LDA is sometimes closer to the experimental values for the lower transitions, the value of OEP lies in it ability to describe both the higher and lower transisions.

2. *Napthalene, a small molecule*

Returning to our benchmark case of Naphthalene, using more accurate LHF exchange-only potentials from Sec. II B together with an LSDA or PBE kernel produces excitation energies in between the GGA and the hybrid results, except for the $1\ ^1A_u$ Rydberg state, whose excitation energy is significantly improved. Whether the LSDA kernel or the PBE GGA kernel is used together with an LHF potential does not change the results significantly.

The $1\ ^1B_{1g}$ and especially the $1\ ^1A_u$ states are diffuse, and it is not surprising that their excitation energy is considerably underestimated in the LSDA and GGA

TABLE IX: Naphthalene: Effect of ground-state potential on the excitations of Table IV. A ground-state calculation using exact exchange OEP (LHF) is performed and the excitations are found using a LDA/PBE kernel respectfully. The result is then compared to that found if the LDA/PBE functional had been used for both steps.

Method	$1\ ^1B_{3u}$	$1\ ^1B_{2u}$	$2\ ^1A_g$	$1\ ^1B_{1g}$	$2\ ^1B_{3u}$	$1\ ^1A_u$
LSDA	4.191	4.026	5.751	4.940	5.623	5.332
LHF/LSDA	4.317	4.143	5.898	5.097	5.752	5.686
PBE	4.193	4.031	5.753	4.957	5.622	5.141
LHF/PBE	4.295	4.121	5.876	5.091	5.741	5.693
"best".	4.0	4.5	5.5	5.5	5.5	5.7

treatment. Using the asymptotically correct LHF potential corrects the excitation energy of the $1\ ^1A_u$, which is a pure one-particle excitation out of the $1a_u$ valence into the $10a_g$ Rydberg orbital; the latter may be viewed as a $3s$ orbital of the $C_{10}H_8^+$ ion. On the other hand, a strong mixture of valence and Rydberg excitations occurs in $1\ ^1B_{1g}$. The LHF potential improves the GGA results only marginally here, suggesting that more accurate XC kernels are necessary to properly account for valence-Rydberg mixing.

C. Analyzing the influence of the XC kernel

In this section, we discuss the importance of the XC kernel in TDDFT calculations. As mentioned earlier, the kernels used in practical TDDFT are local or semi-local in both space and time. Even hybrids are largely semi-local, as they only mix in $20-25\%$ exact exchange.

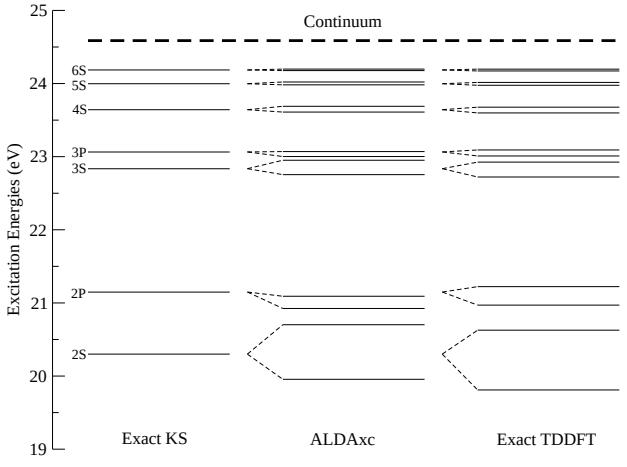

FIG. 5: The spectrum of Helium calculated using the ALDA XC kernel[229] with the exact KS orbitals.

In realistic calculations, both the ground-state XC po-

tential and TDDFT XC kernel are approximated. A simple way to separate the error in the XC kernel is to look at a test case where the exact KS potential is known. Figure 5 shows the spectrum of He using the exact KS potential, but with the ALDA XC kernel. It does rather well[229] (very well, as shall see later in section VI, when we examine atoms in more detail). Very similar results are obtained with standard GGA's.

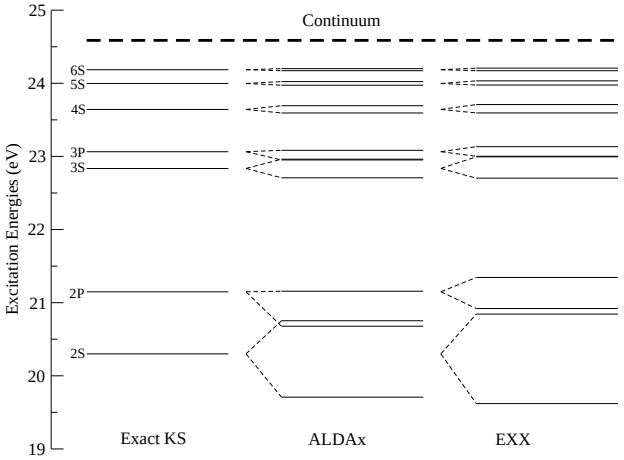

FIG. 6: The spectrum of Helium calculated using the ALDAx kernel and the exact exchange kernel[229]. Again the exact KS orbitals were used. The importance of non-locality for the XC kernel can be seen as the exchange part of ALDA gives a noticeable error compared to the exchange part of the true functional (the AEXX kernel for He).

The errors in such approximate kernels come from the locality in space and time. We can test one of these separately for the He atom, by studying the exchange limit for the XC kernel. For two spin-unpolarized electrons, $f_{\rm x} = -1/2|\mathbf{r}-\mathbf{r}'|$, i.e., it exactly cancels half the Hartree term. Most importantly, it is frequency-independent, so that there is no memory, i.e., the adiabatic approximation is exact. In Fig. 6, we compare ALDAx, i.e., the ALDA for just exchange, to the exact exchange result for He. Clearly, ALDA makes noticeable errors relative to exact exchange, showing that non-locality in space can be important.

Thus the hybrid functionals, by virtue of mixing some fraction of exact exchange with GGA, will have only slightly different potentials (mostly in the asymptotic region), but noticeably different kernels.

D. Errors in potential vs. kernel

In this section, we examine the relative importance of the potential and kernel errors. It has long been believed that fixing the defects in the potential, especially its asymptotic behavior, has been the major challenge to improving TDDFT results[224–226]. We argue here that this is overly simplistic, and is due to tests being carried out on atoms and small molecules. In large molecules, where the interest is in the many low-lying transitions, the potential can be sufficiently accurate, while the kernel may play a larger role.

In fact, our analysis of the general failure of TDDFT in underestimating the ^1L_a transitions in PAH's sheds some light on its origin. Using the self-interaction free LHF potential does not cure this problem, as is obvious from Tab. IX. To the best of our knowledge, the cause of this shortcoming of TDDFT is not well understood. We note, however, that the same incorrect ordering of ^1L_a and ^1L_b occurs in the CIS approximation, which is self-interaction free. The analysis here shows that this is a failure of our approximations to the XC kernel rather than to the ground-state potential.

E. Understanding linear response TDDFT

Several simple methods have evolved for qualitatively understanding TDDFT results. The most basic is the single-pole approximation (SPA), which originated[188] in including only one pole of the response function. The easiest way to see this here is to truncate Eq. (47) to a 1×1 matrix, yielding an (often excellent) approximation to the change in transition frequency away from its KS value[193, 230]:

$$\omega^2 \approx w_{q\sigma}^2 + 2\omega_{q\sigma}K_{q\sigma q\sigma} \quad \text{(SPA)}, \tag{58}$$

(The original SPA was on the unsymmetric system yielding $\omega \approx w_{q\sigma} + K_{q\sigma q\sigma}$, which for a spin-saturated system becomes $\omega \approx \omega_q + 2K_{qq}$ [229]). This can also provide a quick and dirty estimate, since only KS transitions and one integral over $f_{\rm XC}$ are needed. While it allows an estimate of the shift of transitions from their KS energy eigenvalue differences, it says nothing about oscillator strengths, which are unchanged in SPA from their KS values. In fact, a careful analysis of the TDDFT equation shows that oscillator strengths are particularly sensitive to even small off-diagonal matrix elements, whereas transition frequencies are less so[231].

A more advanced analysis is the double pole approximation[232] (DPA), which applies when two transition are strongly coupled to one another, but not strongly to the rest of the transitions. Then one can show explicitly the very strong effect that off-diagonal elements have on oscillator strengths, showing that sometimes an entire peak can have almost no contribution. One also sees pole-repulsion in the positions of the transitions, a phenomenon again missing from SPA.

The DPA was used recently and very successfully to explain X-ray edge spectroscopy results for $3d$-transition metal solids as one moves across the periodic table[233]. These transitions form a perfect test case for DPA, as the only difference between them is caused by the spin-orbit

TABLE X: Transition frequencies and oscillator strengths (O.S) calculated using the double pole approximation (DPA) for the lowest $^1B_{3u}$ transitions in Naphthalene. The PBE functional was used with a aug-TZVP basis set on top of a PBE/TZVP/RI ground state structure

	KS		DPA		Full TDDFT	
	ω	O.S	ω	O.S	ω	O.S
$^1B_{3u}$	4.117	(1.02)	4.245	(0.001)	4.191	(0)
$^2B_{3u}$	4.131	(1.00)	6.748	(2.02)	5.633	(1.14)

splitting (several eV) of the $2p^{1/2}$ and $2p^{3/2}$ levels. In a ground-state KS calculation, this leads to a 2:1 branching ratio for the two peaks, based simply on degeneracy, as all matrix elements are identical for the two transitions. Experimentally, while this ratio is observed for Fe, large deviations occur for other elements.

These deviations could be seen in full TDDFT calculations, and were attributed to strong core-hole correlations. The SPA, while it nicely accounts for the shifts in transition frequencies relative to bare KS transitions, but yields only the ideal 2:1 branching ratio. However, the DPA model gives a much simpler, and more benign interpretation. The sensitivity of oscillator strengths to off-diagonal matrix elements means that, even when the off-diagonal elements are much smaller than diagonal elements (of order 1 eV), they cause rotations in the 2-level space, and greatly alter the branching ratio. Thus a KS branching ratio occurs even with strong diagonal 'correlation', so long as off-diagonal XC contributions are truly negligible. But even small off-diagonal 'correlation', can lead to large deviations from KS branching ratios.

We can use DPA to understand the lowest $^1B_{3u}$ transitions in our naphthalene case. In Table X, we list the TDDFT matrix elements for the PBE calculation for the two nearly degenerate KS transitions, $1a_u \rightarrow 2b_{3g}$ and $2b_{1u} \rightarrow 2b_{2g}$, along with their corresponding KS transition frequencies. Contour plots of the four orbitals involved are shown in Fig. 7. We note first that these two KS transitions are essentially degenerate, so that there is no way to treat them within SPA. The degeneracy is lifted by the off-diagonal elements, which cause the transitions to repel each other, and strongly rotate the oscillator strength between the levels, removing almost all the oscillator strength from the lower peak[232]. The DPA yields almost the correct frequency and oscillator strength (i.e., none) for the lower transition, but the higher one is overestimated, with too much oscillator strength. This must be due to coupling to other higher transitions. In the DPA, in fact the higher transition lands right on top of the third transition, so strong coupling occurs there too. This example illustrates (i), that solution of the full TDDFT equations is typically necessary for large molecules which have many coupled transitions, but also (ii), that simple models can aid the interpretation of such results. All of which shows that, while models developed for well-separated transitions might provide some insight for specific transitions in large molecules, the number and density of transitions make such models only semi-quantitative at best.

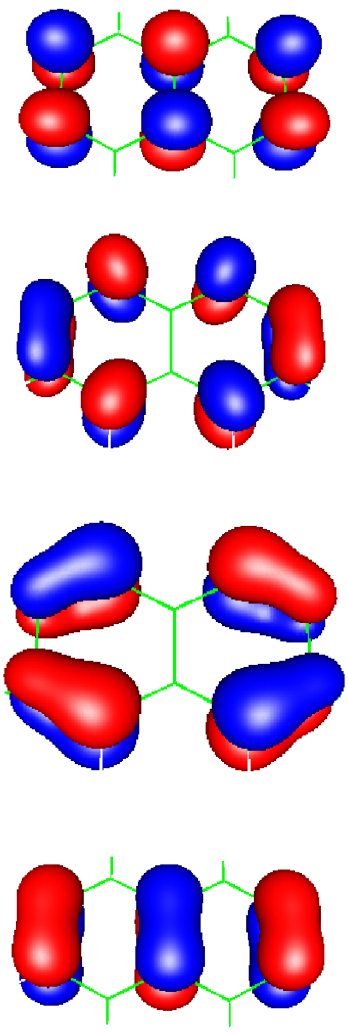

FIG. 7: The four orbitals involved in the first two $^1B_{3u}$ (contour value ± 0.07 a.u.). The PBE functionals and an aug-TZVP basis set were used.

VI. ATOMS AS A TEST CASE

In this section, we look more closely at how well TDDFT performs for a few noble gas atoms. As explained above, this is far from representative of its behavior for large molecules, but this does allow careful study of the electronic spectra without other complications. Most importantly, for the He, Be, and Ne atoms, we have essentially exact ground-state KS potentials from Umrigar and coworkers[156, 234]. This allows us to dissect the sources of error in TDDFT calculations.

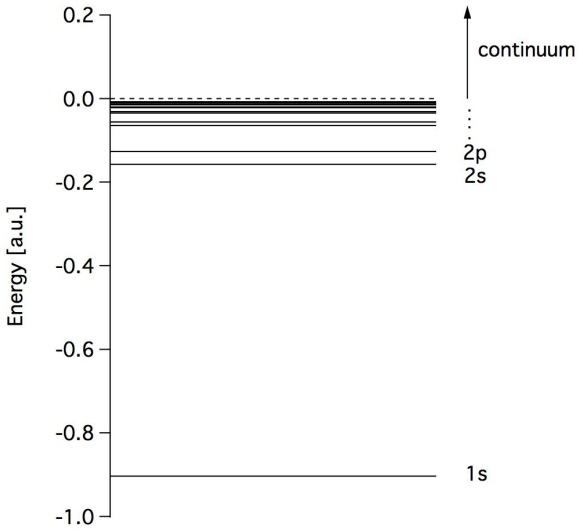

FIG. 8: Singlet energy level diagram for the helium atom. The Rydberg series of transition frequencies clustered below the ionization threshold can be seen. The frequencies cluster together, making it difficult to assess the quality of the TDDFT calculated spectra. As discussed in the text, the quantum defect is preferable for this purpose.

A. Quantum defect

In Fig. 8 we show the KS orbital energy level diagram of the helium atom. The zero is set at the onset of the continuum and is marked with a dotted line. For closed shell atoms and for any spherical one-electron potential that decays as $-1/r$ at large distances, the bound-state transitions form a Rydberg series with frequencies:

$$\omega_{nl} = I - \frac{1}{2(n-\mu_{nl})^2} \tag{59}$$

where I is the ionization potential, and μ_{nl} is called the quantum defect. Quantum defect theory was developed by Ham [235] and Seaton [236] before even the Hohenberg-Kohn theorem[1].

The great value of the quantum defect is its ability to capture all the information about the entire Rydberg series of transitions in a single slowly-varying function, the quantum defect as a function of energy, $\mu_l(E = \omega - I)$, which can often be fit by a straight line or parabola. In Table XI, we report extremely accurate results from wavefunction calculations for the helium atom. We show singlet and triplet values that have been obtained by Drake [198]. We also give results from the exact ground-state KS potential shown in Fig 2 [156]. For each column, on the left are the transition frequencies, while on the right are the corresponding quantum defects. Note how small the differences between transitions become as one climbs up the ladder, and yet the quantum defect remains finite and converges to a definite value.

TABLE XI: Transition energies (ω) and quantum defects (QD) for He atom s-Rydberg series[a.u.]. The ionization energy is 0.90372 a.u.

Transition	Singlet [a]		Triplet [a]		KS[b]	
	ω	QD	ω	QD	ω	QD
$1s \to 2s$	0.7578	0.1493	0.7285	0.3108	0.7459	0.2196
$1s \to 3s$	0.8425	0.1434	0.8350	0.3020	0.8391	0.2169
$1s \to 4s$	0.8701	0.1417	0.8672	0.2994	0.8688	0.2149
$1s \to 5s$	0.8825	0.1409	0.8883	0.2984	0.8818	0.2146
$1s \to 6s$	0.8892	0.1405	0.8926	0.2978	0.8888	0.2144
$1s \to 7s$	0.8931	0.1403	0.8926	0.2975	0.8929	0.2143

[a] Accurate non-relativistic calculations from Ref. [198].
[b] The differences between the KS eigenvalues obtained with the exact potential from Ref. [156].

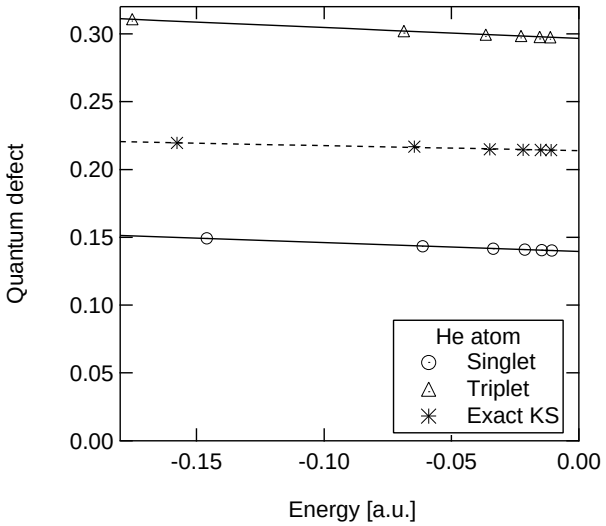

FIG. 9: The exact s KS quantum defect and the exact singlet and triplet quantum defects of He and their parabolic fits. The quantum defect may clearly be described as a smooth function of energy, in this case, a linear fit. Thus knowing the quantum defect for a few transitions allows us to find it for all transitions, and hence their frequencies.

All the information of the levels of Fig. 8 and of Table XI is contained in Fig. 9. This clearly illustrates that the quantum defect is a smooth function of energy, and is well approximated (in these cases) as a straight line. The quantum defect is thus an extremely compact and sensitive test of approximations to transition frequencies. Any approximate ground-state KS potential suggested for use in TDDFT should have its quantum defect compared with the exact KS quantum defect, while any approximate XC-kernel should produce accurate corrections to the ground-state KS quantum defect, on the scale of Fig. 9.

To demonstrate the power of this analysis, we test two common approximations to the ground-state potential, both of which produce asymptotically correct potentials. These are exact exchange [237] (see Sec II B)

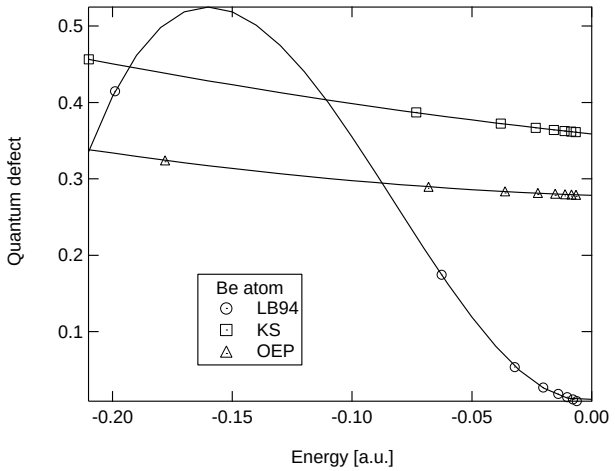

FIG. 10: The Be p quantum defect of LB94, exact exchange (OEP), and KS, and their best fits. While both functionals give the correct asymptotic behavior of the KS potential, by calculating the quantum defect, we can learn more about their performance.

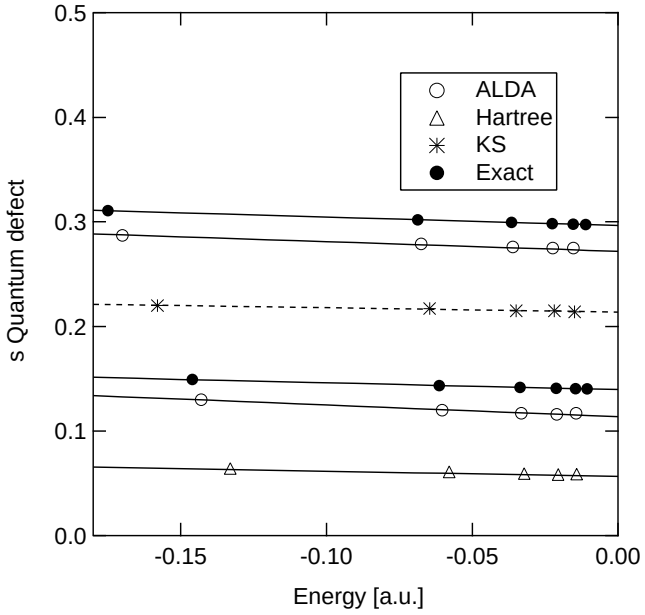

FIG. 11: The corrections due to using the Hartree or ALDA kernel on the exact KS s quantum defect of He. Using the Hartree kernel only effects the singlet values, shifting them too low. If a good XC kernel is then used, it should move both the triplet and singlet quantum defects from the Hartree kernel towards the exact ones[242]. In this case, ALDA does a good job and is performing well.

and LB94 [227]. Exact exchange calculations are more demanding than traditional DFT calculations, but are becoming popular because of the high quality of the potential [238, 239]. On the other hand, LB94 provides an asymptotically correct potential at little extra cost beyond traditional DFT [215, 226, 240]. In Fig. 10 we show the p Be quantum defect obtained with LB94, OEP, and exact KS potentials. Fig. 10 immediately shows the high quality of the exact exchange potential. The quantum defect curve is almost identical to the exact one, apart from being offset by about 0.1 . On the other hand, the quantum defect of LB94 was poor for all cases studied[241, 242]. This shows that just having a potential that is asymptotically correct is not enough to get a good quantum defect.

B. Testing TDDFT

To see how well TDDFT really does, we plot quantum defects for atoms. We take the He atom as our prototype, as usual in this section. In Fig. 11, we plot first the KS quantum defect and the exact singlet and triplet lines, as before in Fig. 9. Then we consider the Hartree approximation. This is equivalent to setting the XC kernel to zero. This changes the postion of the singlet curve, but leaves the triplet unchanged from its KS value, because the direct term includes no spin-flipping. It definitely improves over the KS for the singlet. Lastly, we include ALDA XC corrections. Only if these significantly improve over the Hartree curves can we say TDDFT is really working here. Clearly it does, reducing the Hartree error enormously.

These results are also typical of He P transitions, and Be S and P transitions. For reasons as yet unclear, the $s \to d$ transitions fail badly for both these systems[241, 243].

C. Saving standard functionals

We have a problem with the incorrect long-range behavior of the potential from standard *density* functionals only when Rydberg excitations are needed. But it would be unsatisfactory to have to perform a completely different type of calculation, eg OEP, in order to include such excitations when desired, especially if the cost of that calculation is significantly greater.

However, it is possible, with some thought and care, and using quantum defect theory, to extract the Rydberg series from the short-ranged LDA potential. To see this, consider Fig. 12, which shows both the bare KS response and the TDDFT corrected response of the He atom. The δ-function absorptions at the discrete transitions have been replaced by straightlines, whose height represents the oscillator strength of the absorption, multiplied by the appropriate density of states[247]. In the top panel, just the KS transitions are shown, for both the KS potential and the LDA potential of Fig 3 from section II B. The exact curve has a Rydberg series converging to 0.903, the exact ionization threshold for He. The LDA curve, on the other hand, has a threshold at just below 0.6. But clearly its optical absorption mimics

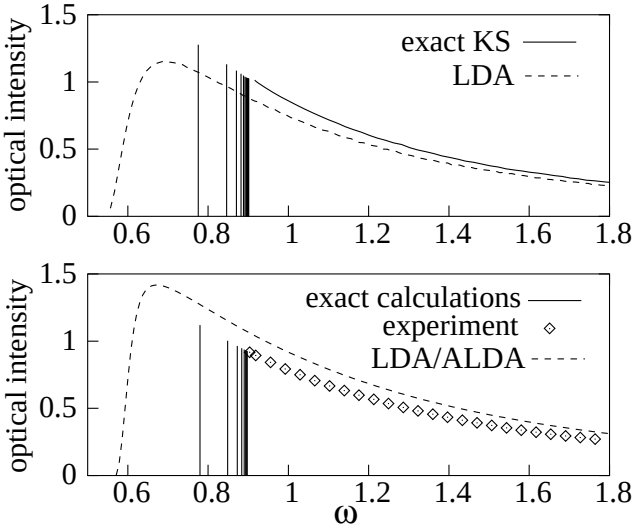

FIG. 12: He atom: The top panel shows the bare exact KS and LDA spectra, and the lower panel shows the TDDFT corrected spectra, LDA/ALDA results are from [244] but unshifted; the exact calculations are from [245], multiplied by the density of states factor (see text), and the experimental results are from [246]

.

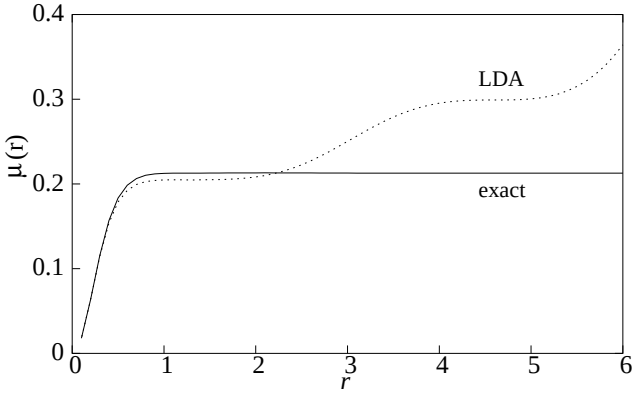

FIG. 13: He atom: solution of Eq.(60) for μ as a function of r; The $n = 20$ orbital was used for the exact case, and the scattering orbital or energy $E = I + \epsilon_{1s}^{LDA}$ was used for the LDA.

that of the exact system, even in the Rydberg series region, and is accurate to about 20%. The TDDFT ALDA corrections are small, and overcorrect the bare LDA results, but clearly are consistent with our observations for the bare spectra.

Why is this the case? Is this a coincidence? Returning to Fig. 3 of the introduction, we notice that the LDA (or GGA) potential runs almost exactly parallel to the true potential for $r \lesssim 2$, i.e., where the density is. Thus the scattering orbitals of the LDA potential, with transition energies between 0.6 and 0.9, almost exactly match the Rydberg orbitals of the exact KS potential with the same energy. When carefully defined, i.e., phase space factors for the continuum relative to bound states, the oscillator strength is about the same. This is no coincidence but, due to the lack of derivative discontinuity of LDA, its potential differs from the exact one by roughly a constant.

The 'fruitfly' of TDDFT benchmarks is the $\pi \rightarrow \pi^*$ transition in benzene. This occurs at about 5 eV in a ground-state LDA calculation, and ALDA shifts it correctly to about 7 eV[230]. Unfortunately, this is in the LDA continuum, which starts at about 6.5 eV! This is an example of the same general phenomenon, where LDA has pushed some oscillator strength into the continuum, but its overall contribution remains about right.

We can go one step further, and even deduce the energies of individual transitions. While the existence of a quantum defect requires a long-ranged potential, its value is determined by the phase-shift caused by the deviation from $-1/r$ in the interior of the atom. The *quantum defect extractor* (QDE)[248], is a formula for extracting the effective quantum defect from a scattering orbital of a short-ranged KS potential, such as that of LDA. The QDE is:

$$\frac{d\ln\phi}{dr} = \frac{1}{n^*} - \frac{n^*}{r} - \frac{1}{r}\frac{U(-n^*;2;2r/n^*)}{U(1-n^*;2;2r/n^*)} \qquad (60)$$

Here $k = \sqrt{2|E|}$ is written as $k = (n^*)^{-1}$, with $n^* = (n - \mu_n)$, where n numbers the bound state, and μ_n is the quantum defect; U is the confluent hypergeometric function [249]. If the extractor is applied to an orbital of a long-ranged potential, it rapidly approaches its quantum defect.

In Fig 13, we plot the results of the QDE for the He atom, applied to both the exact KS potential and the LDA potential. The LDA potential runs almost parallel to the exact one in the region $1 < r < 2$ (where μ_∞ can already be extracted accurately), and orbitals corresponding to the same *frequency* (exact and LDA) are therefore very close in that region. In the spirit of Ref.[250], we compare the exact energy-normalized 20s orbital (which is essentially identical to the zero-energy state in the region $0 < r < 6$) and the LDA orbital of energy $I + \epsilon_{1s}^{LDA} = 0.904 - 0.571 = 0.333$. Notice how good the LDA orbital is in the region $1 < r < 2$. We show in Fig.13 the solution of Eq.(60) when this scattering LDA orbital is employed. Clearly, the plateau of the LDA curve in the $1 < r < 2$ region is an accurate estimate of the quantum defect. The value of μ on this plateau is 0.205, an underestimation of less than 4% with respect to the exact value.

Thus, given the ionization potential of the system, LDA gives a very accurate prediction of the asymptotic quantum defect. The ionization potential is needed to choose the appropriate LDA scattering orbital, but the results are not terribly sensitive to it. We repeated the same procedure with the LDA ionization potential (defined as $E_{\rm LDA}({\rm He}) - E_{\rm LDA}({\rm He}^+) = 0.974$) instead of the exact one, and found $\mu_\infty^{\rm LDA} = 0.216$, overestimating the exact μ_∞ by just 1%.

D. Electron scattering

Lastly in this section, we mention recent progress in developing a theory for low-energy electron scattering from molecules. This was one of the original motivations for developing TDDFT. One approach would be to evolve a wavepacket using the TDKS equations, but a more direct approach has been developed[251, 252], in terms of the response function χ of the $N+1$ electron system (assuming it is bound).

This uses similar technology to the discrete transition case. Initial results for the simplest case, electron scattering from He^+, suggest a level of accuracy comparable to bound-bound transitions, at least for low energies (the most difficult case for traditional methods, due to bound-free correlation[253]). TDDFT, using the exact ground-state potential and ALDA, produces more accurate answers than static exchange[251], a traditional low cost method that is used for larger molecules[254, 255].

However, that TDDFT method fails when applied to electron scattering from Hydrogen, the true prototype, as the approximate solution of the TDDFT equations (very similar to the single pole approximation of Sec V E) fails, due to stronger correlations. To overcome this, a much simpler method has been developed, that uses an old scattering trick[256] to deduce scattering phase shifts from bound-state energies when the system is placed in a box, yielding excellent results for a very demanding case.

VII. BEYOND STANDARD FUNCTIONALS

We have surveyed and illustrated some of the many present successful applications of TDDFT in the previous section. In these applications, standard approximations (local, gradient-corrected, and hybrid, see sec. II B) are used both for the ground-state calculation and the excitations, via the adiabatic approximation (sec. III D). In this section, we survey several important areas in which this approach has been found to *fail*, and what might be done about it.

The errors are due to locality in both space and time, and these are intimately related. In fact, all memory effects, i.e., dependence on the history of the density[184], implying a frequency-dependence in the XC kernel, can be subsumed into an initial-state dependence[180], but probably not vice-versa. Several groups are attempting to build such effects into new approximate functionals [257–266], but none have shown universal applicability yet.

The failure of the adiabatic approximation is most noticeable when higher-order excitations are considered, and found to be missing in the usual linear response treatment[190]. The failure of the local approximation in space is seen when TDDFT is applied to extended systems, e.g., polymers or solids. Local approximations yield short-ranged XC kernels, which become irrelevant compared to Hartree contributions in the long-wavelength limit. The Coulomb repulsion between electrons generally requires long-ranged (ie $1/r$) exchange effects when long-wavelength response is being calculated.

Thus several approaches have been developed and applied in places where the standard formulation has failed. These approaches fall into two distinct categories. On the one hand, where approximations that are local in the *density* fail, approximations that are local (or semi-local) in the *current-density* might work. In fact, for TDDFT, the gradient expansion, producing the leading corrections to ALDA, *only* works if the current is the basic variable[267]. Using the gradient expansion itself is called the Vignale-Kohn (VK) approximation[268, 269], and it has been tried on a variety of problems.

The alternative approach is to construct orbital-dependent approximations with explicit frequency-dependence[270, 271]. This can work well for specific cases, but it is then hard to see how to construct general density functional approximations from these examples. More importantly, solution of the OEP equations is typically far more expensive than the simple KS equations, making OEP impractical for large molecules.

A. Double excitations

As first pointed out by Casida[190], double excitations appear to be missing from TDDFT linear response, within any adiabatic approximation. Experience[272, 273] shows that, like in naphthalene, sometimes adiabatic TDDFT will produce a single excitation in about the right region, in place of two lines, where a double has mixed strongly with a single.

In fact, when a double excitation lies close to a single excitation, elementary quantum mechanics shows that $f_{\rm XC}$ must have a strong frequency dependence [270]. Recently, post-adiabatic TDDFT methodologies have been developed[270, 274, 275] for including a double excitation when it is close to an optically-active single excitation, and works well for small dienes[270, 276]. It might be hoped that, by going beyond linear response, non-trivial double excitations would be naturally included in, e.g., TDLDA, but it has recently been proven that, in the higher-order response in TDLDA, the double excitations occur simply at the sum of single-excitations[277]. Thus we do not currently know how best to approximate these excitations. This problem is particularly severe for quantum wells, where the external potential is parabolic, leading to multiple near degeneracies between levels of excitation[274].

Returning to our naphthalene example, based on a HF reference, the $2\ ^1A_g$ state has, according to the RICC2 results, a considerable admixture of double excitations. This is consistent with the fact that the CIS method yields an excitation energy that is too high by 1.5 eV compared to experiment. The TDDFT results are much closer, yet too high by several tenths of eV.

B. Polymers

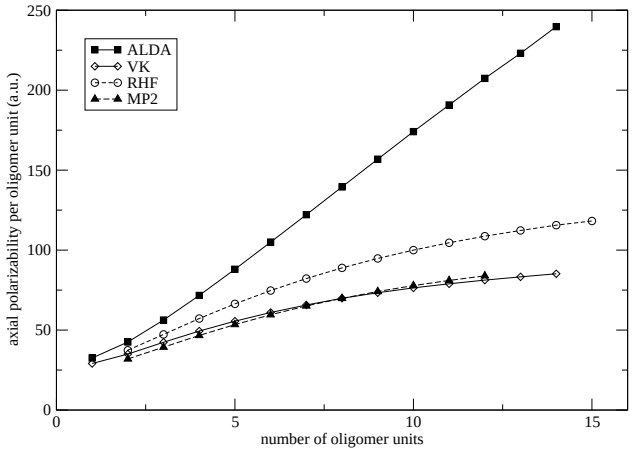

FIG. 14: ALDA and VK static axial polarizability of polyacetylene compared with RHF and MP2 results from Refs. [278–280]. ALDA severely overestimates the polarizability compared to the accurate MP2 calculation. Hartree-Fock is also incorrect. However using the VK functional gives almost exact agreement, at least in this case.

An early triumph of the VK functional was the static polarizabilities of long-chain conjugated polymers. These polarizabilites are greatly underestimated by LDA or GGA, with the error growing rapidly with the number of units[281]. On the other hand, HF does rather well, and does not overpolarize. The VK correction to LDA yields excellent results in many (but not all) cases, showing that a current-dependent functional can correct the over-polarization problem. Naturally, orbital-dependent functionals also account for this effect[282], but at much higher computational cost.

C. Solids

Again, in trying to use TDDFT to calculate the optical response of insulators, local approximations has been shown to fail badly. Most noticeably, they do not describe excitonic effects[283], or the exciton spectrum within the band gap. On top of this, the gap is usually much smaller than experiment, because adiabatic appoximations cannot change the gap size from its KS value.

One approach is using the VK approximation in TDCDFT. This has proven rather successful, although a single empirical factor was needed to get agreement with experiment[284–286]. An alternative is to study the many-body problem[287], and ask which expressions must the XC kernel include in order to yield an accurate absorption spectrum[288, 289]. However, the presently available schemes require an expensive GW calculation in the first place[290]. A recent review can be found in Ref. [291].

D. Charge transfer

As is usually the case whenever a method is shown to work well, it starts being applied to many cases, and specific failures appear. Charge transfer excitations are of great importance in photochemistry, especially of biological systems, but many workers have now found abysmal results with TDDFT for these cases.

This can be understood from the fact that TDDFT is a linear response theory. When an excitation moves charge from one area in a molecule to another, both ends will relax. In fact, charge transfer between molecules can be well-approximated by ground-state density functional calculations of the total energies of the species involved. But TDDFT must deduce the correct transitions by infinitesimal perturbations around the ground-state, without an relaxation. Thus it seems a poor problem to tackle with linear response. Many researchers are studying this problem, to understand it and find practical solutions around it[88, 292–295].

VIII. OTHER TOPICS

In this chapter, we discuss several topics of specialized interest, where TDDFT is being applied and developed in ways other than simple extraction of excitations from linear response.

In the first of these, we show how TDDFT can be used to construct entirely new approximations to the ground-state XC energy. This method is particularly useful for capturing the long-range fluctuations that produce dispersion forces between molecules, which are notoriously absent from most ground-state approximations.

In the second, we briefly survey strong field applications, in which TDDFT is being used to model atoms and molecules in strong laser fields. We find that it works well and easily for some properties, but less so for others.

In the last, we discuss the more recent, hot area of molecular electronics. Here, many workers are using ground-state DFT to calculate transport characteristics, but a more careful formulation can be done only within (and beyond) TDDFT. We review recent progress toward a more rigorous formulation of this problem.

A. Ground-state XC energy

TDDFT offers a method[296, 298–301] to find more sophisticated ground-state approximate energy functional using the frequency-dependent response function. Below we introduce the basic formula and discuss some of the exciting systems this method is being used to study.

This procedure uses the adiabatic connection

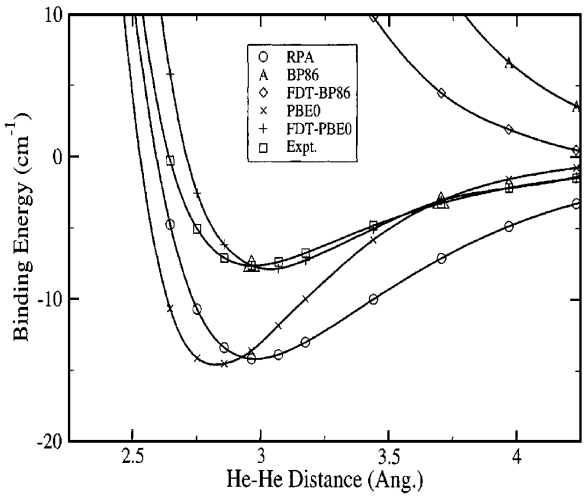

FIG. 15: Binding energy for the Helium dimer interacting via Van der Waals (VdW) forces, from Ref. [296]. Using the fluctuation-dissipation theorem (FDT), new XC energy functionals may be constructed using any ground-state functional. The curves from the standard ground-state functionals BP86[5, 297] and PBE[7] are given, as well as the FDT- curves with these as input. Clearly the FDT is needed to accurately describe VdW interaction.

fluctuation-dissipation formula:

$$E_{\rm XC}[n_0] = \frac{1}{2}\int_0^1 d\lambda \int d^3r \int d^3r' \, \frac{P^\lambda(r,r')}{|\mathbf{r}-\mathbf{r}'|} \qquad (61)$$

where the pair density is

$$P^\lambda(r,r') = -\left(\sum_{\sigma\sigma'}\int_0^\infty \frac{d\omega}{\pi}\chi^\lambda_{\sigma\sigma'}[n_0](\mathbf{r}\mathbf{r}';i\omega)\right) - n_0(\mathbf{r})\delta^{(3)}(\mathbf{r}-\mathbf{r}')$$

and the coupling-constant λ is defined to multiply the electron-electron repulsion in the Hamiltonian, but the external potential is adjusted to keep the density fixed[302, 303]. $\chi^\lambda_{\sigma\sigma'}$ is given by Eq (42) with the XC kernel $f^\lambda_{{\rm XC}\sigma\sigma'}$. Any approximation to the XC kernel yields a sophisticated XC energy $E_{\rm XC}[n]$.

It is interesting that if we set XC effects to zero in conventional DFT, we end up with the highly inaccurate Hartree method of 1928. However when calculating the linear response, if the XC kernel is zero (i.e. within the random phase approximation), the XC energy calculated using Eq. (61) still gives useful results.

Computationally this procedure is far more demanding than conventional DFT, but as the above example has shown, even poor approximations to the XC kernel can still lead to good results. Using this method to find the XC energy has the ability to capture effects such as dynamical correlation or Van der Waal interactions, which are missing from conventional ground-state DFT approximations, and are thought to be important in biological systems.

In particular, the coefficient in the decay of the energy between two such pieces (C_6 in $E \to -C_6/R^6$, where R is their separation) can be accurately (within about 20%) evaluated using a local approximation to the frequency-dependent polarizability[299, 304–306]. In Fig. 15, the binding energy curve for two Helium atoms interacting via Van der Waals is shown. Using the fluctuation-dissipation formula, Eq. (61), and the PBE0 XC kernel clearly gives more accurate results than semi-local functionals. Recently, the frequency integral in Eq. (61) has been performed explicitly but approximately, yielding an explicit non-local density functional[299, 301, 304, 307–312] applicable at all separations. TDDFT response functions have also been used in the framework of symmetry-adapted perturbation theory to generate accurate binding energy curves of Van der Waals molecules [313].

One can go the other way, and try using Eq. (61) for all bond lengths[314, 315].In fact, Eq (61) provides a KS density functional that allows bond-breaking without artifical symmetry breaking[300]. In the paradigm case of the H_2 molecule, the binding energy curve has no Coulson-Fischer point, and the dissociation occurs correctly to two isolated H atoms. Unfortunately, simple approximations, while yielding correct results near equilibrium and at infinity, produce an unphysical repulsion at large but finite separations. This can be traced back[300] to the lack of double excitations in any adiabatic $f_{\rm XC}$. Study of the convergence of $E_{\rm XC}$ with basis sets has also led to an obvious flaw in the ALDA kernel at short distances[296].

Further work is needed to find accurate XC kernels. One method[298] to test these is by examining the uniform electron gas as the frequency dependend susceptibility can be found easily and uses the well known Lindhard function. Hence different approximate XC kernels may be tested and their results compared to highly accurate Monte-carlo simulations.

B. Strong fields

Next we turn our attention to the non-perturbative regime. Due to advances in laser technology over the past decade, many experiments are now possible in regimes where the laser field is stronger than the nuclear attraction[11]. The time-dependent field cannot be treated perturbatively, and even solving the time-dependent Schrödinger equation in three dimensions for the evolution of two interacting electrons is barely feasible with present-day computer technology[316].

For more electrons in a time-dependent field, wavefunc-

tion methods are prohibitive, and in the regime of (not too high) laser intensities, where the electron-electron interaction is still of importance, TDDFT is essentially the only practical scheme available[317–323]. There are a whole host of phenomena that TDDFT might be able to predict: high harmonic generation, multi-photon ionization, above-threshold ionization, above-threshold dissociation, etc., but only if accurate approximations are available.

With the recent advent of atto-second laser pulses, the electronic time-scale has become accessible. Theoretical tools to analyze the dynamics of excitation processes on the attosecond time scale will become more and more important. An example of such a tool is the time-dependent electron localization function (TDELF) [325, 326]. This quantity allows the time-resolved observation of the formation, modulation, and breaking of chemical bonds, thus providing a visual understanding of the dynamics of excited electrons (for an example see Ref. [324]). The natural way of calculating the TDELF is from the TDKS orbitals.

High harmonic generation (HHG) is the production from medium intensity lasers of very many harmonics (sometimes hundreds) of the input intensity. Here TDDFT calculations have been rather succesful for atoms [327–329] and molecules[330, 331]. Recent experiments have used the HHG response of molecules to determine their vibrational modes[332]. Calculations have been performed using traditional scattering theory[333]. If this method grows to be a new spectroscopy, perhaps the electron scattering theory of Sec VI D will be used to treat large molecules.

Multi-photon ionization occurs when an atom or molecule loses more than one electron in an intense field. About a decade ago, this was discovered to be a non-sequential process, i.e., the probability of double ionization can be much greater than the product of two independent ionization events, leading to a 'knee' in the double ionization probability as a function of intensity[334–336]. TDDFT calculations have so far been unable to accurately reproduce this knee, and it has recently been shown that a correlation-induced derivative discontinuity is needed in the time-dependent KS potential[185].

Above-threshold ionization (ATI) refers to the probability of ionization when the laser frequency is less than the ionization potential, i.e., it does not occur in linear response[337, 338]. Again, this is not well given by TDDFT calculations, but both this and MPI require knowledge of the correlated wavefunction, which is not directly available in a KS calculation.

Since the ionization threshold plays a crucial role in most strong field phenomena, Koopmans theorem relating the energy level of the KS HOMO to the ionization energy must be well satisfied. This suggests the use of self-interaction free methods such as OEP[159, 173] or LDA-SIC rather than the usual DFT approximations (LDA,GGA,etc), with their poor potentials (see Fig. 3 in Sec. II B).

The field of quantum control has mainly concentrated on the motion of the nuclear wave packet on a given set of precalculated potential energy surfaces, the ultimate goal being the femto-second control of chemical reactions [339]. With the advent of atto-second pulses, control of electronic dynamics has come within reach. A marriage of optimal-control theory with TDDFT appears to be the ideal theoretical tool to tackle these problems[340, 341]. Recent work[342–344] has shown the ability of TDDFT to predict the coherent control of quantum wells using Terahertz lasers. However they remains many difficulties and challenges, including the coupling between nuclei and electrons[345–347], in order to develop a general purpose theory.

C. Transport

There is enormous interest in transport through single molecules as a key component in future nanotechnology[348]. Present formulations use ground-state density functionals to describe the stationary non-equilibrium current-carrying state[349]. But several recent suggestions consider this as a time-dependent problem[350–353], and use TD(C)DFT for a full description of the situation. Only time will tell if TDDFT is really needed for an accurate description of these devices.

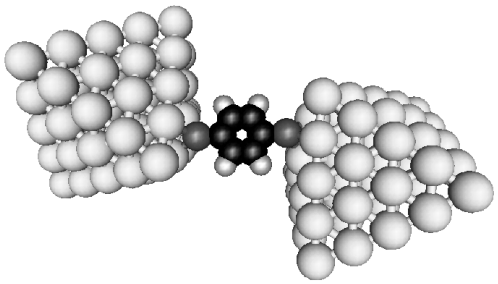

FIG. 16: Schematic representation of a benzene-1,4-di-thiol molecule between two gold contacts. The molecule plus gold pyramids (55 atoms each) constitute the *extended molecule* as used in the DFT calculations for the Landauer approach.

Imagine the setup shown in Fig. 16 where a conducting molecule is sandwiched between two contacts which are connected to semi-infinity leads. The Landauer formula for the current is

$$I = \frac{1}{\pi}\int_{-\infty}^{\infty} dE\; T(E)[f_L(E) - f_R(E)] \qquad (62)$$

where $T(E)$ is the transmission probability for a given energy and $f_{L/R}(E)$ is the Fermi distribution function

for the left/right lead. The transmission probability can be written using the non-equilibrium Green's functions (NEGF) of the system. Ground-state DFT is used to find the KS orbitals and energies of the extended molecule and used to find the self-energies of the leads. These are then fed into the NEGF method, which will determine $T(E)$ and hence the current.

The NEGF scheme has had a number of successes, most notably for atomic-scale point contacts and metallic wires. Generally it does well for systems where the conductance it high. However, it was found that for molecular wires, the conductance is overestimated by $1-3$ orders of magnitude. Various explanations for this and the problems with DFT combined with NEGF in general have been suggested.

Firstly, the use of the KS orbitals and energy levels has no theoretical basis. The KS orbitals are those orbitals for the non-interacting problem that reproduce the correct ground-state density. They should not be thought of as the true single-particle excitations of the true system. However as we have seen they often reproduce these excitations qualitatively, so it is not clear to what extent this problem affects the conductance.

The geometry of the molecules was also suggested as a source of error. DFT first relaxes the molecule to find its geometry, whereas in the experiments the molecule may be subject to various stresses that could rotate parts of it and/or squash parts together. However calculations have shown that the geometry corrections are small[354].

The approximation that the non-equilibrium XC functional is the same as for the static case has been suggested as a major source of error. In fact neither the HK theorem nor the RG theorem are strictly valid for current-carrying systems in homogeneous electric fields. A dynamical correction to the LDA functional for the static case has been derived using the Vignale-Kohn functional TDCDFT but were found to yield only small corrections to ALDA[355].

In a similar vein, the lack of the derivative discontinuity and self interacting errors (SIE) in the approximations to the XC functional may be the source of the problem[354]. In Hartree-Fock (HF) calculations (and also in OPM calculations[282] with EXX, exact exchange), which have no SIE, the conductances come out a lot lower in most regions[356]. Also calculations have been done using a simple model[357] with a KS potential with a derivative discontinuity. The I-V curves for this system are significantly different from those predicted by LDA. This problem is most severe when the molecule is not strongly coupled to the leads, but goes away when it is covalently bonded. Recent OEP calculations of the transmission along a H-atom chain verify these features[356].

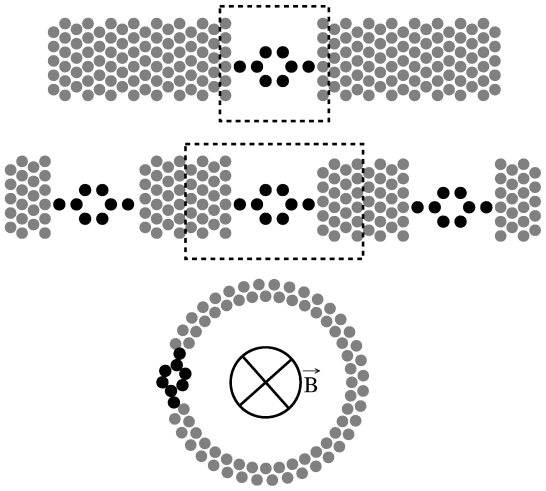

FIG. 17: Ring geometry for gauge transformation of electric fields.

Despite these problems, quantitative results can be found for molecular devices. By looking at what bias a KS energy level gets moved between the two chemical potentials of the leads (and hence by Eq. (62) there should be a conductance peak), one can qualitatively predict postitions of these peaks[358], although the magnitude of the conductance may be incorrect by orders of magnitude.

Since transport is a non-equilibrium process, we should expect that using static DFT will not be able to accurately predict all the features. Recently a number of methods have been suggested to use TDDFT to calculate transport. In Ref. [359], the authors present a practical scheme using TDDFT to calculate current. The basic idea is to 'pump' the system into a non-equilibrium initial state by some external bias and then allow the KS orbitals to evolve in time via the TDKS equations. The RG theorem then allows one to extract the longitudinal current using the continuity equation. Using transparent boundary conditions in the leads (these solve problems with propagating KS in the semi-infinite leads) and using an iterative procedure to get the correct initial state, they are able to find the steady state current.

An alternative formulation uses periodic boundary conditions and includes dissipation[360]. In the Landauer-Büttiker formulism, dissipation effects due to electron-electron interaction and electron-phonon interaction are neglected as the molecule is smaller than the scattering length. However, there would be scattering in the leads. Imagine a molecule in the ring geometry, with a spatially constant electric field. Via a gauge transformation, this can be replaced by a constant time-dependent magnetic field through the center of the ring. If there is no dissipation, the electrons would keep accelerating indefinitely and never reach a steady state.

In the classical Boltzmann equation for transport, scattering is included via a dissipation term using τ, the average collision time. A master equation approach is basically a generalization of the Boltzmann equation to a fully quantum mechanical system. The master equation is based on the Louville equation in quantum mechanics and for a quantum mechanical density coupled to a heat bath (or reservoir), it is written as

$$\frac{d}{dt}\hat{\rho}(t) = -\imath[H, \hat{\rho}(t)] + \mathbf{C}[\hat{\rho}(t)] \tag{63}$$

where $\mathbf{C}$ is a superoperator acting on the density whose elements are calculated using Fermi's Golden rule with V_{el-ph} in a certain approximation (weak coupling and instantaneous processes). A KS master equation[353] can be set up, modifying $\mathbf{C}$ for single particle reduced density matrices so that it will give the correct steady state. The TDKS equations are then used to propagate forward in time until the correct steady state density is found. The current in then extracted from this. Recent calculations have shown it can give correct behaviour, such as hysteresis in I-V curves.[352, 361]

IX. SUMMARY

We hope we have conveyed some of the spirit and excitement of TDDFT in this non-comprehensive review. We have explained what TDDFT is, and where it comes from. We have shown that it is being used, and often works well, for many molecular excitations. Its usefulness lies neither in high accuracy nor reliability, but in its qualitative ability to yield roughly correct absorption spectra for molecules of perhaps several hundred atoms. Thus we emphasize that, usually, there are many excitations of the same symmetry, all coupled together, and that these are the circumstances under which the theory should be tested. For many molecular systems, TDDFT is now a routine tool that produces useful accuracy with reasonable confidence.

That said, we have discussed some of the areas where TDDFT in its current incarnation is not working, such as double excitations, charge transfer, and extended systems. But there has been significant progress in two out of three of these, both in understanding the origin of the problem, and finding alternative approaches that may ultimately yield a practical solution. We also studied how well TDDFT works for a few cases where the exact ground-state solution is known, describing the accuracy of different functionals. We also surveyed some applications beyond simple linear response for optical absorption, such as ground-state functionals from the adiabatic connection, strong fields, and transport. In each of these areas, more development work seems needed before TDDFT calculations can become a routine tool with useful accuracy.

Many wonder how long DFT's preemminence in electronic structure can last. For sure, Kohn-Sham DFT is a poor player that struts and frets his hour upon the stage of electronic structure, and then is heard no more. After all, its predecessor, Thomas-Fermi theory, is now obsolete, being too inaccurate for modern needs. Many alternatives for electronic excitations, such as GW, are becoming computationally feasible for interesting systems. But we believe DFT, and TDDFT, should dominate for a few decades yet.

We thank Michael Vitarelli for early work and Dr. Meta van Faassen and Dr. Max Koentopp for providing figures. K.B. gratefully acknowledges support of the US Department of Energy, under grant number DE-FG02-01ER45928, and the NSF, under grant CHE-0355405. This work was supported, in part, by the Center for Functional Nanostructures (CFN) of the Deutsche Forschungsgemeinschaft (DFG) within project C3.9, the EXC!TiNG Research and Training Network of the European Union and the NANOQUANTA Network of Excellence.

[1] *Inhomogeneous electron gas*, P. Hohenberg and W. Kohn, Phys. Rev. **136**, B 864 (1964).

[2] *Self-consistent equations including exchange and correlation effects*, W. Kohn and L.J. Sham, Phys. Rev. **140**, A 1133 (1965).

[3] R.M. Dreizler and E.K.U. Gross, *Density Functional Theory* (Springer-Verlag, Berlin, 1990).

[4] *Electron densities in search of Hamiltonians*, M. Levy, Phys. Rev. A **26**, 1200 (1982).

[5] *Density-functional exchange-energy approximation with correct asymptotic behavior*, A.D. Becke, Phys. Rev. A **38**, 3098 (1988).

[6] *Development of the Colle-Salvetti correlation-energy formula into a functional of the electron density*, C. Lee, W. Yang, and R.G. Parr, Phys. Rev. B **37**, 785 (1988).

[7] *Generalized gradient approximation made simple*, J.P. Perdew, K. Burke, and M. Ernzerhof, Phys. Rev. Lett. **77**, 3865 (1996); **78**, 1396 (1997) (E).

[8] *Density-functional thermochemistry. III. The role of exact exchange*, A.D. Becke, J. Chem. Phys. **98**, 5648 (1993).

[9] *The performance of semi-local and hybrid density functionals in 3d transition metal chemistry*, F. Furche and J.P. Perdew, J. Chem. Phys. **124**, 044103 (2006).

[10] *see www.turbomole.com*

[11] *Time-Dependent Density-Functional Theory*, M.A.L. Marques and E.K.U. Gross, Annu. Rev. Phys. Chem. **55**, 427 (2004).

[12] *Time-dependent density functional theory in quantum chemistry*, F. Furche and K. Burke, in *Annual Reports*

in Computational Chemistry, Vol 1, ed by D. Spellmeyer (Elsevier, Amsterdam, 2005), pg. 19-30.

[13] *Ten topical questions in time-dependent density functional theory*, N. T. Maitra, K. Burke, H. Appel, E.K.U. Gross, and R. van Leeuwen, in *Reviews in Modern Quantum Chemistry: A celebration of the contributions of R. G. Parr*, ed. K. D. Sen, (World-Scientific, 2001).

[14] *A guided tour of time-dependent density functional theory*, K. Burke and E.K.U. Gross, in *Density functionals: Theory and applications*, ed. D. Joubert (Springer, Berlin, 1998).

[15] *Density Functional Theory of Time-Dependent Phenomena*, E.K.U. Gross, J.F. Dobson, and M. Petersilka, Topics in Current Chemisty, **181**, 81 (1996).

[16] *Density-functional theory for time-dependent systems*, E. Runge and E.K.U. Gross, Phys. Rev. Lett. **52**, 997 (1984).

[17] *Dichtefunktionalmethoden für elektronisch angeregte Moleküle. Theorie, Implementierung und Anwendung*, F. Furche, Ph.D. thesis, Universität Karlsruhe, (2002).

[18] *Auxiliary basis sets for main row atoms and transition metals and their use to approximate Coulomb potentials*, K. Eichkorn, F. Weigend, O. Treutler and R. Ahlrichs, Theor. Chem. Acc. **97**, 119 (1997).

[19] *Absolute configuration of chiral fullerenes and covalent derivatives from their calculated circular dichroism spectra*, H. Goto, N. Harada, J. Crassous and F. Diederich, J. Chem. Soc., Perkin Trans. **2**, 1719 (1998).

[20] *Pentacyanoiron(II) as an electron donor group for nonlinear optics: Medium-responsive properties and comparisons with related pentaammineruthenium(II) complexes*, B.J. Coe, J.L. Harries,M. Helliwell, L.A. Jones, I. Asselberghs, K. Clays, B.S. Brunschwig, J.A. Harris, J. Garin and J. Orduna, J. Amer. Chem. Soc. **128**, 12192 (2006).

[21] *Studies of the 5 '-substituted phenylisoquinoline-based iridium complexes using density functional theory*, C.H. Yang, W.L. Su, K.H. Fang, S.P. Wang and I.W. Sun, Organometallics **25**, 4514 (2006).

[22] *Density-functional theory investigation of the geometric, energetic, and optical properties of the cobalt(II)tris(2,2 '-bipyridine) complex in the high-spin and the Jahn-Teller active low-spin states*, A. Vargas, M. Zerara, E. Krausz, A. Hauser and L.M.L. Daku, J. Chem. Theory Comput. **2**, 1342 (2006).

[23] *Photon-, electron-, and proton-induced isomerization behavior of ferrocenylazobenzenes*, A. Sakamoto, A. Hirooka, K. Namiki, M. Kurihara, M. Murata, M. Sugimoto and H. Nishihara, Inorg. Chem. **44**, 7547 (2005).

[24] *Computational and spectroscopic studies of Re(I) bipyridyl complexes containing 2,6-dimethylphenylisocyanide (CNx) ligand*, S.R. Stoyanov, J.M. Villegas, A.J. Cruz, L.L. Lockyear, J.H. Reibenspies and D.P. Rillema, J. Chem. Theory Comput. **1**, 95 (2005).

[25] *Theoretical study of Ln(III) complexes with polyazaaromatic ligands: Geometries of [LnL(H2O)(n)](3+) complexes and successes and failures of TD-DFT*, F. Gutierrez, C. Rabbe, R. Poteau and J.P. Daudey, J. Phys. Chem. A **109**, 4325 (2005).

[26] *Importance of vibronic effects on the circular dichroism spectrum of dimethyloxirane*, J. Neugebauer, E.J. Baerends, M. Nooijen and J. Autschbach, J. Chem. Phys. **122**, 234305 (2005).

[27] *Vibronic coupling in square planar complexes of palladium(II) and platinum(II)*, E. Lanthier, C. Reber and T. Carrington, Chem. Phys. **329**, 90 (2006).

[28] *X-ray absorption spectroscopy of titanium oxide by time dependent density functional calculations*, G. Fronzoni, R. Francesco, M. Stener and M. Causa, J. Phys. Chem. B **110**, 9899 (2006).

[29] *First hyperpolarizability of a sesquifulvalene transition metal complex by time-dependent density-functional theory*, W. Hieringer and E.J. Baerends, J. Phys. Chem. A **110**, 1014 (2006).

[30] *Theoretical studies of cyclometalated phenylpyrazol Ir(III) complex using density functional theory*, N.G. Park, G.C. Choi, J.E. Lee and Y.S. Kim, Current Appl. Phys. **5**, 79

[31] *Synthesis, characterization, and photochemical and computational investigations of Ru(II) heterocyclic complexes containing 2,6-dimethylphenylisocyanide (CNx) ligand*, J.M. Villegas, S.R. Stoyanov, W. Huang, L.L. Lockyear, J.H. Reibenspies and D.P.Rillema, Inorg. Chem. **43**, 6383 (2004).

[32] *Contrasting linear and quadratic nonlinear optical behavior of dipolar pyridinium chromophores with 4-(dimethylamino)phenyl or ruthenium(II) ammine electron donor groups*, B.J. Coe, J.A. Harris, B.S. Brunschwig, J. Garin, J. Orduna, S.J. Coles and M.B. Hursthouse, J. Am. Chem. Soc. **126**, 10418 (2004).

[33] *The charge transfer band solvent-dependence of [Ru(bpy)(2)(CNx)Cl](+) CNx=2,6-dimethylphenylisocyanide: a polarizable continuum model/time-dependent density functional theory study*, S.R. Stoyanov, J.M. Villegas and D.P. Rillema, Inorg. Chem. Comm. **7**, 838 (2004).

[34] *Time-dependent density functional theory study of the absorption spectrum of [Ru(4,4 '-COOH-2,2 '-bpy)(2)(NCS)(2)] in water solution: influence of the pH*,
F. De Angelis, S. Fantacci and A. Selloni, Chem. Phys. Lett. **389**, 204 (2004).

[35] *On the origin of the optical activity in the d-d transition region of tris-bidentate Co(III) and Rh(III) complexes*, F.E. Jorge,J. Autschbach and T. Ziegler, Inorg. Chem. **42**, 8902 (2003).

[36] *Simulation of x-ray absorption near-edge spectra and x-ray fluorescence spectra of optically excited molecules*, R.K. Pandey and S. Mukamel, J. Chem. Phys. **124**, 094106 (2006).

[37] *Time-dependent density functional theory calculations of ligand K edge and metal L edge X-ray absorption of a series of oxomolybdenum complexes*, G. Fronzoni, A. Stener, A. Reduce and P. Decleva, J. Phys. Chem. A **108**, 8467 (2004).

[38] *TD-DFT investigation on the low-lying excited states of spiro-bithiophene*, S.Y. Yang, Y.H. Kan, G.C. Yang, Z.M. Su and L. Zhao, Chem. Phys. Lett. **429**, 180 (2006).

[39] *Structure absorption spectra correlation in a series of 2,6-dimethyl-4-arylpyrylium salts*, N. Manoj, G. Ajayakumar, K.R. Gopidas and C.H. Suresh, J. Phys. Chem. A **110**, 11338 (2006).

[40] *Optical properties of N-succinimidyl bithiophene and the effects of the binding to biomolecules: Comparison between coupled-cluster and time-dependent density functional theory calculations and experiments*, E. Fabiano,

F. Della Sala, G. Barbarella, S. Lattante, M. Anni, G. Sotgiu, C. Hattig, R. Cingolani and G. Gigli, J. Phys. Chem. B **110**, 18651 (2006).

[41] *Time dependent density functional theory study of electronic absorption properties of lead(II) complexes with a series of hydroxyflavones*, C. Lapouge and J.P. Cornard, J. Phys. Chem. A **109**, 6752 (2005).

[42] *Optical properties and delocalization of excess negative charges on oligo(phenylenevinylene)s: A quantum chemical study*, S. Fratiloiu, F.C. Grozema and L.D.A. Siebbeles, J. Phys. Chem. B **109**, 5644 (2005).

[43] *A first principles calculations and experimental study of the ground- and excited-state properties of ladder oligo(p-aniline)s*, M. Belletete, G. Durocher, S. Hamel, M. Cote, S. Wakim and M. Leclerc, J. Chem. Phys. **122**, 104303 (2005).

[44] *Electronic and optical properties of functionalized carbon chains with the localized Hartree-Fock and conventional Kohn-Sham methods*, M. Weimer, W. Hieringer, F. Della Sala and A. Gorling, Chem. Phys. **309**, 77 (2005).

[45] *Structural, electronic, and optical properties of the diindenoperylene molecule from first-principles density-functional theory*, L.M. Ramaniah and M. Boero, Phys. Rev. A **74**, 042505 (2006).

[46] *On the electronic properties of dehydrogenated polycyclic aromatic hydrocarbons*, D.L. Kokkin and T.W. Schmidt, J. Phys. Chem. A **110**, 6173 (2006).

[47] *Electronic transitions of thiouracils in the gas phase and in solutions: Time-dependent density functional theory (TD-DFT) study*, M.K. Shukla and J. Leszczynski, J. Phys. Chem. A **108**, 10367 (2004).

[48] *s-tetrazine in aqueous solution: A density functional study of hydrogen bonding and electronic excitations*, M. Odelius, B. Kirchner and J. Hutter, J. Phys. Chem. A **108**, 2044 (2004).

[49] *Observation and interpretation of annulated porphyrins: Studies on the photophysical properties of meso-tetraphenylmetalloporphyrins*, J.E. Rogers, K.A. Nguyen, D.C. Hufnagle, D.G. McLean, W.J. Su, K.M. Gossett, A.R. Burke, S.A. Vinogradov, R. Pachter and P.A. Fleitz, J. Phys. Chem. A **107**, 11331 (2003).

[50] *DFT and TDDFT study related to electron transfer in nonbonded porphine center dot center dot center dot C-60 complexes*, T.L.J. Toivonen, T.I. Hukka, O. Cramariuc, T.T. Rantala and H. Lemmetyinen, J. Phys. Chem. A **110**, 12213 (2006).

[51] *Optical absorption and electron energy loss spectra of carbon and boron nitride nanotubes: a first-principles approach*, A.G. Marinopoulos, L. Wirtz, A. Marini, V. Olevano, A. Rubio and L. Reining, Appl. Phys. A **78**, 1157 (2004).

[52] *Real-time Ab initio simulations of excited carrier dynamics in carbon nanotubes*, Y. Miyamoto, A. Rubio and D. Tomanek, Phys. Rev. Lett. **97**, 126104 (2006).

[53] *Photoelectron spectroscopy of C-84 dianions*, O.T. Ehrler, J.M. Weber, F. Furche and M.M. Kappes, Phys. Rev. Lett. **91**, 113006 (2003).

[54] *Photoelectron spectroscopy of fullerene dianions C-76(2-), C-78(2-), and C-84(2-)*, O.T. Ehrler, F. Furche, J.M. Weber and M.M. Kappes, J. Chem. Phys. **122**, 094321 (2005).

[55] *Optical and loss spectra of carbon nanotubes: Depolarization effects and intertube interactions*, A.G. Marinopoulos, L. Reining, A. Rubio, and N. Vast, Phys. Rev. Lett. **91**, 046402 (2003).

[56] *Structures and electronic absorption spectra of a recently synthesised class of photodynamic therapy agents*, A.D. Quartarolo, N. Russo and E. Sicilia, Chem.-Eur. J. **12**, 6797 (2006).

[57] *Are conical intersections responsible for the ultrafast processes of adenine, protonated adenine, and the corresponding nucleosides?*, S.B. Nielsen and T.I. Solling, ChemPhysChem **6**, 1276 (2005).

[58] *Molecular dynamics in electronically excited states using time-dependent density functional theory*, I. Tavernelli, U.F. Rohrig and U. Rothlisberger, Mol. Phys. **103**, 963 (2005).

[59] *A TDDFT study of the optical response of DNA bases, base pairs, and their tautomers in the gas phase*, A. Tsolakidis and E. Kaxiras, J. Phys. Chem. A **109**, 2373 (2005).

[60] *Calculating absorption shifts for retinal proteins: Computational challenges*, M. Wanko, M. Hoffmann, P. Strodet, A. Koslowski, W. Thiel, F. Neese, T. Frauenheim and M. Elstner, J. Phys. Chem. B **109**, 3606 (2005).

[61] *A time-dependent density functional theory investigation of the spectroscopic properties of the beta-subunit in C-phycocyanin*, Y.L. Ren, J. Wan, X. Xu, Q.Y. Zhang and G.F. Yang, J. Phys. Chem. B **110**, 18665 (2006).

[62] *Linear and nonlinear optical response of aromatic amino acids: A time-dependent density functional investigation*, J. Guthmuller and D. Simon, J. Phys. Chem. A **110**, 9967 (2006).

[63] *Time dependent density functional theory modeling of chiroptical properties of small amino acids in solution*, M.D. Kundrat and J. Autschbach, J. Phys. Chem. A **110**, 4115 (2006).

[64] *Theoretical study on photophysical and photosensitive properties of aloe emodin*, L. Shen, H.F. Ji and H.Y. Zhang, Theochem-J. Mol. Struct. **758**, 221 (2006).

[65] *Electronically excited states of tryptamine and its microhydrated complex*, M. Schmitt, R. Brause, C.M. Marian, S. Salzmann and W.L. Meerts, J. Chem. Phys. **125**, 124309 (2006).

[66] *Photoinduced processes in protonated tryptamine*, H. Kang, C. Jouvet, C. Dedonder-Lardeux, S. Martrenchard, C. Charriere, G. Gregoire, C. Desfrancois, J.P. Schermann, M. Barat and J.A. Fayeton, J. Chem. Phys. **122**, 084307 (2005).

[67] *A TDDFT study of the excited states of DNA bases and their assemblies*, D. Varsano, R. Di Felice, M.A.L. Marques and A. Rubio, J. Phys. Chem. B **110**, 7129 (2006).

[68] *TD-DFT calculations of the potential energy curves for the trans-cis photo-isomerization of protonated Schiff base of retinal*, H. Tachikawa and T. Iyama, J. Photochem. Photobiol. B: Biol. **76**, 55 (2004)

[69] *Time-dependent density-functional approach for biological chromophores: The case of the green fluorescent protein*, M. A. L. Marques, X. Lopez, D. Varsano, A. Castro, and A. Rubio, Phys. Rev. Lett. **90**, 258101 (2003).

[70] *Optical absorption of the blue fluorescent protein: A first-principles study*, X. Lopez, M.A.L. Marques, A. Castro and A. Rubio, J. Am. Chem. Soc. **127**, 12329 (2005).

[71] *Single-Reference Calculations of Photochemical Potential Energy Surfaces:Time-Dependent Density-*

Functional Theory Calculations of the Con- and Disrotatory Surfaces for the Woodward-Hoffmann CC Ring-Opening of Oxirane, F. Cordova, L.J. Doriol, A. Ipatov, M.E. Casida and A. Vela, to be published (2006).

[72] *Theoretical predictions for occurrence of charge transfer complex within the two synthesized bichromophores considering the role of their spacers in interactions with the pi-orbitals of the redox centers*, A.K. De and T. Ganguly, Chem. Phys. Lett. **428**, 213 (2006).

[73] *Three-dimensional non linear optical chromophores based on metal-to-ligand charge-transfer from ruthenium(II) or iron(II) centers*, B.J. Coe, J.A. Harris, B.S. Brunschwig, I. Asselberghs, K. Clays, J. Garin and J. Orduna, J. Amer. Chem. Soc. **127**, 13399 (2005).

[74] *NLO properties of metallabenzene-based chromophores: A time-dependent density functional study*, A. Karton, M.A. Iron, M.E. van der Boom and J.M.L. Martin, J. Phys. Chem. A **190**, 5454 (2005).

[75] *A time dependent density functional theory study of alpha-84 phycocyanobilin in C-phycocyanin*, J. Wan, X. Xu, Y.L. Ren and G.F. Yang, J. Phys. Chem. B **109**, 11088 (2005).

[76] *Photoionization cross section and angular distribution calculations of carbon tetrafluoride*, B. Toffoli, M. Stener, G. Fronzoni and P. Decleva, J. Chem. Phys. **124**, 214313 (2006).

[77] *Time-dependent density functional theory determination of the absorption spectra of naphthoquinones*, D. Jacquemin, J. Preat, V. Wathelet and E.A. Perpete, Chem. Phys. **328**, 324 (2006).

[78] *A Theoretical Investigation of the Ground and Excited States of Coumarin 151 and Coumarin 120*, R.J. Cave, K. Burke, and E.W. Castner Jr., J. Phys. Chem. A **106**, 9294 (2002).

[79] *A TD-DFT study on triplet excited-state properties of curcumin and its implications in elucidating the photo sensitizing mechanisms of the pigment*, L. Shen, H.F. Ji and H.Y. Zhang, Chem. Phys. Lett. **409**, 300 (2005).

[80] *Time-dependent density functional theory investigation of the absorption, fluorescence, and phosphorescence spectra of solvated coumarins*, D. Jacquemin, E.A. Perpete, G. Scalmani, M.J. Frisch, X. Assfeld, I. Ciofini and C. Adamo, J. Chem. Phys. **125**, 164324 (2006).

[81] *TDDFT investigation of the optical properties of cyanine dyes*, B. Champagne, M. Guillaume and F. Zutterman, Chem. Phys. Lett. **425**, 105 (2006).

[82] *Excitation spectra of nitro-diphenylaniline: Accurate time-dependent density functional theory predictions for charge-transfer dyes*, D. Jacquemin, M. Bouhy and E.A. Perpete, J. Chem. Phys. **124**, 204321 (2006).

[83] *Spectral properties of bipyridyl ligands by time-dependent density functional theory*, F. Labat, P.P. Laine, I. Ciofini and C. Adamo, Chem. Phys. Lett. **417**, 445 (2006).

[84] *Photoinduced intramolecular charge transfer reaction in (E)-3-(4-Methylamino-phenyl)-acrylic acid methyl ester: A fluorescence study in combination with TDDFT calculation*, A. Chakraborty, S. Kar, D.N. Nath and N. Guchhait, J. Phys. Chem. A **110**, 12089 (2006).

[85] *Theoretical analysis of low-lying charge transfer states in [Ru(X) (Me)(CO)(2)(Me-DAB)] (X=Cl, I; DAB=1 4-diaza-1,3-butadiene) complexes by TDDFT and CASSCF/CASPT2 methods*, N. Ben Amor, S. Zalis and C. Daniel, Int. J. Quant. Chem. **106**, 2458 (2006).

[86] *Charge-transfer pi pi* excited state in the 7-azaindole dimer. A hybrid configuration interactions singles/time-dependent density functional theory description*, R. Gelabert, M. Moreno and J.M. Lluch, J. Phys. Chem. A **110**, 1145 (2006).

[87] *Hartree-Fock exchange in time dependent density functional theory: application to charge transfer excitations in solvated molecular systems*, L. Bernasconi, M. Sprik and R.Hutter, Chem. Phys. Lett. **394**, 141 (2004).

[88] *Time-dependent density-functional theory investigation of the fluorescence behavior as a function of alkyl chain size for the 4-(N,N-dimethylamino)benzonitrile-like donor-acceptor systems 4-(N,N-diethylamino)benzonitrile and 4-(N,N-diisopropylamino)benzonitrile*, C.J. Jamorski and M.E. Casida, J. Phys. Chem. B **108**, 7132 (2004).

[89] *Failure of time-dependent density functional theory for long-range charge-transfer excited states: The zincbacteriochlorin-bacterlochlorin and bacteriochlorophyll-spheroidene complexes*, A. Dreuw and M. Head-Gordon, J. Am. Chem. Soc. **126**, 4007 (2004).

[90] *Photoinduced intramolecular charge transfer in 4-(dimethyl)aminobenzonitrile - A theoretical perspective*, D. Rappoport and F. Furche, J. Am. Chem. Soc. **126**, 1277 (2004).

[91] *Relationship between long-range charge-transfer excitation energy error and integer discontinuity in Kohn-Sham theory*, D.J. Tozer, J. Chem. Phys. **119**, 12697 (2003).

[92] *Rational classification of a series of aromatic donor-acceptor systems within the twisting intramolecular charge transfer model, a time-dependent density-functional theory investigation*, C.J. Jamorski and H.P. Luthi, J. Chem. Phys. **119**, 12852 (2003).

[93] *Electronic transitions in [Re6S8X6](4-) (X = Cl, Br, I): Results from time-dependent density functional theory and solid-state calculations*, L.E. Roy and T. Hughbanks, Inorg. Chem. **45**, 8273 (2006).

[94] *Size dependence of the static polarizabilities and absorption spectra of Ag-n (n=2-8) clusters*, J.C. Idrobo, S. Ogut and J. Jellinek, Phys. Rev. B **72**, 085445 (2005).

[95] *Finite lifetime effects on the polarizability within time-dependent density-functional theory*, L. Jensen, J. Autschbach, and G.C. Schatz, J. Chem. Phys. **122**, 224115 (2005).

[96] *Polarization effects and charge separation in AgCl-water clusters*, S.S.M.C. Godinho, P.C. do Couto and B.J.C. Cabral, J. Chem. Phys. **122**, 044316 (2005).

[97] *Core excitations in MgO: a DFT study with cluster models*, M. Stener, G. Fronzoni and R. De Francesco, Chem. Phys. **309**, 49 (2005).

[98] *Absorption spectra of small silver clusters Ag-n (n=4, 6, 8): A TDDFT study*, G.F. Zhao, Y. Lei and Z. Zeng, Chem. Phys. **327**, 261 (2006).

[99] *Excitonic effects and optical properties of passivated CdSe clusters*, M.L. del Puerto, M.L. Tiago and J.R. Chelikowsky, Phys. Rev. Lett. **97**, 096401 (2006).

[100] *Optical properties of sila-adamantane nanoclusters from density-functional theory*, O. Lehtonen and D. Sundholm, Phys. Rev. B **74**, 045433 (2006).

[101] *A theoretical investigation of hyperpolarizability for small GanAsm (n+m=4-10) clusters*, Y.Z. Lan, W.D.

Cheng, D.S. Wu, J. Shen, S.P. Huang, H. Zhang, Y.J. Gong and F.F. Li, J. Chem. Phys. **124**, 094302 (2006).

[102] *Photochemistry of AgCl-water clusters: Comparison with Cl–water clusters*, S.S.M.C. Godinho, P.C. do Couto and B.J.C. Cabral, Chem. Phys. Lett. **419**, 340 (2006).

[103] *Electronic excited states of Si(100) and organic molecules adsorbed on Si(100)*, N.A. Besley and A.J. Blundy, J. Phys. Chem. B **110**, 1701 (2006).

[104] *Quantum chemical modeling of electrochromism of tungsten oxide films*, E. Broclawik, A. Gora, P. Liguzinski, P. Petelenz and H.A. Witek, J. Chem. Phys. **124**, 054709 (2006).

[105] *Different approaches for the calculation of electronic excited states of nonstoichiometric alkali halide clusters: The example of Na_3F*, G. Durand, M.C. Heitz, F. Spiegelman, C. Meier, R. Mitric, V. Bonacic-Koutecky and J. Pittner, J. Chem. Phys. **121**, 9898 (2004).

[106] *Simple DFT model of clusters embedded in rare gas matrix: Trapping sites and spectroscopic properties of Na embedded in Ar*, B. Gervais, E. Giglio, E. Jacquet, A. Ipatov, P.G. Reinhard and E. Suraud, J. Chem. Phys. **121**, 8466 (2004).

[107] *Real-time study of the adiabatic energy loss in an atomic collision with a metal cluster*, R. Baer and N. Siam, J. Chem. Phys. **121**, 6341 (2004).

[108] *Angular distribution of electrons emitted from Na clusters*, A. Pohl, P.G. Reinhard and E. Suraud, Phys. Rev. A **70**, 023202 (2004).

[109] *Excited states of tetrahedral single-core Si_{29} nanoparticles*, R. Rao, J. Sutin, R. Clegg, E. Gratton, M.H. Nayfeh, S. Habbal, A. Tsolakidis and R.M. Martin, Phys. Rev. B **69**, 205319 (2004).

[110] *Quantum and thermal fluctuation effects on the photoabsorption spectra of clusters*, F. Della Sala, R. Rousseau, A. Gorling and D. Marx, Phys. Rev. Lett. **92**, 183401 (2004).

[111] *Enhanced absorption induced by a metallic nanoshell*, R. Baer, D. Neuhauser and S. Weiss, Nano Lett. **4**, 85 (2004).

[112] *Photoabsorption spectra of Ti8C12 metallocarbohedrynes: Theoretical spectroscopy within time-dependent density functional theory*, J.I. Martinez, A. Castro, A. Rubio and J.A. Alonso, J. Chem. Phys. **125**, 074311 (2006).

[113] *Calculation of the optical spectrum of the Ti8C12 and V8C12 Met-Cars*, J.I. Martinez, A. Castro, A. Rubio, J.M. Poblet and J.A. Alonso, Chem. Phys. Lett. **398**, 292 (2004).

[114] *Electronic distribution and solvatochromism investigation of a model radical (2,2,6,6-tetramethylpiperidine N-oxyl : tempo) through TD-DFT calculations including PCM solvation*, J. Lalevee, X. Allonas and P. Jacques, Theochem-J. Mol. Struct. **767**, 143 (2006).

[115] *The merits of the frozen-density embedding scheme to model solvatochromic shifts*, J. Neugebauer, M.J. Louwerse, E.J. Baerends and T.A. Wesolowski, J. Chem. Phys. **122**, 094115 (2005).

[116] *Solvatochromism of a novel betaine dye derived from purine*, A. Masternak, G. Wenska, J. Milecki, B. Skalski and S. Franzen, J. Phys. Chem. A **109**, 759 (2005).

[117] *On the performance of gradient-corrected approximation functionals and polarizable continuum model in the study of 1,2,3-triazine in water*, C. Zazza and A. Grandi and L. Bencivenni and M. Aschi, Theochem-J. Mol. Struct. **764**, 87 (2006).

[118] *Photophysical properties of trans-3-(4-monomethylamino-phenyl)-acrylonitrile: Evidence of twisted intramolecular charge transfer (TICT) process*, A. Chakraborty, S. Kar and N. Guchhait, Chem. Phys. **324**, 733 (2006).

[119] *Water solvent effect on the first hyperpolarizability of p-nitrophenol and p-nitrophenylphosphate: A time-dependent density functional study*, J. Guthmuller and D. Simon, J. Chem. Phys. **124**, 174502 (2006).

[120] *Geometry and solvent dependence of the electronic spectra of the amide group and consequences for peptide circular dichroism*, J. Sebek, Z. Kejik and P. Bour, J. Phys. Chem. A **110**, 4702 (2006).

[121] *Absorption and emission spectra in gas-phase and solution using TD-DFT: Formaldehyde and benzene as case studies*, D. Jacquemin, E.A. Perpete, G. Scalmani, M.J. Frisch, M. Ciofini, C. Adamo, Chem. Phys. Lett. **421**, 272 (2006).

[122] *Geometries and properties of excited states in the gas phase and in solution: Theory and application of a time-dependent density functional theory polarizable continuum model*, G. Scalmani, M.J. Frisch, B. Mennucci, J. Tomasi, R. Cammi and V. Barone, J. Chem. Phys. **124**, 094107 (2006).

[123] *Density functional calculation of the electronic absorption spectrum of Cu+ and Ag+ aqua ions*, L. Bernasconi,J. Blumberger, M. Sprik, and R. Vuilleumier, J. Chem. Phys. **121**, 11885 (2004).

[124] *Magnitude of zero-point vibrational corrections to optical rotation in rigid organic molecules: A time-dependent density functional study*, B.C. Mort and J. Autschbach, J. Phys. Chem. A **109**, 8617 (2005).

[125] *Determination of absolute configurations of chiral molecules using ab initio time-dependent density functional theory calculations of optical rotation: How reliable are absolute configurations obtained for molecules with small rotations?*, P.J. Stephens, D.M. Mccann, J.R. Cheeseman and M.J. Frisch, Chirality **17**, S52 (2005).

[126] *A theoretical study of the chiroptical properties of molecules with isotopically engendered chirality*, M. Dierksen and S. Grimme, J. Chem. Phys. **124**, 174301 (2006).

[127] *Time-dependent density functional calculations of optical rotatory dispersion including resonance wavelengths as a potentially useful tool for determining absolute configurations of chiral molecules*, J. Autschbach, L. Jensen, G.C. Schatz, Y.C.E. Tse and M. Krykunov, J. Phys. Chem. A **110**, 2461 (2006).

[128] *On the origin of optical activity in tris-diamine complexes of Co(III) and Rh(III): A simple model based on time-dependent density function theory*, F.E. Jorge, J. Autschbach and T. Ziegler, J. Amer. Chem. Soc. **127**, 975 (2005).

[129] *Circular dichroism spectrum of [Co(en)(3)](3+) in water: A discrete solvent reaction field study*, L. Jensen, M. Swart, P.T. Van Duijnen and J. Autschbach, Int. J. Quant. Chem. **106**, 2479 (2006).

[130] *Determination of absolute configuration using concerted ab initio DFT calculations of electronic circular dichroism and optical rotation: Bicyclo[3.3.1]nonane diones*, P.J. Stephens, D.M. McCann, E. Butkus, S. Stoncius, J.R. Cheeseman and M.J. Frisch, J. Org. Chem. **69**,

1948 (2004).

[131] *Calculation of the A term of magnetic circular dichroism based on time dependent-density functional theory I. Formulation and implementation*, M. Seth, T. Ziegler, A. Banerjee, J. Autschbach, S.J.A. van Gisbergen and E.J. Baerends, J. Chem. Phys. **120**, 10942 (2004).

[132] *Open shells in reduced-density-matrix-functional theory*, N.N. Lathiotakis, N. Helbig, and E.K.U. Gross, Phys. Rev. A **72**, 030501 (R) (2005).

[133] *One-pot synthesis of helical aromatics: Stereoselectivity, stability against racemization, and assignment of absolute configuration assisted by experimental and theoretical circular dichroism*, M. Watanabe, H. Suzuki, Y. Tanaka, T. Ishida, T. Oshikawa and A. Tori-i, J. Org.Chem. **69** 7794 (2004).

[134] *Circular-dichroism studies on artemisinin and epi-artemisinin and their beta-cyclodextrin complexes in solution*, G. Marconi, S. Monti, F. Manoli, A.D. Esposti and A. Guerrini, Helv. Chim. Acta **87**, 2368 (2004).

[135] *Field emission and electronic structures of carbon allotropes*, K. Watanabe, M. Araidai and K. Tada, Thin Solid Films **464-65**, 354 (2004).

[136] *Effects of the crystal structure in the dynamical electron density-response of hcp transition metals*, G. Gurtubay, W. Ku, J.M. Pitarke and A.G. Eguiluz, Comp. Mater. Sci. **30**, 104 (2004).

[137] *Time-dependent density functional theory of excitation energies of closed-shell quantum dots*, K. Hirose, Y. Meir, and N.S. Wingreen, Physica E **22** 486 (2004).

[138] *Long-range contribution to the exchange-correlation kernel of time-dependent density functional theory*, S. Botti, F. Sottile, N. Vast, V. Olevano, L. Reining, H.C. Weissker, A. Rubio, G. Onida, R. Del Sole and R.W. Godby, Phys. Rev. B **69**, 155112 (2004).

[139] *Electronic and structural effects on the nonlinear optical behavior in push-pull TTF/tricarbonyl chromiun arene complexes*, B. Insuasty, C. Atienza, C. Seoane, N. Martin, J. Garin, J. Orduna, R. Alcala and B. Villacampa, J. Org. Chem. **69**, 6986 (2004).

[140] *Experimental and ab initio calculational studies on 2,3-diketo-benzopiperazine*, F.F. Jian and P.S. Zhao, J. Mol. Str. **705**, 133 (2004).

[141] *Calculations of the third-order nonlinear optical responses in push-pull chromophores with a time-dependent density functional theory*, N. Kobko, A. Masunov and S. Tretiak, Chem. Phys. Lett. **392**, 444 (2004).

[142] *Prediction of two-photon absorption properties for organic chromophores using time-dependent density-functional theory*, A.M. Masunov and S. Tretiak, J. Phys. Chem. B **108**, 899 (2004).

[143] *Prediction of second-order optical nonlinearity of trisorganotin-substituted beta-Keggin polyoxotungstate*, W. Guan, G.C. Yang, L.K. Yan and Z.M. Su, Inorg. Chem. **45**, 7864 (2006).

[144] *Theoretical study on the second-order nonlinear optical properties of asymmetric spirosilabifluorene derivatives*, G.C. Yang, Z.M. Su and C.S. Qin, J. Phys. Chem. A **110**, 4817 (2006).

[145] *Origin of the photoinduced optical second harmonic generation arising in N-phenyl microcrystalline films*, M. Makowska-Janusik, S. Tkaczyk and I.V. Kityk, J. Phys. Chem. B **110**, 6492 (2006).

[146] *Calculation of two-photon absorption spectra of donor-pi-acceptor compounds in solution using quadratic response time-dependent density functional theory*, P.N. Day, K.A. Nguyen and R. Pachter, J. Chem. Phys. **125**, 094103 (2006).

[147] *Calculations of two-photon absorption cross-sections of stibene and bis(styry1) benzene derivatives by means of TDDFT-SOS method*, G.C. Yang, C.S. Qin, Z.M. Su and S. Dong, Theochem-J. Mol. Struct. **726**, 61 (2005).

[148] *Effects of (multi)branching of dipolar chromophores on photophysical properties and two-photon absorption*, C. Katan, F. Terenziani, O. Mongin, M.H.V. Werts, L. Porres, T. Pons, J. Mertz, S. Tretiak and M. Blanchard-Desce, J. Phys. Chem. A **109**, 3024 (2005).

[149] *TDDFT study of one- and two-photon absorption properties: Donor-pi-acceptor chromophores*, P.N. Day, K.A. Nguyen and R. Pachter, J. Phys. Chem. B **109**, 1803 (2005).

[150] *Theoretical investigation of two-photon absorption allowed excited states in symmetrically substituted diacetylenes by ab initio molecular-orbital method*, K. Ohta and K. Kamada, J. Chem. Phys. **124**, 124303 (2006).

[151] *Time-dependent density functional theory studies of the photoswitching of the two-photon absorption spectra in stilbene, metacyclophenadiene, and diarylethene chromophores*, A.E. Clark, J. Phys. Chem. A **110**, 3790 (2006).

[152] *Effects of conjugation length, electron donor and acceptor strengths on two-photon absorption cross sections of asymmetric zinc-porphyrin derivatives*, O. Rubio-Pons, Y. Luo and H. Agren, J. Chem. Phys. **124**, 094310 (2006).

[153] *Two-photon excitation of substituted enediynes*, J.F. Kauffman, J.M. Turner, I.V. Alabugin, B. Breiner, S.V. Kovalenko, E.A. Badaeva, A. Masunov and S. Tretiak, J. Phys. Chem. A **110**, 241 (2006).

[154] *A Primer in Density Functional Theory*, ed. C. Fiolhais, F. Nogueira, and M. Marques (Springer-Verlag, NY, 2003).

[155] *Universal variational functionals of electron densities, first order density matrices, and natural spin-orbitals and solution of the v-representability problem* M. Levy, Proc. Natl. Acad. Sci. (U.S.A.) **76**, 6062 (1979).

[156] *Accurate exchange-correlation potentials and total-energy components for the helium isoelectronic series*, C. J. Umrigar and X. Gonze, Phys. Rev. A **50**, 3827 (1994).

[157] *Density-functional theory for fractional particle number: Derivative discontinuities of the energy*, J.P. Perdew, R.G. Parr, M. Levy, and J.L. Balduz, Jr., Phys. Rev. Lett. **49**, 1691 (1982).

[158] *Orbital-Dependent Functionals for the Exchange-Correlation Energy: A Third Generation of Density Functionals*, E. Engel, in *A Primer in Density Functional Theory*, ed. C. Fiolhais, F. Nogueira, and M. Marques (Springer-Verlag, NY, 2003), pg 56.

[159] *Orbital functionals in density functional theory: the optimized effective potential method*, T. Grabo, T. Kreibich, S. Kurth, and E.K.U. Gross, in *Strong Coulomb correlations in electronic structure: Beyond the local density approximation*, ed. V.I. Anisimov (Gordon and Breach, Tokyo, 1998).

[160] *Orbital- and state-dependent functionals in density-functional theory*, A. Görling, J. Chem. Phys. **123**,

062203 (2005).

[161] *Ground state of the electron gas by a stochastic method*, D. M. Ceperley and B. J. Alder, Phys. Rev. Lett. **45**, 566 (1980).

[162] *Self-interaction correction to density-functional approximations for many-electron systems*, J.P. Perdew and A. Zunger, Phys. Rev. B **23**, 5048 (1981).

[163] *Accurate spin-dependent electron liquid correlation energies for local spin-density calculations - a critical analysis*, S. H. Vosko, L. Wilk, and M. Nusair, Can. J. Phys. **58**, 1200 (1980).

[164] *Pair distribution function and its coupling-constant average for the spin-polarized electron gas*, J. P. Perdew and Y. Wang, Phys. Rev. B **46**, 12947 (1992); ibid. **56**, 7018 (1997) (E).

[165] *Correlation energy of an electron gas with a slowly varying high density*, S.-K. Ma and K.A. Brueckner, Phys. Rev. **165**, 18 (1968).

[166] *The adiabatic connection method: A non-empirical hybrid*, K. Burke, M. Ernzerhof, and J.P. Perdew, Chem. Phys. Lett. **265**, 115 (1997).

[167] *A new mixing of Hartree-Fock and local density-functional theories*, A.D. Becke, J. Chem. Phys. **98**, 1372 (1993).

[168] *Relevance of the slowly-varying electron gas to atoms, molecules, and solids*, J. P. Perdew, L. A. Constantin, E. Sagvolden, and K. Burke, Phys. Rev. Lett. **97**,223002 (2006).

[169] *Rationale for mixing exact exchange with density functional approximations*, J.P. Perdew, M. Ernzerhof, and K. Burke, J. Chem. Phys. **105**, 9982 (1996).

[170] *Unambiguous exchange-correlation energy density*, K. Burke, F.G. Cruz, and K.C. Lam, J. Chem. Phys. **109**, 8161 (1998).

[171] *Ensemble-Hartree-Fock scheme for excited states. The optimized effective potential method*, N.I. Gidopoulos, P.G. Papaconstantinou and E.K.U. Gross, PHYSICA B **318**, 328 (2002).

[172] *Time-dependent optimized effective potential in the linear response regime*, M. Petersilka, U.J. Gossmann, and E.K.U. Gross, in *Electronic Density Functional Theory: Recent Progress and New Directions*, eds. J.F. Dobson, G. Vignale, and M.P. Das (Plenum, NY, 1998).

[173] *Time-dependent optimized effective potential*, C.A. Ullrich, U.J. Gossman, and E.K.U. Gross, Phys. Rev. Lett. **74**, 872 (1995).

[174] *Efficient localized Hartree-Fock methods as effective exact-exchange Kohn-Sham methods for molecules*, F. Della Sala and A. Görling, J. Chem. Phys. **115**, 5718 (2001).

[175] *The asymptotic region of the Kohn-Sham exchange potential in molecules*, F. Della Salla and A. Görling, J. Chem. Phys. **116**, 5374 (2002).

[176] *Basis set selection for molecular calculations*, E.R. Davidson and D. Feller, Chem. Rev. **86**, 681 (1986).

[177] *Improvements on the direct SCF method*, M. Häser and R. Ahlrichs, J. Comput. Chem. **10**, 104 (1989).

[178] *Neutral Thermochemical Data*, H.Y. Afeefy, J.F. Liebman, and S.E. Stein in NIST Chemistry WebBook *http://webbook.nist.gov*, Eds. P.J. Linstrom and W.G. Mallard, June (2005).

[179] E.K.U. Gross and W. Kohn, in *Advances in Quantum Chemistry, Vol. 21: Density Functional Theory of Many-Fermion Systems*, edited by S. B. Trickey (Academic Press, San Diego, 1990).

[180] *Memory in time-dependent density functional theory*, N.T. Maitra, K. Burke, and C. Woodward, Phys. Rev. Letts, **89**, 023002 (2002).

[181] *Demonstration of initial-state dependence in time-dependent density functional theory*, N.T. Maitra and K. Burke, Phys. Rev. A **63**, 042501 (2001); **64** 039901 (E).

[182] *A Time-dependent spin-density functional theory for the dynamic spin susceptibility*, K.L. Liu and S.H. Vosko, Can. J. Phys. **67**, 1015 (1989).

[183] I. D'Amico and G. Vignale, *Exact exchange-correlation potential for a time-dependent two electron system*, Phys. Rev. B **59**, 7876 (1999).

[184] *Correlation in time-dependent density functional theory*, P. Hessler, N.T. Maitra, and K. Burke, J. Chem. Phys. **117**, 72 (2002).

[185] *Exact Time-Dependent Exchange-Correlation Potentials for Strong-Field Electron Dynamics*, M. Lein, and S. Kümmel, Phys. Rev. Lett. **94**, 143003 (2005).

[186] *Propagators for the time-dependent Kohn-Sham equations*, A.Castro, M.A.L. Marques and A. Rubio, J. Chem. Phys. **121**, 3425 (2004).

[187] *Mapping from Densities to Potentials in Time-Dependent Density-Functional Theory*, R. van Leeuwen, Phys. Rev. Lett. **82**, 3863, (1999).

[188] *Excitation energies from time-dependent density-functional theory*, M. Petersilka, U.J. Gossmann, and E.K.U. Gross, Phys. Rev. Lett. **76**, 1212 (1996).

[189] *Exact conditions in TDDFT*, K. Burke, Lect. Notes Phys **706**, 181 (2006).

[190] *Time-dependent density functional response theory of molecular systems: Theory, computational methods, and functionals*, M.E. Casida, in *Recent developments and applications in density functional theory*, ed. J.M. Seminario (Elsevier, Amsterdam, 1996).

[191] *Treatment of electronic excitations within the adiabatic approximation of time dependent density functional theory*, R. Bauernschmitt, R. Ahlrichs, Chem. Phys. Lett., **256**, 454 (1996).

[192] *An Undulatory Theory of the Mechanics of Atoms and Molecules*, E. Schrödinger, Phys. Rev. **28**, 1049 (1926).

[193] *Ab Initio Excitation Spectra and Collective Electronic Response in Atoms and Clusters*, I. Vasiliev, S. Ögüt, and J.R. Chelikowsky, Phys. Rev. Lett. **82**, 1919 (1999).

[194] *Octopus: a first-principles tool for excited electron-ion dynamics*, M.A.L. Marques, A. Castro, G.F. Bertsch and A. Rubio, Comput. Phys. Commun. **151**,60 (2003).

[195] *CPMD*, J. Hutter et al., Copyright IBM Zürich Research Laboratory and MPI für Festkörperforschung 1995-2001.

[196] *On the density matrix based approach to time-dependent density functional theory*, F. Furche, J. Chem. Phys. **114**, 5982 (2001).

[197] *A theoretical study of the electronic spectrum of naphthalene*, M. Rubio, M. Merchán, E. Ortí and B.O. Roos, Chem. Phys. **179**, 395 (1994).

[198] *Hohenberg-Kohn density-functional theory as an implicit Poisson equation for density changes from summed fragment densities*, A.E. DePristo, Phys. Rev. A **54**, 3863 (1996).

[199] *Gaussian basis sets of quadruple zeta valence quality for atoms H–Kr*, F. Weigend, F. Furche and R. Ahlrichs, J.

Chem. Phys. **119**, 12753 (2003).

[200] *Electron affinities of the first-row atoms revisited. Systematic basis sets and wave functions*, R.A. Kendall, T.H. Dunning and R.J. Harrison, J. Chem. Phys. **96**, 6796 (1992).

[201] *Fully optimized contracted Gaussian basis sets for atoms Li to Kr*, A. Schäfer, H. Horn and R. Ahlrichs, J. Chem. Phys. **97**, 2571 (1992).

[202] *Self-consistent molecular orbital methods. XII. Further extensions of Gaussian-type basis sets for use in molecular orbital studies of organic molecules*, W.J. Hehre, R. Ditchfield and J.A. Pople, J. Chem. Phys. **56**, 2257 (1972).

[203] *The influence of polarization functions on molecular orbital hydrogenation energies*, P.C. Hariharan and J.A. Pople, Theoret. Chim. Acta **28**, 213 (1973).

[204] *Balanced basis sets of split valence, triple zeta valence and quadruple zeta valence quality for H to Rn: Design an assessment of accuracy*, F. Weigend and R. Ahlrichs, Phys. Chem. Chem. Phys. **7**, 3297 (2005).

[205] *Gaussian basis sets for use in correlated molecular calculations. I. The atoms boron through neon and hydrogen*, T.H. Dunning Jr., J. Chem. Phys. **90**, 1007 (1989).

[206] *Fitting the Coulomb potential variationally in linear-combination-of-atomic-orbitals density-functional calculations*, J.W. Mintmire and B.I. Dunlap, Phys. Rev. A **25**, 88 (1982).

[207] *Auxiliary basis sets to approximate Coulomb potentials*, K. Eichkorn, O. Treutler, H. Öhm, M. Häser and R. Ahlrichs, Chem. Phys. Lett. **240**, 283 (1995).

[208] *Analytical time-dependent density functional derivative methods within the RI-J approximation, an approach to excited states of large molecules*, D. Rappoport and F. Furche, J. Chem. Phys. **122**, 064105 (2005).

[209] *Adiabatic time-dependent density functional methods for excited state properties*, F. Furche and R. Ahlrichs, J. Chem. Phys. **117**, 7433 (2002).

[210] *The second-order approximate coupled cluster singles and doubles model CC2*, O. Christiansen, H. Koch and P. Jørgensen, Chem. Phys. Lett. **243**, 409 (1995).

[211] *CC2 excitation energy calculations on large molecules using the resolution of the identity approximation*, C. Hättig and F. Weigend, J. Chem. Phys. **113**, 5154 (2000).

[212] *Transition moments and excited state first-order properties in the second-order coupled cluster model CC2 using the resolution of the identity approximation*, C. Hättig and A. Köhn, J. Chem. Phys. **117**, 6939 (2002).

[213] *A TDDFT study of the lowest excitation energies of polycyclic aromatic hydrocarbons*, M. Parac and S. Grimme, Chem. Phys. **292**, 11 (2003).

[214] *On the required shape corrections to the local density and generalized gradient approximations to the Kohn-Sham potentials for molecular response calculations of (hyper)polarizabilities and excitation energies*, M. Grüning, O.V. Gritsenko, S.J.A. van Gisbergen, and E.J. Baerends, J. Chem. Phys. **116**, 9591 (2002).

[215] *Density-functional theory calculations with correct long-range potentials*,Q. Wu, P.W. Ayers, and W. Yang, J. Chem. Phys. **119**, 2978 (2003).

[216] *Excitation energies of molecules by time-dependent density functional theory based on effective exact exchange Kohn-Sham-potentials*, F. Della Sala and A. Gorling, Int. J. Quantum Chem. **91**, 131 (2003).

[217] *Medium-size polarized basis-sets for high-level-correlated calculations of molecular electric properties .2. 2nd-row atoms - Si through Cl*, A.J. Sadlej, Theor. Chim. Acta **79**, 123 (1991).

[218] *Molecular excitation energies from time-dependent density functional theory*, T. Grabo, M. Petersilka, and E.K.U. Gross, in J. Mol. Structure (Theochem), **501**, 353 (2000).

[219] *Dynamic polarizabilities and excitation spectra from a molecular implementation of time-dependent density functional response theory: N_2 as a case study*, C. Jamorski, M.E. Casida, D.R. Salahub, J. Chem. Phys. **104**, 5134 (1996).

[220] *Molecular excitation energies to high-lying bound states from time-dependent density-functional response theory: Characterization and correction of the time-dependent local density approximation ionization threshold* M.E. Casida, C. Jamorski, K.C. Casida, and D.R. Salahub, J. Chem. Phys. **108**, 4439 (1998).

[221] *Comparison between equation of motion and polarization propagator calculations*, J. Oddershede, N.E. Grüner and G.H.F. Diercksen, Chem. Phys. **97**, 303 (1985).

[222] K.P. Huber and G. Herzberg, *Molecular Spectra and Molecular Structure IV: Constants of Diatomic Molecules*, Van Nostrand Reinhold, New York, 1979.

[223] *Relationship of Kohn-Sham eigenvalues to excitation energies*, A. Savin, C.J. Umrigar, X. Gonze, Chem. Phys. Lett. **288**, 391 (1998).

[224] *The development of new exchange-correlation functionals*, D.J. Tozer and N.C. Handy, J. Chem. Phys. **108**, 2545 (1998).

[225] *A direct optimization method for calculating density functionals and exchange-correlation potentials from electron densities*, Q. Wu and W. Yang, J. Chem. Phys. **118**, 2498 (2003).

[226] *Asymptotic correction approach to improving approximate exchange-correlation potentials: Time-dependent density-functional theory calculations of molecular excitation spectra*, M.E. Casida, D.R. Salahub, J. Chem. Phys. **113**, 8918 (2000).

[227] *Exchange-correlation potential with correct asymptotic behavior*, R. van Leeuwen and E.J. Baerends, Phys. Rev. A. **49**, 2421 (1994).

[228] J. B. Krieger, Y. Li, and G. J. Iafrate, in *Density Functional Theory*, eds. R. Dreizler and E. K. U. Gross, NATO ASI Series B (Plenum, New York, 1995).

[229] *Excitation energies from time-dependent density functional theory using exact and approximate functionals*, M. Petersilka, E.K.U. Gross, and K. Burke, Int. J. Quantum Chem. **80**, 534 (2000).

[230] *First-principles density-functional calculations for optical spectra of clusters and nanocrystals*, I. Vasiliev, S. Öğüt, and J.R. Chelikowsky, Phys. Rev. B **65**, 115416 (2002).

[231] *Excitations in Time-Dependent Density-Functional Theory*, H. Appel, E.K.U.Gross, and K. Burke, Phys. Rev. Lett. **90**, 043005 (2003).

[232] *Double-Pole Approximation in Time-Dependent Density Functional Theory* H. Appel, E.K.U. Gross, K. Burke, Int. J. Quant. Chem. **106**, 2840-2847 (2006).

[233] *Measuring the kernel of time-dependent density functional theory with X-ray absorption spectroscopy of 3d*

transition metals, A. Scherz, E.K.U. Gross, H. Appel, C. Sorg, K. Baberschke, H. Wende, and K. Burke, Phys. Rev. Lett. 95, 253006 (2005)

[234] *Comparison of approximate and exact density functionals: A quantum monte carlo study*, C. J. Umrigar and X. Gonze, in *High Performance Computing and its Application to the Physical Sciences*, Proceedings of the Mardi Gras 1993 Conference, edited by D. A. Browne et al. (World Scientific, Singapore, 1993).

[235] *The quantum defect method*, F. Ham, Solid State Phys. **1**, 127 (1955).

[236] *The quantum defect method*, M. J. Seaton, Mon. Not. R. Astron. Soc. **118**, 504 (1958).

[237] *Optimized effective atomic central potential*, J.D. Talman and W.F. Shadwick, Phys. Rev. A **14**, 36 (1976).

[238] *New Kohn-Sham method for molecules based on an exchange charge...*, A. Görling, Phys. Rev. Letts. **83**, 5459 (1999).

[239] *Exact exchange treatment for molecules in finite-basis-set Kohn-Sham theory*, S. Ivanov, S. Hirata, and R.J. Bartlett, Phys. Rev. Letts. **83**, 5455 (1999).

[240] *Shape corrections to exchange-correlation potentials by gradient-regulated seamless connection of model potentials for inner and outer region*, M. Gruning, O.V. Gritsenko, S.J.A. van Gisbergen, and E.J. Baerends, J. Chem. Phys. **114**, 652 (2001).

[241] *The quantum defect: the true measure of TDDFT results for atoms*, M. van Faassen and K. Burke, J. Chem. Phys. **124**, 094102 (2006).

[242] *The quantum defect as a powerful tool for studying Rydberg transition energies from density functional theory*, M. van Faassen, Int. J. Quant. Chem. **106**, 3235 (2006).

[243] *A new challenge for time-dependent density functional theory*, M. van Faassen and K. Burke, Chem. Phys. Lett. **431**, 410 (2006).

[244] *The role of exchange and correlation in time-dependent density- functional theory for photoionization*, M. Stener, P. Decleva, and A. Gorling, J. Chem. Phys., **114**, 7816 (2001).

[245] *Accurate oscillator strengths for neutral helium*, A. Kono and S. Hattori, Phys. Rev. A **29**, 2981 (1984).

[246] *Precision measurements of the absolute photoionization cross sections of He*, J.A.R. Samson, Z.X. He, L. Yin and G.N. Haddad, J. Phys. B **27**, 887 (1994).

[247] *Theoretical Atomic Physics*, H. Friedrich, 2nd ed. (Springer-Verlag, 1998).

[248] *Rydberg transition frequencies from the Local Density Approximation*, A. Wa sserman and K. Burke, Phys. Rev. Lett. **95**, 163006 (2005).

[249] *Handbook of Mathematical Functions*, eds. M. Abramowitz and I.A. Stegun (Dover, New York, 1972).

[250] *Accurate Rydberg transitions from LDA potentials*, A. Wasserman, N.T. Maitra, and K. Burke, Phys. Rev. Lett. **91**, 263001 (2003).

[251] *Electron-molecule scattering from time-dependent density functional theory*, A. Wasserman, N.T. Maitra, and K. Burke, J. Chem. Phys. **122**, 133103(2005).

[252] *Scattering amplitudes from TDDFT*, A. Wasserman and K. Burke, Lect. Notes Phys **706**, 493 (2006).

[253] *Bound-free correlation in electron scattering by atoms and molecules*, R.K. Nesbet, Phys. Rev. A **62**, 040701(R) (2000).

[254] *Electron-molecule scattering calculations in a 3D finite element R-matrix approach*, S. Tonzani and C. H. Greene, J. Chem. Phys. **122**, 014111 (2005).

[255] *Low-energy electron scattering from DNA and RNA bases: Shape resonances and radiation damage*, S. Tonzani and C. H. Greene, J. Chem. Phys. **124**, 054312 (2006).

[256] *On the absorption spectrum of noble gases at the arc spectrum limit*, U. Fano, cond-mat/0502210, (2005).

[257] *Excitation energies from time-dependent density-functional theory beyond the adiabatic approximation*, C.A. Ullrich and K. Burke, J. Chem. Phys. **121**, 28 (2004).

[258] *Nonadiabatic electron dynamics in time-dependent density-functional theory*, C.A. Ullrich and I.V. Tokatly, Phys. Rev. B **73**, 235102 (2006).

[259] *Time-dependent density-functional theory beyond the adiabatic approximation: insights from a two-electron model system*, C. A. Ullrich, cond-mat/0610341 (2006).

[260] *Time-dependent density functional theory beyond the adiabatic approximation*, G. Vignale, Int. J. Mod. Phys. B **15**, 1714 (2001).

[261] *Time-dependent density-functional theory beyond the local-density approximation*, J.M. Tao and G. Vignale, Phys. Rev. Lett. **97**, 036403 (2006).

[262] *Time-dependent exchange-correlation current density functionals with memory*, Y. Kurzweil and R. Baer, J. Chem. Phys. **121**, 8731 (2004).

[263] *Generic Galilean-invariant exchange-correlation functionals with quantum memory*, Y. Kurzweil and R. Baer, Phys. Rev. B **72**, 035106 (2005).

[264] *Quantum memory effects in the dynamics of electrons in gold clusters*, Y. Kurzweil and R. Baer, Phys. Rev. B **73**, 075413 (2006).

[265] *Quantum many-body dynamics in a Lagrangian frame: I. Equations of motion and conservation laws*, I.V. Tokatly, Phys. Rev. B **71**, 165104 (2005).

[266] *Quantum many-body dynamics in a Lagrangian frame: II. Geometric formulation of time-dependent density functional theory*, I.V. Tokatly, Phys. Rev. B **71**, 165105 (2005).

[267] *Current Density Functional Theory* G. Vignale, Lect. Notes Phys **706**, 75 (2006).

[268] *Current-Dependent Exchange-Correlation Potential for Dynamical Linear Response Theory*, G. Vignale and W. Kohn, Phys. Rev. Lett. **77**, 2037 (1996).

[269] *Time-dependent density functional theory beyond the adiabatic local density approximation*, G. Vignale, C.A. Ullrich, and S. Conti, Phys. Rev. Lett. **79**, 4878 (1997).

[270] *Double excitations in time-dependent density functional theory linear response*, N.T. Maitra, F. Zhang, R.J. Cave and K. Burke, J. Chem. Phys. **120**, 5932 (2004).

[271] *Approximate Functionals from Many-Body Perturbation Theory*, A. Marini, R. Del Sole and A. Rubio, Lect. Notes Phys **706**, 161 (2006).

[272] *Does Density Functional Theory Contribute to the Understanding of Excited States of Unsaturated Organic Compounds?*, D.J. Tozer, R.D. Amos, N.C. Handy, B.O. Roos, and L. Serrano-Andres, Mol. Phys. **97**, 859 (1999).

[273] *On the determination of excitation energies using density functional theory*, D.J. Tozer and N.C. Handy, Phys. Chem. Chem. Phys. **2**, 2117 (2000).

[274] *Adiabatic connection for near degenerate excited states*, F. Zhang and K. Burke, Phys. Rev. A **69**, 052510 (2004).

[275] *Propagator corrections to adiabatic time-dependent*

density-functional theory linear response theory, M.E. Casida, J. Chem. Phys. 122, 054111 (2005).

[276] *A dressed TDDFT treatment of the 2^1A_g states of butadiene and hexatriene*, R.J. Cave, F. Zhang, N.T. Maitra, and K. Burke, Chem. Phys. Lett. **389**, 39 (2004)

[277] *Resonant nonlinear polarizabilities in the time-dependent density functional (TDDFT) theory*, S. Tretiak and V. Chernyak, J. Chem. Phys. **119**, 8809 (2003).

[278] *Ultranonlocality in time-dependent current-density-functional theory: application to conjugated polymers*, M. van Faassen, P.L. de Boeij, R. van Leeuwen, J.A. Berger, and J.G. Snijders, Phys. Rev. Lett. **88**, 186401 (2002).

[279] *Application of time-dependent current-density-functional theory to nonlocal exchange-correlation effects in polymers*, M. van Faassen, P.L. de Boeij, R. van Leeuwen, J.A. Berger, and J.G. Snijders, J. Chem. Phys. **118**, 1044 (2003).

[280] *Time-dependent current-density-functional theory applied to atoms and molecules*, M. van Faassen, Int. J. Mod. Phys. B **20**, 3419 (2006).

[281] *Electric field dependence of the exchange-correlation potential in molecular chains*, S.J.A. van Gisbergen, P.R.T. Schipper, O.V. Gritsenko, E.J. Baerends, J.G. Snijders, B. Champagne, B. Kirtman, Phys. Rev. Lett., **83**, 694 (1999).

[282] *Electrical Response of Molecular Chains from Density Functional Theory*, S. Kummel, L. Kronik, and J.P. Perdew, Phys. Rev. Lett. **93**, 213002 (2004).

[283] *Optical excitations of Si by time-dependent density functional theory based on exact-exchange Kohn-Sham band structure*, Y. H. Kim, M. Stadele, and A. Gorling, Int. J. Quantum Chem. **91**, 257 (2003).

[284] *Efficient real-space approach to time-dependent density functional theory for the dielectric response of nonmetallic crystals*, F. Kootstra, P.L. Boeij, and J.G. Snijders, J. Chem. Phys. **112**, 6517 (2000).

[285] *Application of time-dependent density-functional theory to the dielectric function of various nonmetallic crystals*, F. Kootstra, P. L. De boeij, and J. G. Snijders, Phys. Rev. B, **62**, 7071 (2000).

[286] *Current density functional theory for optical spectra: A polarization functional*, P.L. de Boeij, F. Kootstra, J.A. Berger, R. van Leeuwen, and J.G. Snijders, J. Chem. Phys. **115**, 1995 (2001).

[287] *Electronic excitations: density-functional versus many-body Green's-function approaches*, G. Onida, L. Reining, and A. Rubio, Rev. Mod. Phys. **74**, 601 (2002).

[288] *Parameter-free calculation of response functions in time-dependent density-functional theory*, F. Sottile, V. Olevano, and L. Reining, Phys. Rev. Lett. **91**, 056402 (2003).

[289] *Bound Excitons in Time-Dependent Density-Functional Theory: Optical and Energy-Loss Spectra*, Andrea Marini, Rodolfo Del Sole, and Angel Rubio, Phys. Rev. Lett. **91**, 256402 (2003)

[290] *Electron linewidths of wide-gap insulators: Excitonic effects in LiF*, A. Marini and A. Rubio, Phys. Rev. B **70**, 081103 (2004).

[291] *Time-dependent density functional theory*, edited by M. Marques, C.A. Ullrich, F. Noguiera, A. Rubio, K. Burke, and E.K.U. Gross (Springer, Heidelberg, 2006).

[292] *Undoing static correlation: long-range charge transfer in time-dependent density functional theory*, N. T. Maitra, J. Chem. Phys. **122**, 234104 (2005).

[293] *Long-range excitations in time-dependent density functional theory*, N.T. Maitra, and D.G. Tempel, cond-mat/0510588 (2005).

[294] *Failure of time-dependent density functional methods for excitations in spatially separated systems*, W. Hieringer, and A. Görling, Chem. Phys. Lett. **419**, 557 (2006).

[295] *Charge-transfer correction for improved time-dependent local density approximation excited-state potential energy curves: Analysis within the two-level model with illustration for H-2 and LiH*, M.E. Casida, F. Gutierrez, J.G. Guan, F.X. Gadea, D. Salahub, and J.P. Daudey, J. Chem. Phys. **113**, 7062 (2000).

[296] *Fluctuation-dissipation theorem density-functional theory*, F. Furche and T. Van Voorhis, J. Chem. Phys. **122**, 164106 (2005).

[297] *Density functional approximation for the correlation energy of the inhomogeneous gas*, J.P. Perdew, Phys. Rev. B **33**, 8822 (1986); **34**, 7406 (1986) (E).

[298] *Electron correlation energies from scaled exchange-correlation kernels: Importance of spatial vs. temporal nonlocality*, M. Lein, E.K.U. Gross, and J.P. Perdew, Phys. Rev. B **61**, 13431 (2000).

[299] *van der Waals Interactions in Density-Functional Theory*, Y. Andersson, D.C. Langreth, and B.I. Lunqvist, Phys. Rev. Lett. **76**, 102 (1996).

[300] *Describing static correlation in bond dissociation by Kohn-Sham density fun ctional theory*, M. Fuchs, Y.-M. Niquet, X. Gonze, and K. Burke, J. Chem. Phys. **122**, 094116

[301] *van der Waals density functional for general geometries*, M. Dion, H. Rydberg, E. Schr̈der, D.C. Langreth, and B.I. Lundqvist, Phys. Rev. Lett. **92**, 246401 (2004).

[302] *The exchange-correlation energy of a metallic surface*, D.C. Langreth and J.P. Perdew, Solid State Commun. **17**, 1425 (1975).

[303] *Exchange and correlation in atoms, molecules, and solids by the spin-density-functional formalism*, O. Gunnarsson and B.I. Lundqvist, Phys. Rev. B **13**, 4274 (1976).

[304] *Density Functional for van der Waals Forces at Surfaces*, Y. Andersson, B.I. Lunqvist, and D.C. Langreth, Phys. Rev. Lett. **77**, 2029 (1996).

[305] *Density functional results for isotropic and anisotropic multipole polarizabilities and C_6, C_7, and C_8 Van der Waals dispersion coefficients for molecules*, V.P. Osinga, S.J.A. van Gisbergen, J.G. Snijders, and E.J. Baerends, J. Chem. Phys. **106**, 5091 (1997).

[306] *Van der Waals energies in density functional theory*, W. Kohn, Y. Meir, and D.E. Makarov, Phys. Rev. Lett., **80**, 4153 (1998).

[307] *Van der Waals interactions in density functional theory*, Y. Andersson, E. Hult, H. Rydberg, P. Apell, B.I. Lundqvist, and D.C. Langreth, in *Electronic Density Functional Theory: Recent Progress and New Directions*, eds. J.F. Dobson, G. Vignale, and M.P. Das (Plenum, NY, 1997).

[308] *Tractable nonlocal correlation density functionals for flat surfaces and slabs*, H. Ryberg, B.I. Lundqvist, D.C. Langreth, and M. Dion, Phys. Rev. B **62**, 6997 (2000).

[309] *Van der Waals Density Functional for Layered Structures*, H. Rydberg, M. Dion, N. Jacobson, E. Schröder,

P. Hyldgaard, S.I. Simak, D.C. Langreth, and B.I. Lundqvist, Phys. Rev. Lett. (to appear).

[310] *Application of van der Waals Density Functional to an Extended System: Adsorption of Benzene and Naphthalene on Graphite*, S.D. Chakarova Käck, E. Schröder, B.I. Lundqvist, and D.C. Langreth, cond-mat/0601161v1 (2006).

[311] *Binding energies in benzene dimers: Nonlocal density functional calculations*, A. Puzder, M. Dion, and D.C. Langreth, J. Chem. Phys. **124**, 164105

[312] *Interaction energies of monosubstituted benzene dimers via nonlocal density functional theory*, T. Thonhauser, A. Puzder, and D.C. Langreth, J. Chem. Phys. **124**, 164106

[313] *Dispersion Energy from Density-Functional Theory Description of Monomers*, A.J. Misquitta, B. Jeziorski, and K. Szalewicz, Phys. Rev. Lett. **91**, 033201 (2003).

[314] *Molecular tests of the random phase approximation to the exchange-correlation energy functional* F. Furche, Phys. Rev. B **64**, 195120 (2001).

[315] *Accurate density functionals: Approaches using the adiabatic-connection fluctuation-dissipation theorem*, M. Fuchs and X. Gonze, Phys. Rev. B **65**, 235109 (2002).

[316] *Double ionization of helium at 390 nm*, J. Parker, L.R. Moore, D. Dundas and K.T. Taylor, J. Phys. B: At. Mol. Opt. Phys. **33**, L691-L698 (2000).

[317] *Time-Dependent Variational Approach to Molecules in Strong Laser Fields*, T. Kreibich, R. van Leeuwen, and E.K.U. Gross, Chem. Phys. **304**, 183 (2004).

[318] *Towards time-dependent density-functional theory for molecules in strong laser pulses*, T. Kreibich, N.I. Gidopoulos, R. van Leeuwen, E.K.U. Gross, Progress in Theoretical Chemistry and Physics 14, 69 (2003).

[319] *Strong-Field double Ionization of Helium: A Density-Functional perspective*, M. Petersilka and E.K.U. Gross, Laser Physics **9**,1 (1999).

[320] *The Effect of the Electron-Electron Interaction in Above-Threshold Double Ionization*, M. Lein, E.K.U. Gross, and V. Engel, Laser Physics **12**, 487 (2002).

[321] *Strong-field ionization dynamics of a model H_2 molecule*, M. Lein, T. Kreibich, E.K.U Gross, and V. Engel, Phys. Rev. A **65**, 033403 (2002).

[322] *Phase-space analysis of double ionization*, M. Lien, V. Engel and E.K.U. Gross, Optics Express **8**, 411 (2001).

[323] *Intense-Field Double Ionization of Helium: Identifying the Mechanism*, M. Lein, E.K.U. Gross, and V. Engel, Phys. Rev. Lett. **85**, 4707 (2000).

[324] *http://www.physik.fu-berlin.de/˜ag-gross/tdelf*

[325] *Time-dependent electron localization function*, T. Burnus, M.A.L. Marques, E.K.U. Gross, Phys. Rev. A **71**, 010501 (R) (2005).

[326] *Time-dependent electron localization functions for coupled nuclear-electronic motion*, M. Erdmann, E.K.U. Gross, V. Engel, J. Chem. Phys. 121, 9666 (2004).

[327] *Time-dependent density-functional approach to atoms in strong laser pulses*, C.A. Ullrich, S. Erhard and E.K.U. Gross, in: Super Intense Laser Atom Physics IV, H.G. Muller and M.V. Fedorov, ed(s), (Kluwer, 1996), p 267 - 284.

[328] *High harmonic generation in hydrogen and helium atoms subject to one- and two-color laser pulses*, S. Erhard and E.K.U. Gross, in: Multiphoton Processes 1996, P. Lambropoulus and H. Walther, ed(s), (IOP, 1997), p 37.

[329] *Excited states dynamics in time-dependent density functional theory - High-field molecular dissociation and harmonic generation*, A. Castro, M.A.L. Marques, J.A. Alonso, G.F. Bertsch and A. Rubio, Eur. Phys. J. D **28**, 211 (2004).

[330] *Self-interaction-free time-dependent density-functional theory for molecular processes in strong fields: high-order harmonic generation of H_2 in intense laser fields - art. no. 023411*, X. Chu and S. I. Chu, Phys. Rev. A, **6302**, 3411 (2001).

[331] *Ionization and High-order harmonic generation in aligned benzene by a short intense circularly polarized laser pulse*, R. Baer, D. Neuhauser, P. R.Ždánská and N. Moiseyev, Phys. Rev. A **68**,043406 (2003).

[332] *Monitoring molecular dynamics using coherent electrons from high harmonic generation*, N.L. Wagner, A. Wüest, I.P. Christov, T. Popmintchev, X. Zhou, M.M. Murnane and H.C. Kapteyn, PNAS **103**, 13279 (2006).

[333] *see http://online.itp.ucsb.edu/online/atto06/moletomo/*

[334] *Precision measurement of stong field double ionization of helium*, B. Walker, B. Sheehy, L.F. DiMauro, P. Agostini, K.J. Schafer, and K.C. Kulander, Phys. Rev. Lett. **73**, 1227 (1994).

[335] *Observation of nonsequential double ionization of Helium with optical tunnelling*, D.N. Fittinghoff, P.R. Bolton, B. Chang, and K.C. Kulander, Phys. Rev. Letts. **69**, 2642 (1992).

[336] *Wavelength dependence of nonsequential double ionization in He* , K. Kondo, A. Sagisaka, T. Tamida, Y. Nabekawa and S. Watanabe, Phys. Rev. A **48**, R2531 (1993).

[337] *Towards Single-Particle spectroscopy of Small Metal Clusters*, A. Pohl, P.-G. Reinhard and E. Suraud, Phys. Rev. Lett **84**,5090 (2000).

[338] *Asymmetry of above-threshold ionization of metal clusters in two-color laser fields: A time-dependent density-functional study*, H.S. Nguyen, A.D. Bandrauk and C.A. Ullrich, Phys. Rev. A **69**, 063415 (2004).

[339] *Optical Control of Molecular Dynamics*, S.A. Rice and M. Zhao (John Wiley and Sons, 2000).

[340] *Tailoring laser pulses with spectral and fluence constraints using optimal control theory*, J. Werschnik, and E.K.U. Gross, J. Opt. B: Quantum Semiclass. Opt. **7**,

[341] *Laser-induced control of (multichannel) intracluster reactions - The slowest is always the easiest to take*, A.G. Urena, K. Gasmi, S. Skowronek, A. Rubio and P.M. Echenique, Eur. Phys. J. D **28**, 193 (2004).

[342] *Coherent control of intersubband optical bistability in quantum wells*, H.O. Wijewardane and C.A. Ullrich, Appl. Phys. Lett. **84**, 3984 (2004).

[343] *Theory of the linewidth of intersubband plasmons in quantum wells*, C.A. Ullrich and G. Vignale, Phys. Rev. Lett. **87**, 037402 (2001).

[344] *Collective charge-density excitations of noncircular quantum dots in a magnetic field*, C. A. Ullrich and G. Vignale, Phys. Rev. B, **61**, 2729 (2000).

[345] *Theoretical studies of molecular scale near-field electron dynamics*, R. Baer and D. Neuhauser, J. Chem. Phys. **125**, 074709 (2006).

[346] *Time-dependent density-functional studies of the D-2 Coulomb explosion*, E. Livshits and R. Baer, J. Phys. Chem. A **110**, 8443 (2006).

[347] *Rotational aspects of short-pulse population transfer in*

diatomic molecules, Y.B. Band, S. Kallush and R. Baer, Chem. Phys. Lett. **392**, 23 (2004).

[348] *Electron transport in molecular wire junctions*, A. Nitzan and M.A. Ratner, Science **300**, 1384 (2003).

[349] *Density functional method for nonequilibrium electron transport* M. Brandbyge, J.-L. Mozos, P. Ordejon, J. Taylor, and K. Stokbro, Phys. Rev. B **65**, 165401 (2002).

[350] *Time-Dependent Partition-Free Approach in Resonant Tunneling Systems*, G. Stefanucci and C.- O. Almbladh, Phys. Rev. B **69**, 195318 (2004).

[351] *Transport in nanoscale systems: the microcanonical versus grand-canonical picture*, M. Di Ventra, T.N. Todorov, J Phys Cond Matt **16**, 8025 (2004).

[352] *Kinetic theory of quantum transport at the nanoscale*, R. Gebauer and R. Car, Phys. Rev. B **70**, 125324 (2004).

[353] *Density Functional Theory of the Electrical Conductivity of Molecular Devices*, K. Burke, Roberto Car, and Ralph Gebauer, Phys. Rev. Lett. **94**, 146803 (2005).

[354] *The conductance of molecular wires and DFT based transport calculations*, F. Evers, F. Weigend, M. Koentopp, Phys Rev. B **69**, 25411 (2004).

[355] *Dynamical Corrections to the DFT-LDA Electron Conductance in Nanoscale Systems*, N. Sai, M. Zwolak, G. Vignale, and M. Di Ventra, Phys. Rev. Lett. **94**, 186810 (2005).

[356] *The Dramatic Role of the Exchange-Correlation Potential in ab initio Electron Transport Calculations*, S-H Ke, H.U. Baranger and W. Yang, cond-mat/0609637 (2006).

[357] *Self-interaction errors in density functional calculations of electronictransport*, C. Toher, A. Filippetti, S. Sanvito, and K. Burke, Phys. Rev. Lett. **95**, 146402 (2005)

[358] *Zero-bias molecular electronics: Exchange-correlation corrections to Landauer's formula*, M. Koentopp, K. Burke, and F. Evers, Phys. Rev. B Rapid Comm., **73**, 121403 (2006).

[359] *Time-dependent quantum transport: A practical scheme using density functional theory*, S. Kurth, G. Stefanucci, C.O. Almbladh, A. Rubio and E.K.U. Gross, Phys. Rev. B **72**, 035308 (2005).

[360] *Kohn-Sham master equation approach to transport through single molecules*, R. Gebauer, K. Burke, and R. Car, Lect. Notes Phys **706**, 463 (2006).

[361] *Electron transport with dissipation: a quantum kinetic approach* R. Gebauer and R. Car, Int. J. Quantum Chem. **101**, SI 564, (2005).